Prepared for:

Dutch Ministry of Transport, Public Works and Water Management, Tidal Waters Division

The importance of internal waves for mixing in a stratified estuarine tidal flow

Part two: tables and figures

November 1993

Z694

delft hydraulics

The importance of internal waves for mixing in a stratified estuarine tidal flow

Part two: tables and figures

R.E. Uittenbogaard
J. Imberger

delft hydraulics

Contents

List of Tables

List of Figures

Table 1. Mean values for Rotterdam Waterway (day 156) and Caland channel (day 157).

Data derived from Table 2.

Mean values for day 156, Rotterdam Waterway:

Lower estimate/tot KE	[-]	0.74
Upper estimate/tot KE	[-]	1.02
$\int\{G_{\partial u \partial u} + \chi \lvert Q \rvert_{\rho u}\}/\langle u'^2 \rangle$	[-]	0.55
$\chi \lvert Q \rvert_{\rho v}/\langle v'^2 \rangle$	[-]	1.10
$\chi \lvert Q \rvert_{\rho w}/\langle w'^2 \rangle$	[-]	1.29
α	[-]	0.43
Br	[mm²/s³]	310.

Mean values for day 157, Caland channel:

Lower estimate/tot KE	[-]	0.42
Upper estimate/tot KE	[-]	0.60
$\int\{G_{\partial u \partial u} + \chi \lvert Q \rvert_{\rho u}\}/\langle u'^2 \rangle$	[-]	0.39
$\chi \lvert Q \rvert_{\rho v}/\langle v'^2 \rangle$	[-]	1.01
$\chi \lvert Q \rvert_{\rho w}/\langle w'^2 \rangle$	[-]	0.90
α	[-]	0.47
Br	[mm²/s³]	5.

Table 2. Summary of platform data per time series measurement of 30 minutes.

Data averaged from Table 3.

Reference number		1	2	3	4	5	6	7	8	9	10
M.E.T time/Julian day	[h:min/d]	12:53/156	13:32/156	14:07/156	14:59/156	15:36/156	16:15/156	09:13/157	09:53/157	10:35/157	11:11/157
Total KE: $\frac{1}{2}\langle \underline{u}' \cdot \underline{u}' \rangle$	[mm²/s²]	2211	1560	1992	2878	992	977	452	833	1076	682.
Upper estimate KIWE	[mm²/s²]	2342	885	1915	3720	2129	117	281	390	870	345
Lower estimate KIWE	[mm²/s²]	1666	1308	1946	1915	1029	189	235	368	634	97.
Lower estimate/tot KE	[-]	0.75	0.84	0.98	0.67	1.04	0.19	0.52	0.44	0.59	0.14
Upper estimate/tot KE	[-]	1.06	0.57	0.96	1.29	2.15	0.12	0.62	0.47	0.81	0.51
$\int \{G_{\partial u \partial u} + \chi \lvert Q \rvert_{\rho u}\} / \langle u'^2 \rangle$	[-]	0.55	0.56	0.61	0.68	0.72	0.16	0.47	0.41	0.54	0.16
$\chi \lvert Q \rvert_{\rho v} / \langle v'^2 \rangle$	[-]	1.53	1.18	1.40	0.73	1.38	0.37	1.51	1.24	1.07	0.23
$\chi \lvert Q \rvert_{\rho w} / \langle w'^2 \rangle$	[-]	1.47	0.96	1.27	0.85	2.21	0.98	0.79	0.97	1.54	0.30
L_E	[mm]	569	297	494	761	469	138	499	643	1094	786
L_E from $\int \{\lvert Q \rvert_{\rho u_i} \lvert Q \rvert_{\rho u_i}\}^{1/2}$	[mm]	480	361	498	546	326	175	456	625	933	416
L_C	[mm]	200	110	60	70	50	70	30	20	30	50
α from L_E	[-]	0.54	0.26	0.48	0.72	0.47	0.13	0.31	0.42	0.68	0.46
W	[-]	2	2	17	30	22	1	69	259	332	62.
Br	[mm²/s³]	692	328	236	306	260	38	5	3	7	4.

Table 3. Summary of microstructure and finescale observations at platform level.

Reference number		1	2	3	4	5	6	7	8	9	10
M.E.T time/Julian day		12:53/156	13:32/156	14:07/156	14:59/156	15:36/156	16:15/156	09:13/157	09:53/157	10:35/157	11:11/157
Depth	[m]	11	12	12	10	10	12	6	6	6	9
Start after ref time	[min]	26	65	100	152	189	228	19	59	101	137
End after ref time	[min]	56	95	130	182	219	258	49	89	131	167
Finescale profile	[-]	1+2	3+4	5+6	7+8	9+10	11+12	16	17+18	19+20	21
$-\langle \partial\rho/\partial z \rangle$	[kg/m^4]	3.14	2.35	1.46	3.02	2.81	3.21	0.70	0.65	0.41	0.39
dU/dz	[1/s]	0.17	0.24	0.22	0.15	0.22	-0.13	0.048	0.036	0.043	0.025
U	[mm/s]	604	389	272	444	286	693	165	263	253	61
Ri	[-]	1.18	0.43	0.55	0.48	0.63	2.20	4.90	0.85	3.85	3.59
N	[rad/s]	0.17	0.15	0.12	0.17	0.17	0.18	0.082	0.079	0.063	0.062
$\langle \rho'^2 \rangle$	[kg^2/m^6]	0.799	0.122	0.130	1.32	0.435	0.0489	0.0305	0.0437	0.0503	0.0235
$\langle u'^2 \rangle$	[mm^2/s^2]	3298	2520	3361	3708	1509	1613	477	1096	1601	696
$\langle v'^2 \rangle$	[mm^2/s^2]	675	390	378	1217	361	270	85.7	303	276	523
$\langle w'^2 \rangle$	[mm^2/s^2]	449	209	245	831	114	71.8	341	266	274	145
$\langle \rho'u' \rangle$	[kg.mm/s.m^3]	-29.5	-9.93	-13.3	-38.5	-12.4	1.62	0.773	-1.31	-0.347	0.0879
$\langle \rho'v' \rangle$	[kg.mm/s.m^3]	14.5	-0.941	-1.45	11.8	3.68	0.606	-0.264	0.448	-0.486	0.247
$\langle \rho'w' \rangle$	[kg.mm/s.m^3]	1.58	0.282	0.204	3.0	-0.0625	0.275	-0.0273	-0.172	0.426	-0.0164
$\lvert Q \rvert_{\rho u}$	[kg.mm/s.m^3]	18.96	7.818	7.349	30.54	7.754	3.630	1.420	3.159	4.358	0.5989
$\lvert Q \rvert_{\rho v}$	[kg.mm/s.m^3]	19.03	7.230	6.458	15.77	8.231	1.804	1.106	3.083	1.923	0.7593
$\lvert Q \rvert_{\rho w}$	[kg.mm/s.m^3]	12.23	3.136	3.787	12.60	4.156	1.253	2.307	2.129	2.750	0.2765
$\int \{ \lvert Q \rvert_{\rho u_i} \lvert Q \rvert_{\rho u_i} \rvert \}^{1/4}$	[kg.mm/s.m^3]	30.77	11.51	10.86	38.25	12.72	4.430	2.990	5.008	5.626	1.046
$\langle u'w' \rangle$	[mm^2/s^2]	-18.7	6.36	-68.0	34.8	-16.3	-49.9	-34.4	96.4	140	31.7
L_C	[mm]	200	110	60	70	50	70	30	20	30	50
H	[m]	6	8	8	8	8	8	15	15	15	15

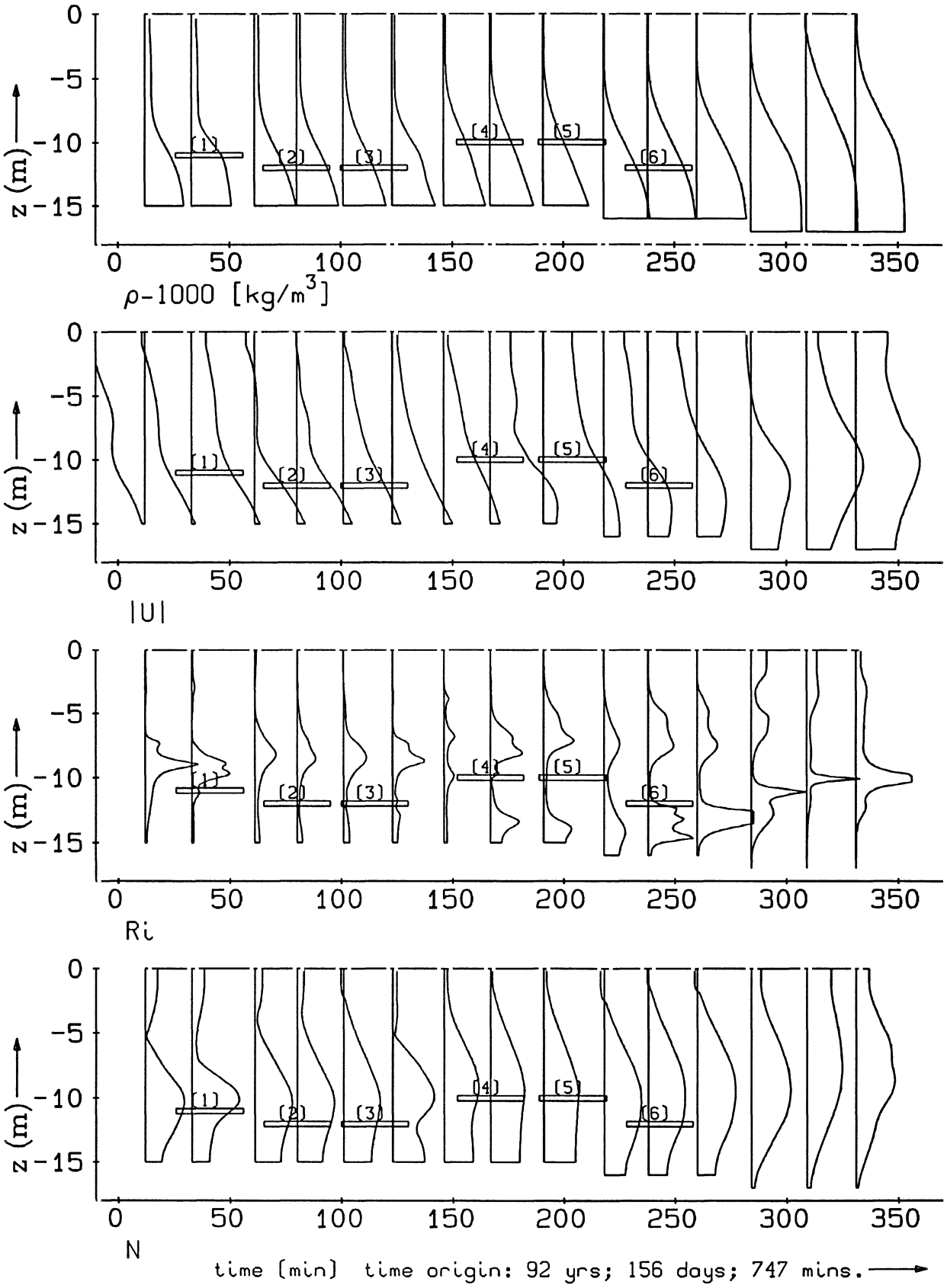

Density, vel. magnitude, Ri-number and buoyancy freq.
Rotterdam Waterway; day 156 [RWS].

day.156

DELFT HYDRAULICS

Z 694

Fig.1a

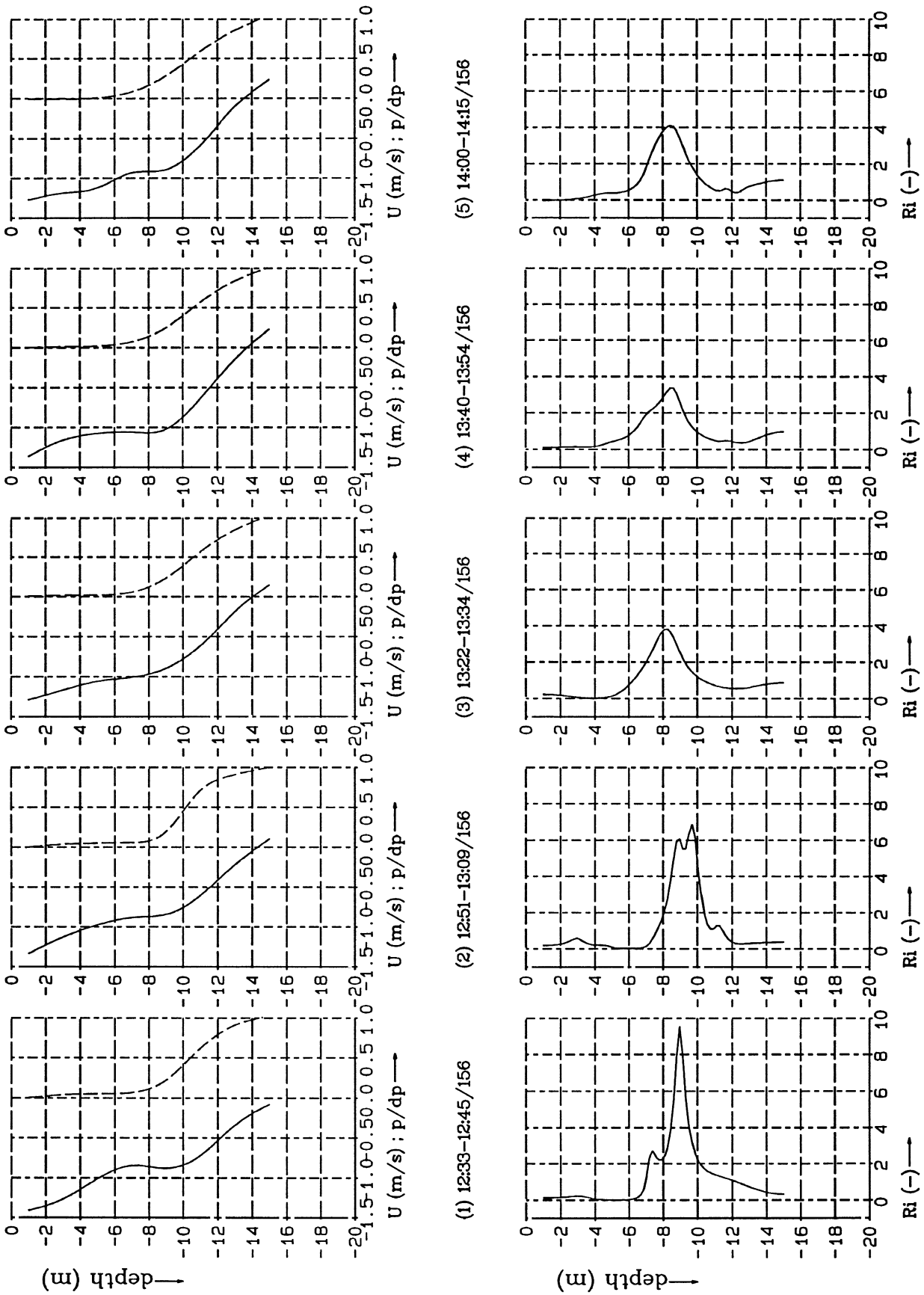

Vertical finescale profiles of |U|, rel. density and Richardson number (RWS).

Profiles 1-5

Ri1-5.inv

DELFT HYDRAULICS

Z694

Fig.1[b]

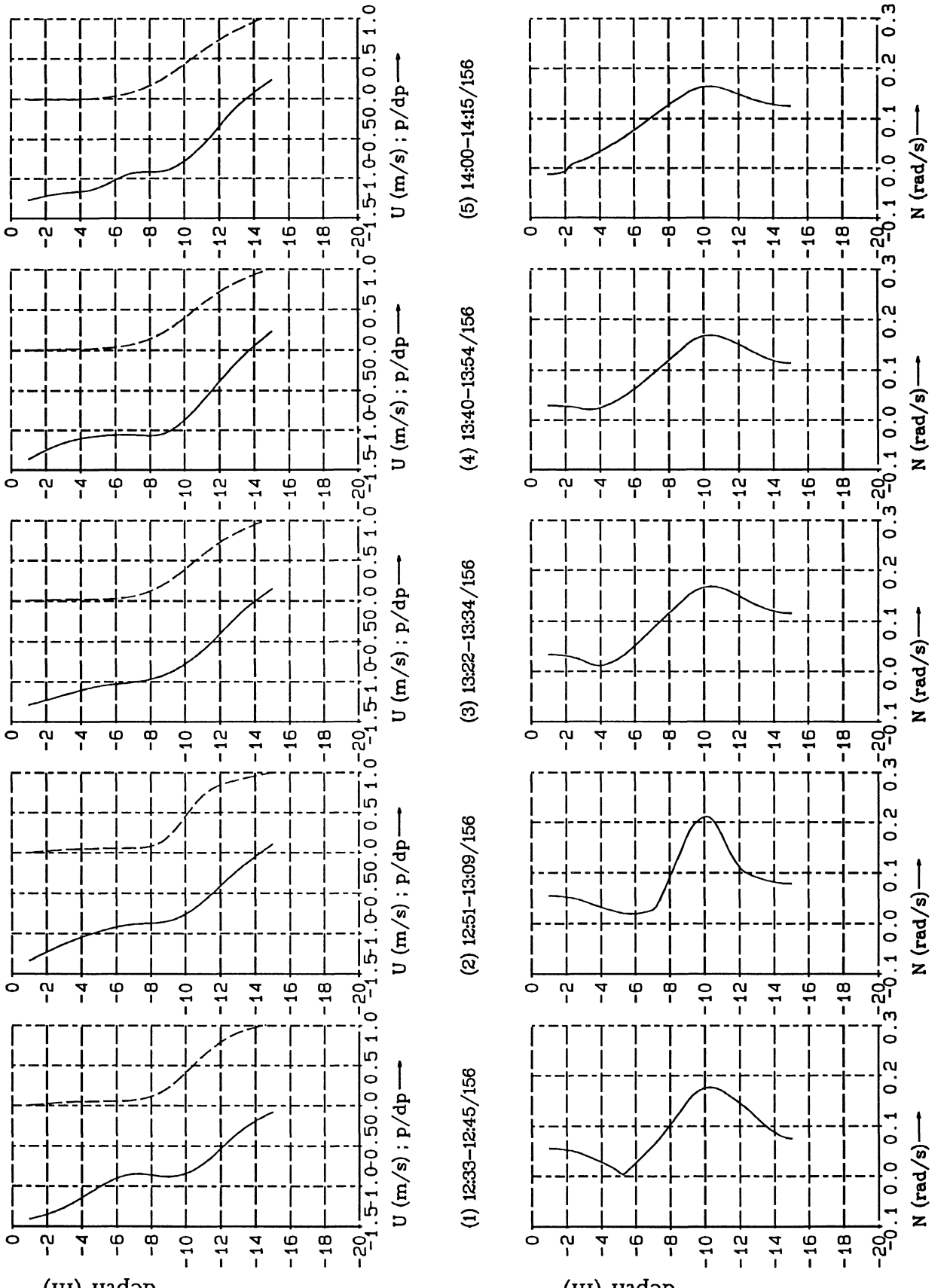

Vertical finescale profiles of |U|, rel. density and Brunt-Vaisaila freq.(RWS).

Profiles 1-5

bv1-5.inv

DELFT HYDRAULICS

Z694

Fig.1c

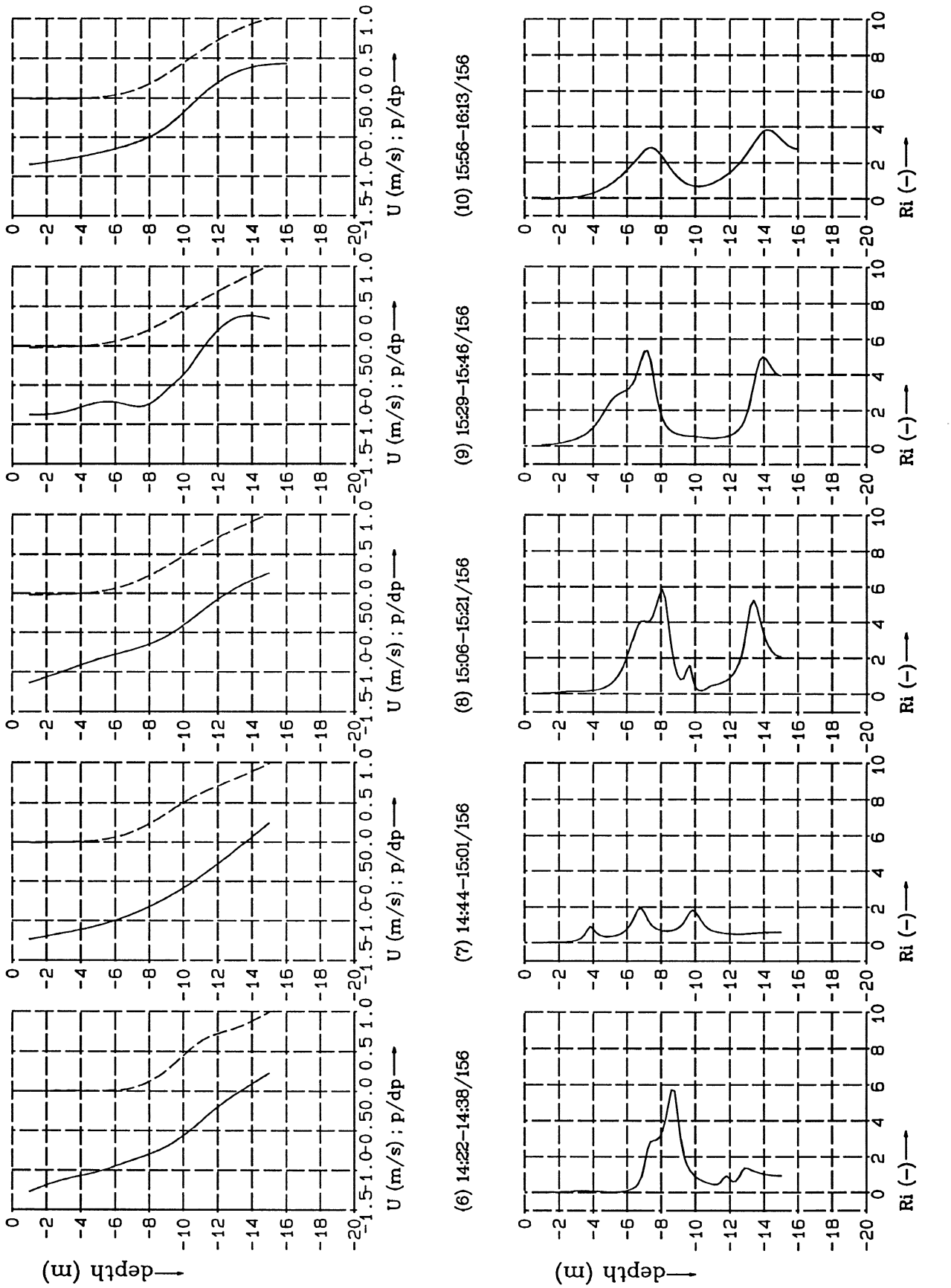

Vertical finescale profiles of |U|, rel. density and Richardson number (RWS).

Profiles 6-10

Ri6-10.inv

DELFT HYDRAULICS

Z694

Fig.1[d]

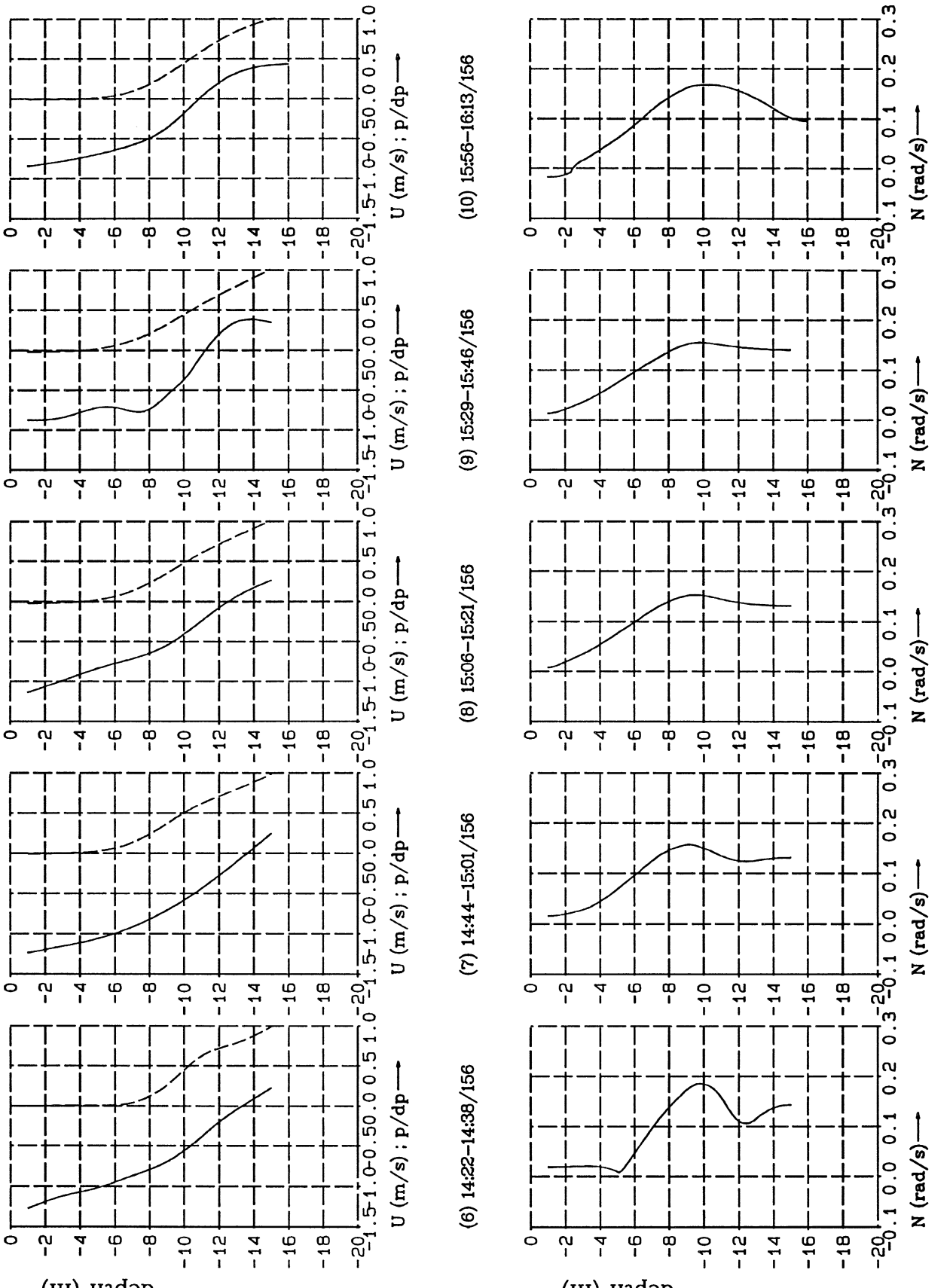

Vertical finescale profiles of |U|, rel. density and Brunt-Vaisaila freq. (RWS).

Profiles 6-10

bv6-10.inv

DELFT HYDRAULICS

Z694

Fig.1e

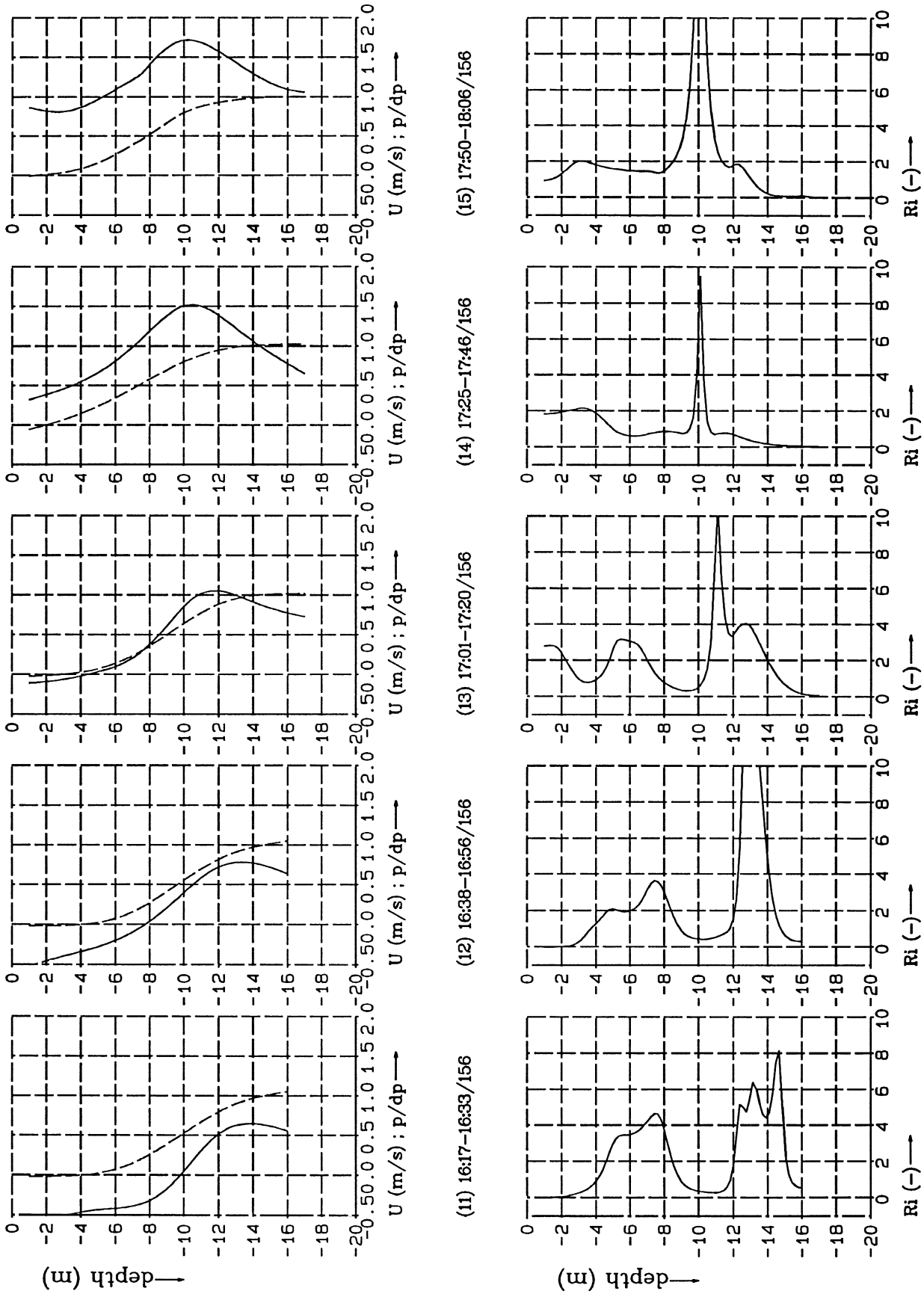

Vertical finescale profiles of |U|, rel. density and Richardson number (RWS).

Profiles 11-15

Ri11-15.inv

DELFT HYDRAULICS

Z694

Fig.1[f]

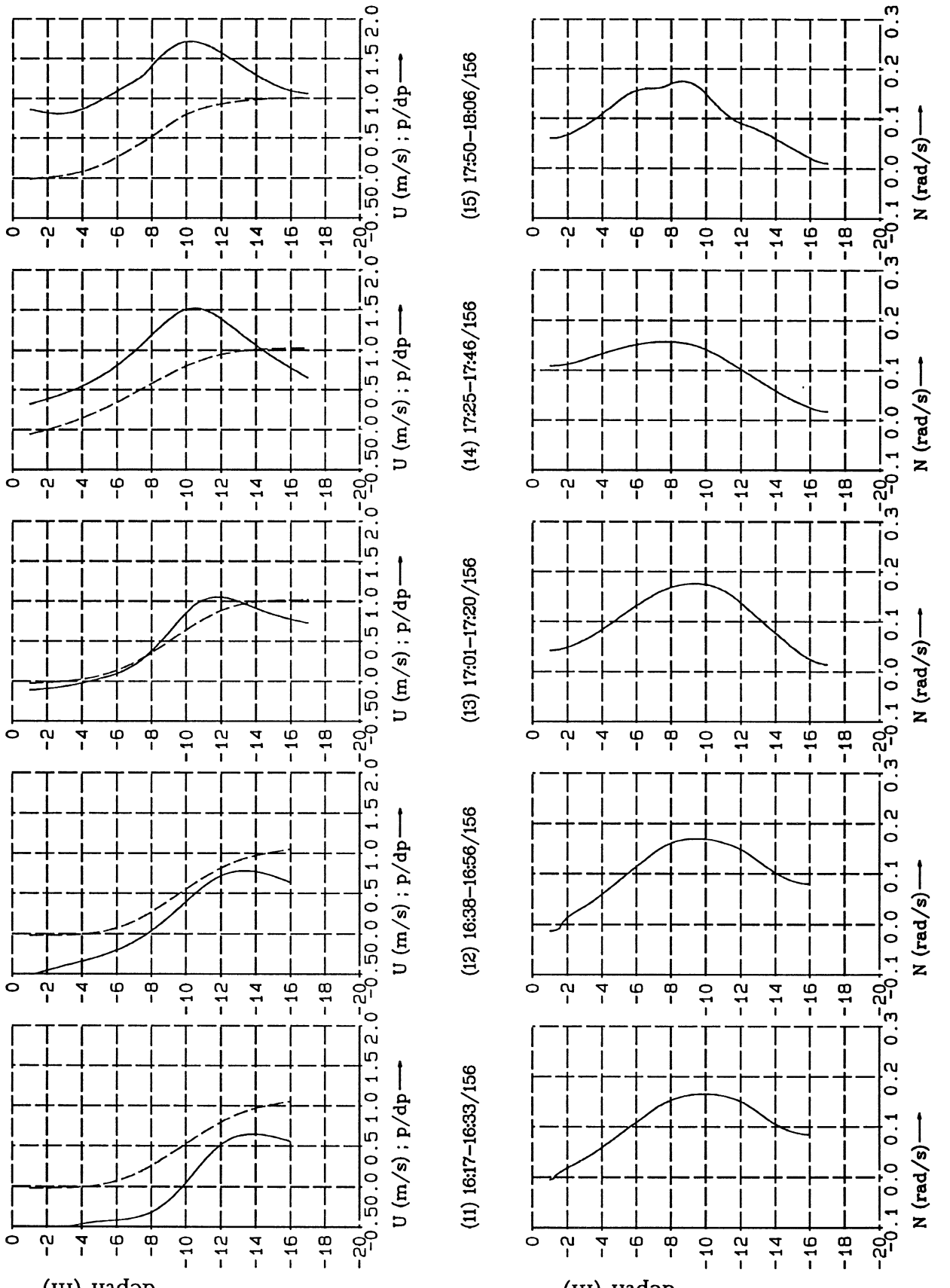

Vertical finescale profiles of |U|, rel. density and Brunt-Vaisaila freq. (RWS).

Profiles 11-15

bv11-15.inv

DELFT HYDRAULICS

Z694

Fig.1[9]

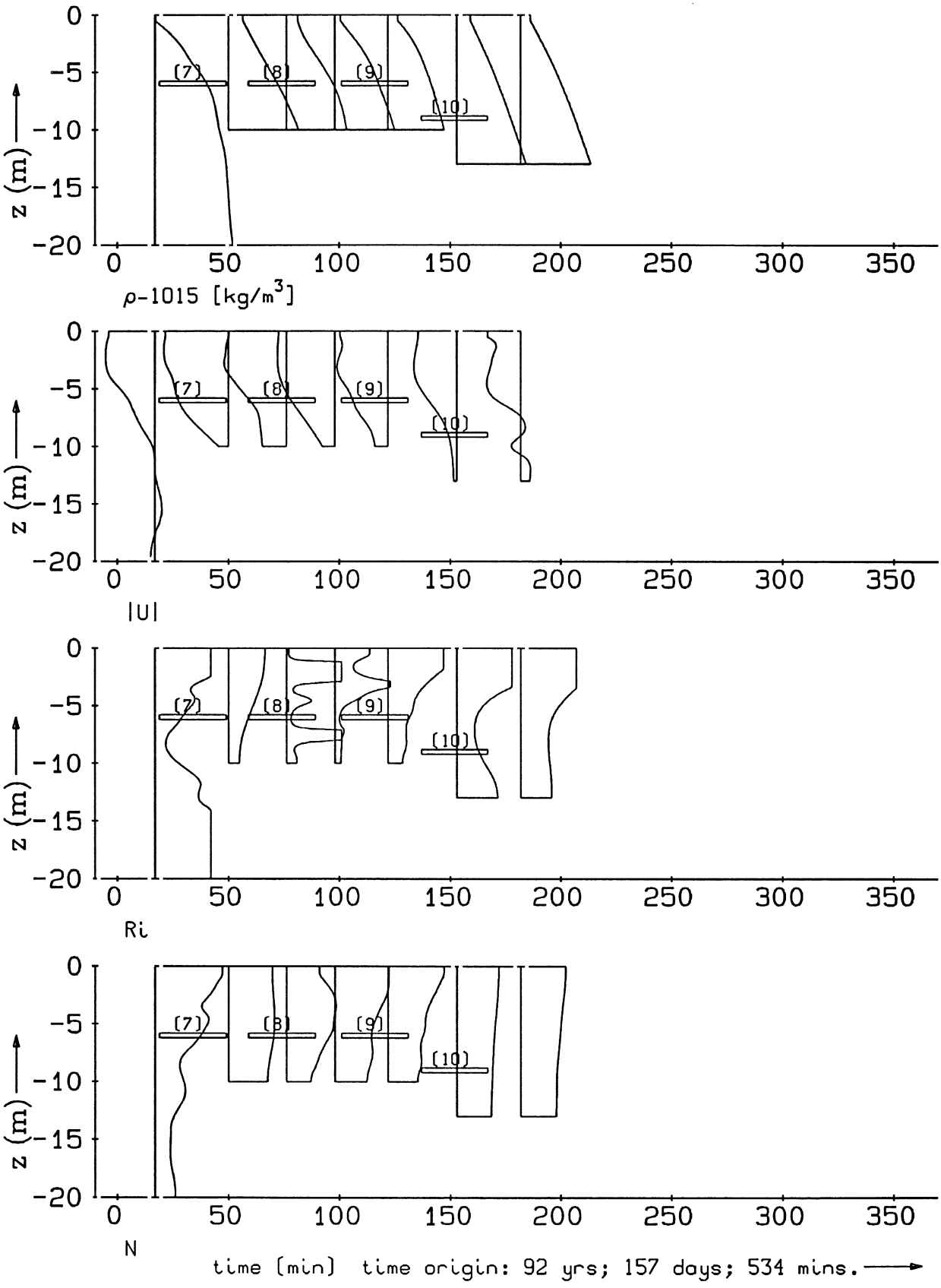

Density, vel. magnitude, Ri-number and buoyancty freq.
Caland channel; day 157 (RWS).

day.157

DELFT HYDRAULICS

Z 722

Fig.2a

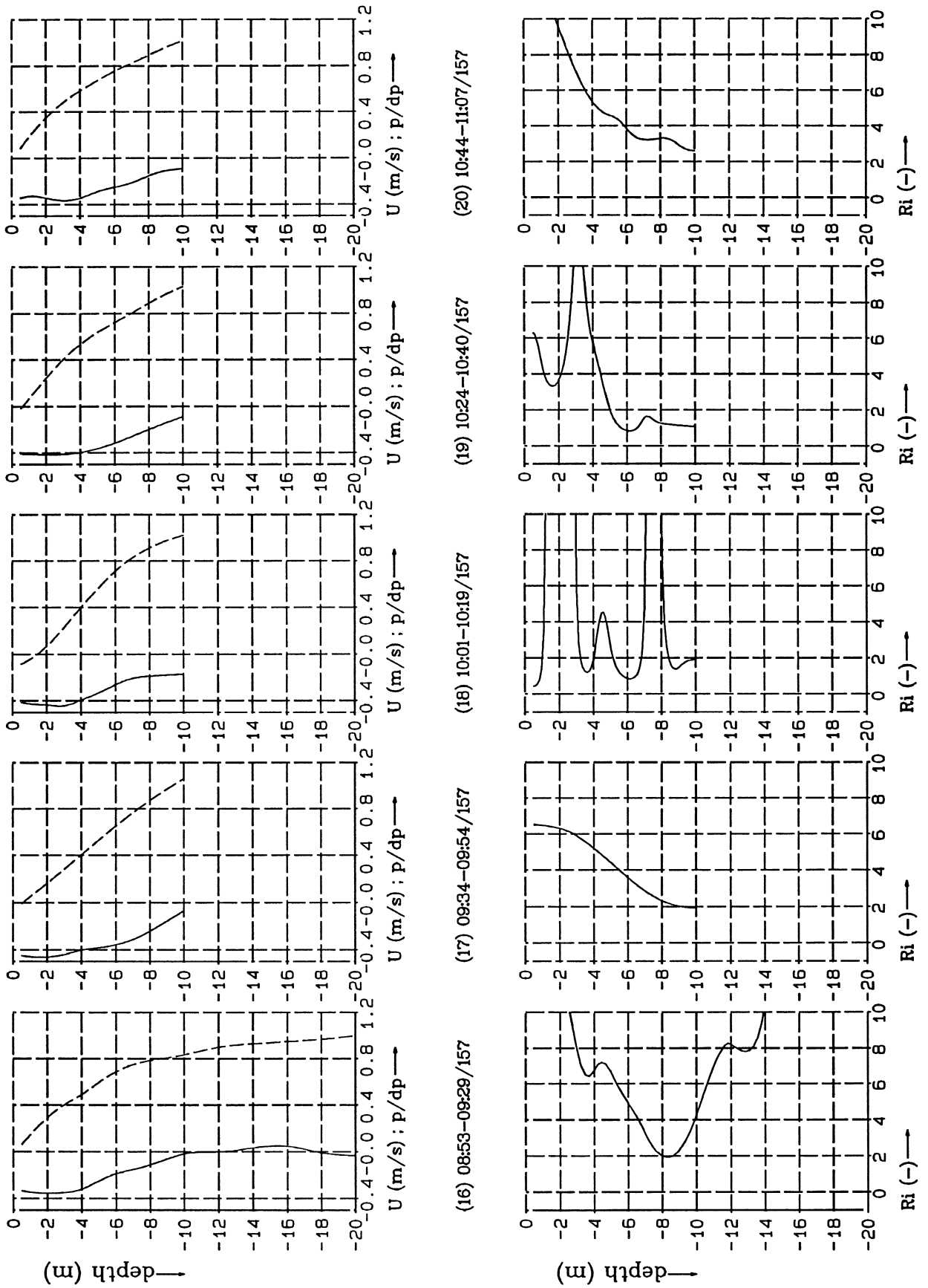

Vertical finescale profiles of |U|, rel. density and Richardson number (RWS).

Profiles 16-20

Ri16-20.inv

DELFT HYDRAULICS

Z694

Fig.2[b]

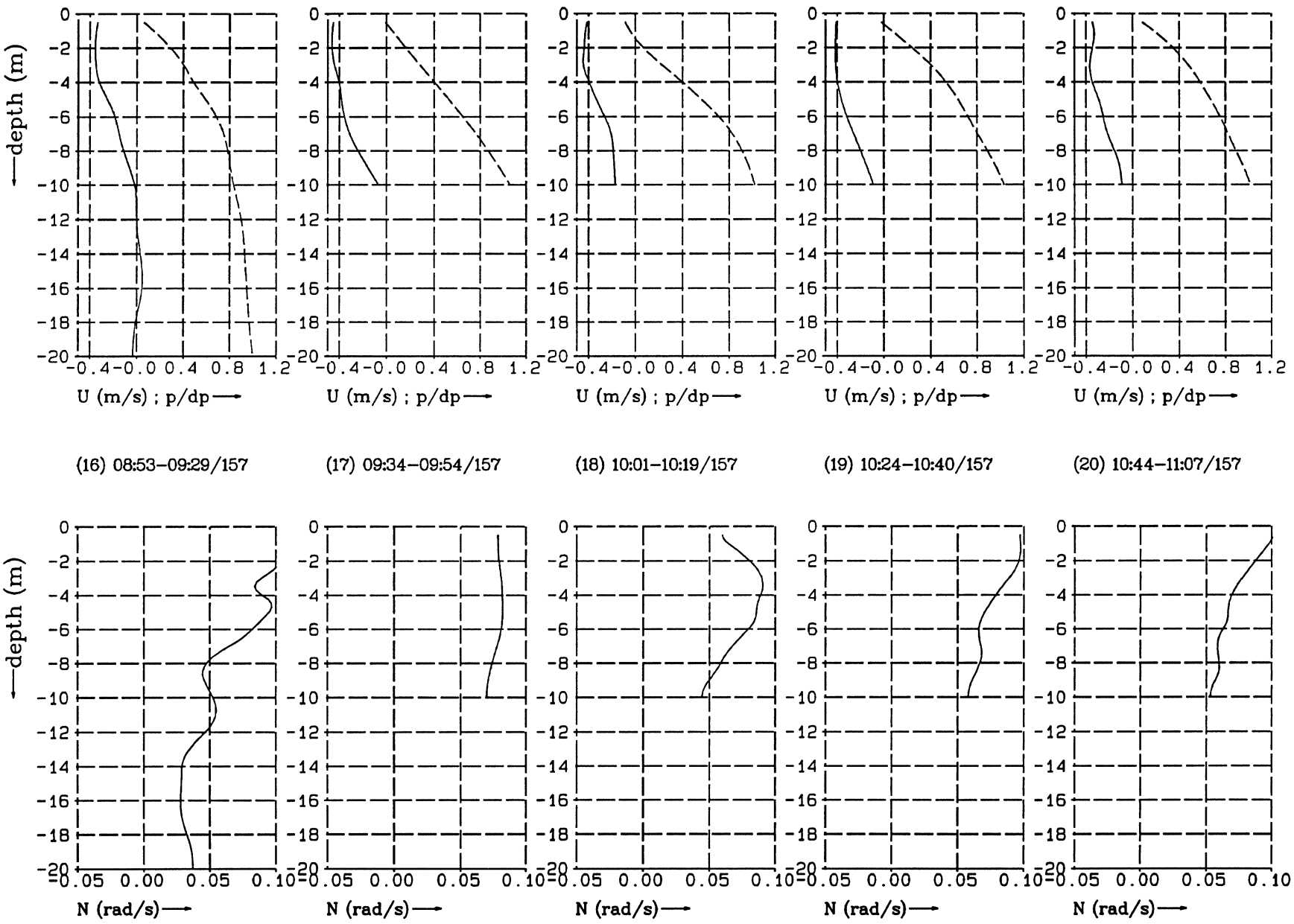

Vertical finescale profiles of |U|, rel. density and Brunt-Vaisala freq. [RMS].

DELFT HYDRAULICS

Z694	bv16-20.inv	Profiles 16-20
Fig.2c		

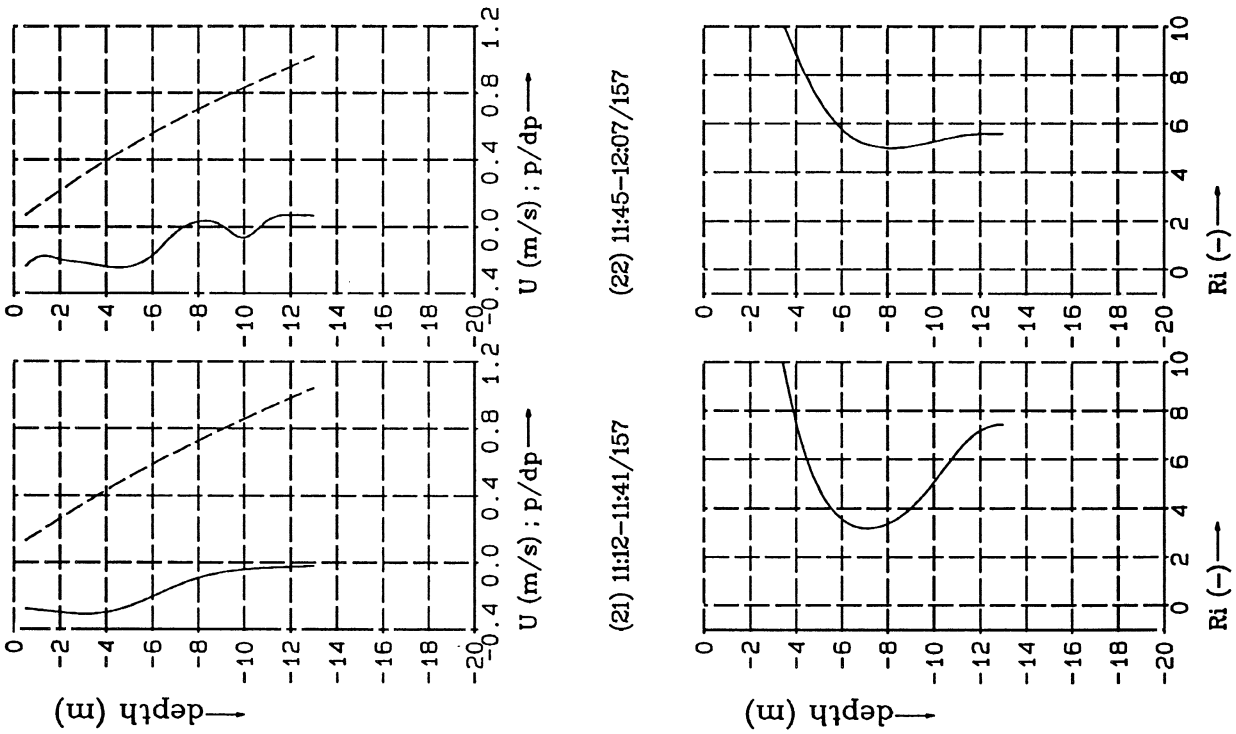

Vertical finescale profiles of |U|, rel. density and Richardson number (RWS).

Profiles 21-22

Ri21-22.inv

DELFT HYDRAULICS

Z694

Fig.2d

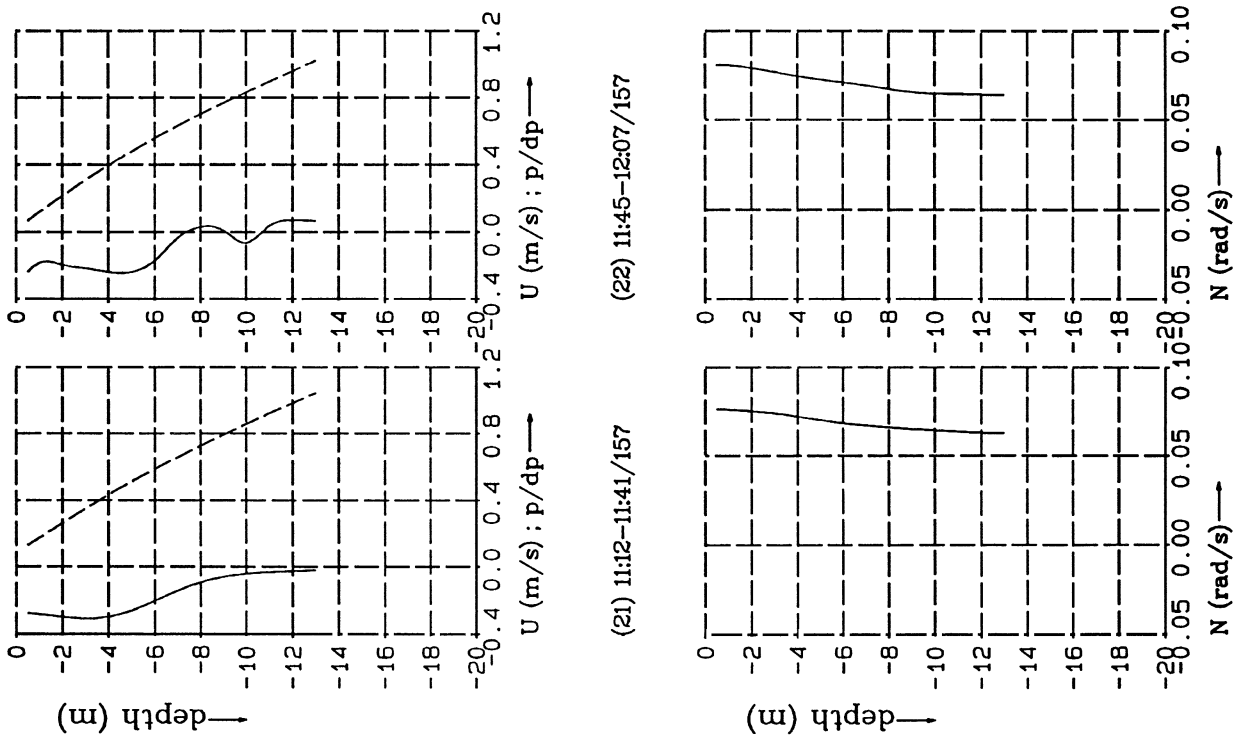

Vertical finescale profiles of |U|, rel. density and Brunt-Vaisaila freq. (RWS).

Profiles 21-22

bv21-22.inv

DELFT HYDRAULICS

Z694

Fig.2e

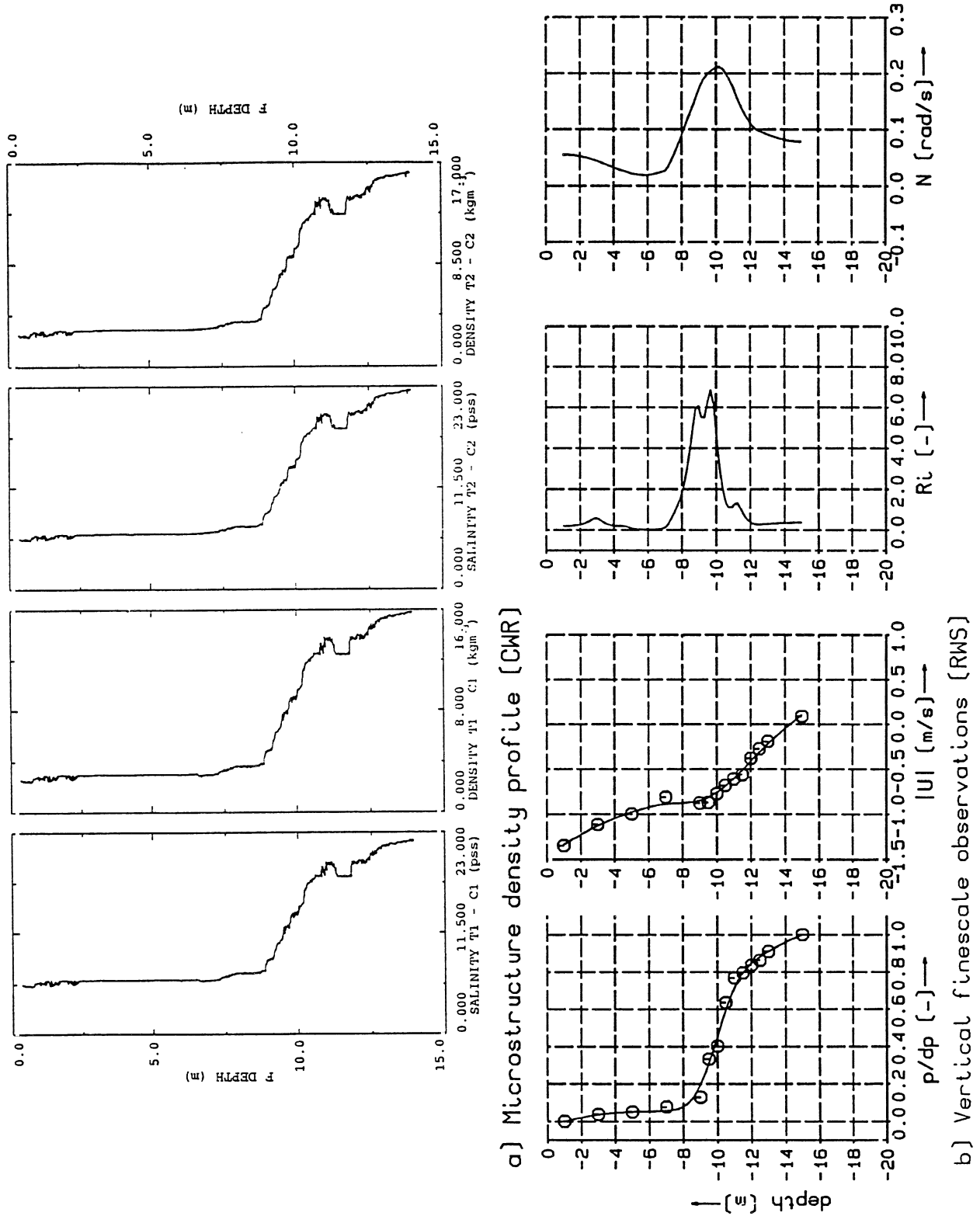

Microstructure density profile in the Rotterdam Waterway and vertical finescale structure.	12:51/156	
	prof 2	
DELFT HYDRAULICS	Z 694	Fig. 3

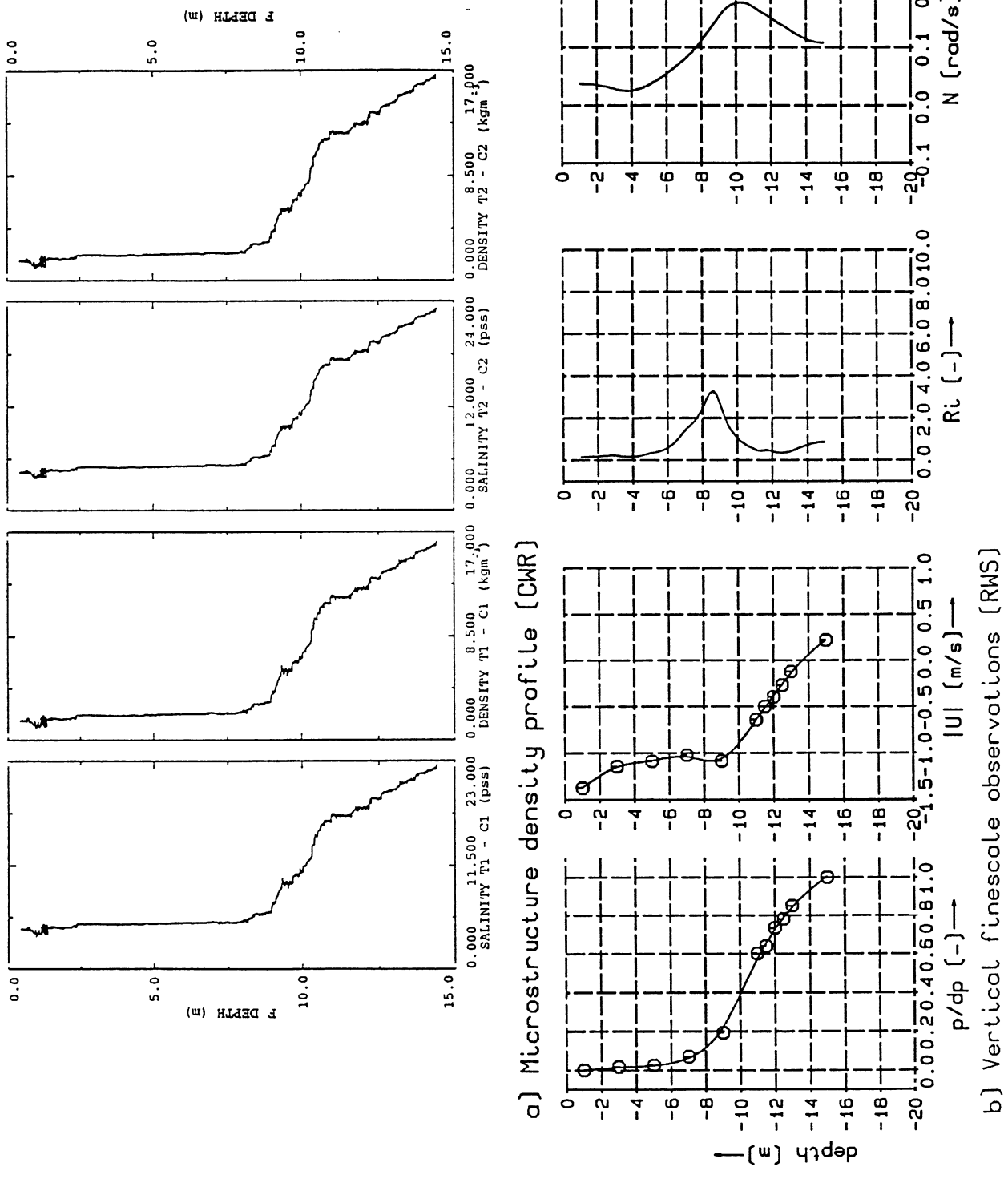

Microstructure density profile in the Rotterdam Waterway and vertical finescale structure.	13:50/156	
	prof 4	
DELFT HYDRAULICS	Z 694	Fig. 4

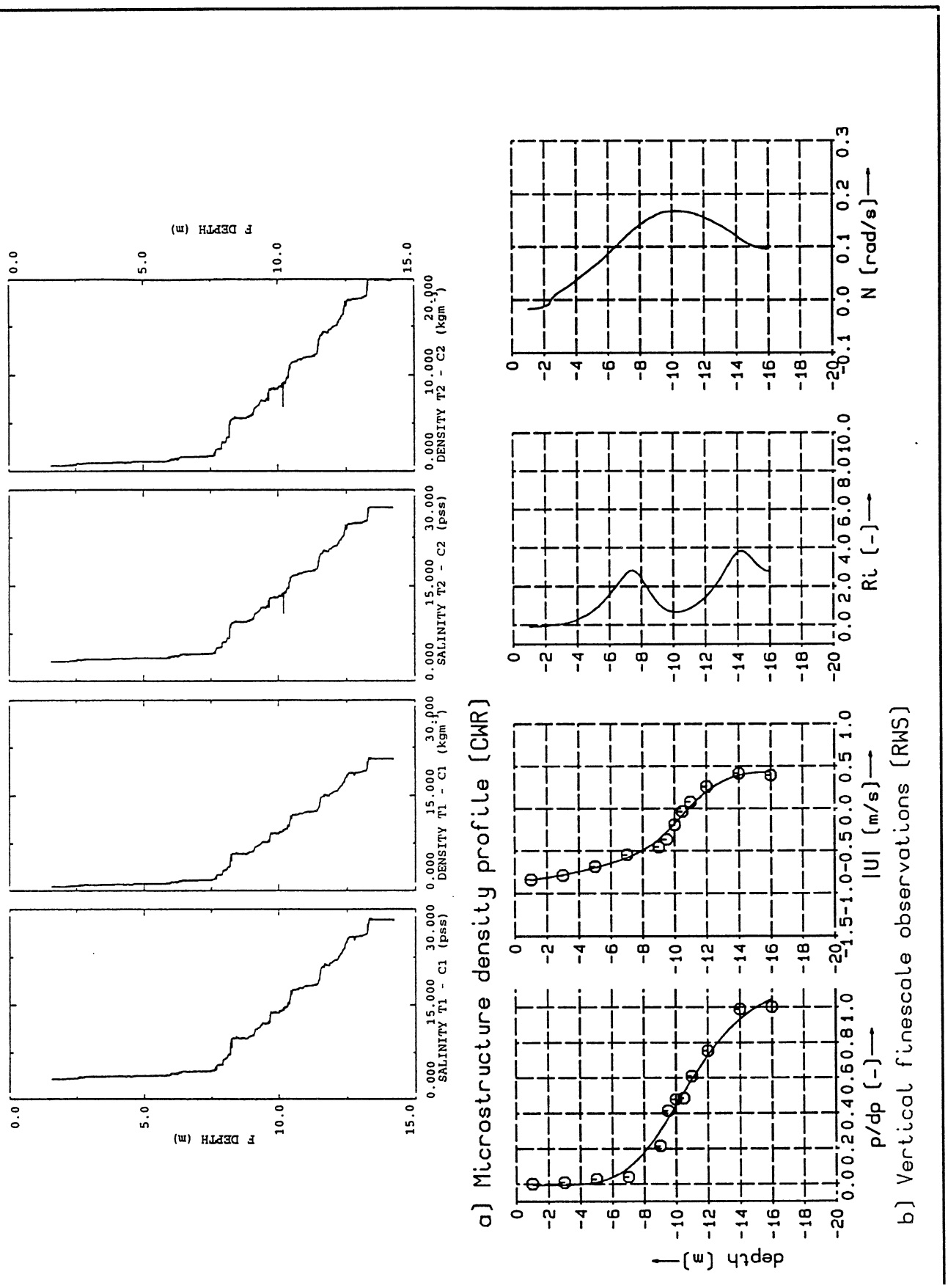

Microstructure density profile in the Rotterdam Waterway and vertical finescale structure.	16:13/156	
	prof 10	
DELFT HYDRAULICS	Z 694	Fig. 5

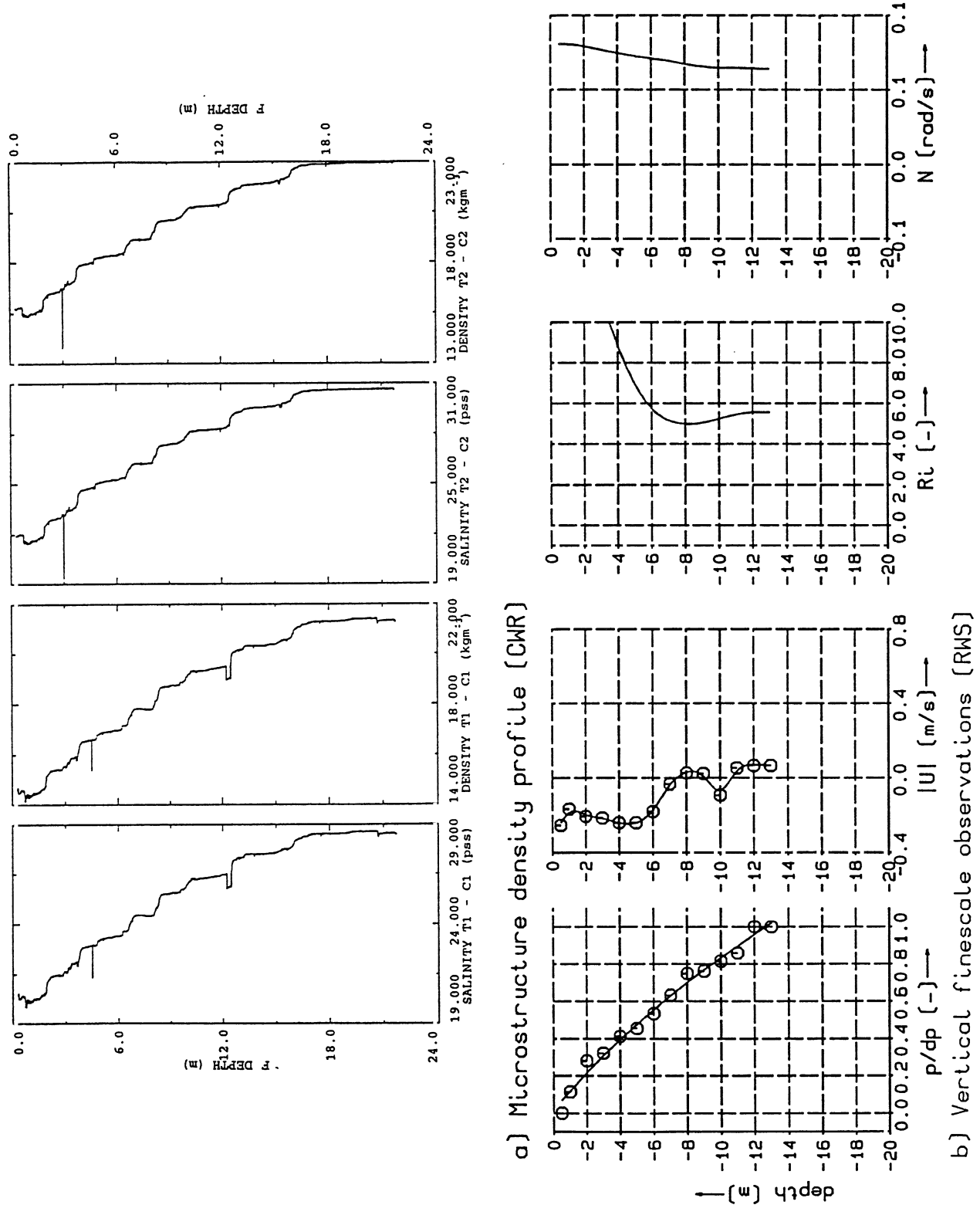

Microstructure density profile in the Rotterdam Waterway and vertical finescale structure.	11:46/157	
	prof 22	
DELFT HYDRAULICS	Z 694	Fig. 6

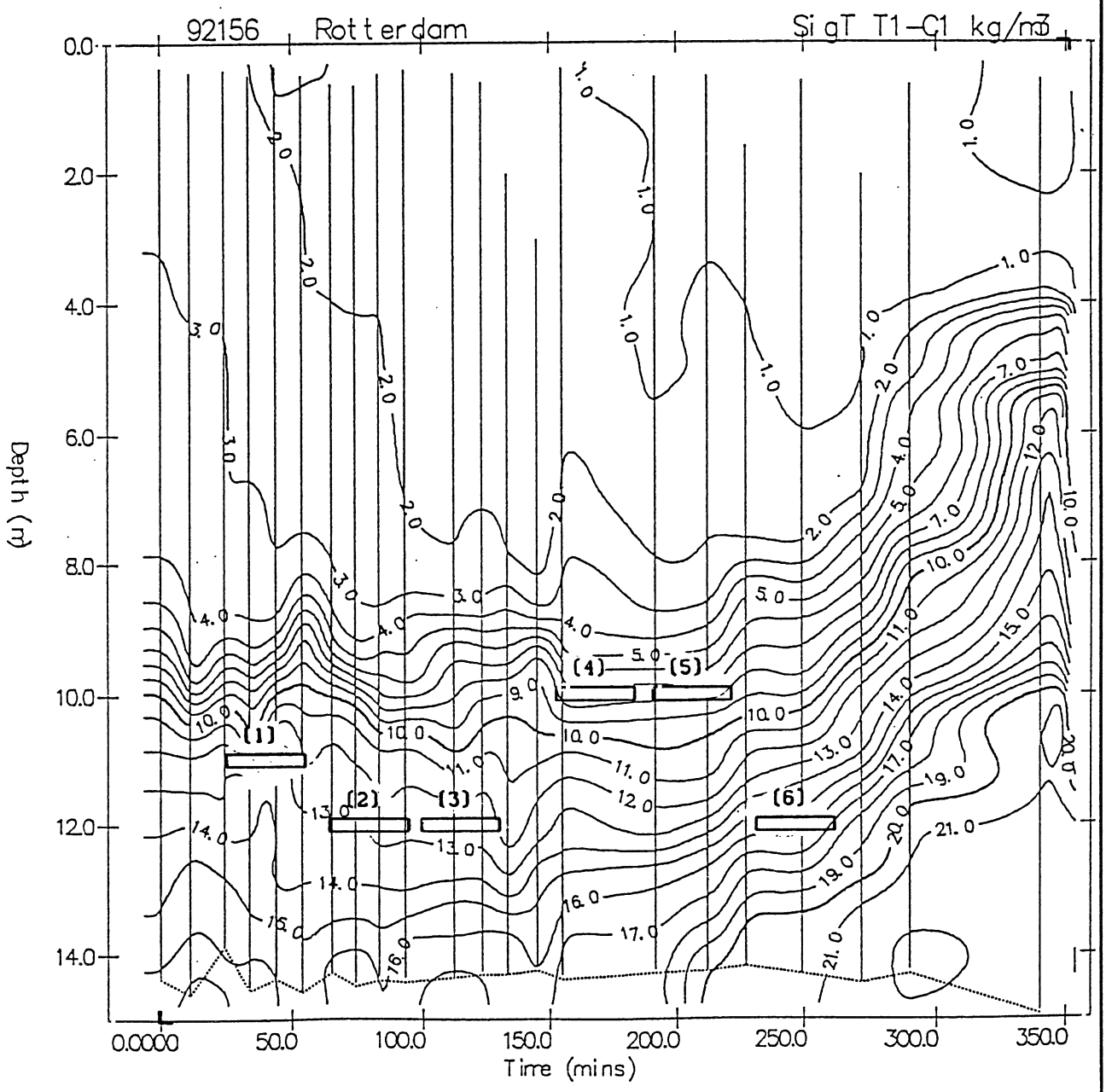

Density isolines. Rotterdam Waterway (CWR) on day 156.

DELFT HYDRAULICS | Z 694 | Fig. 7

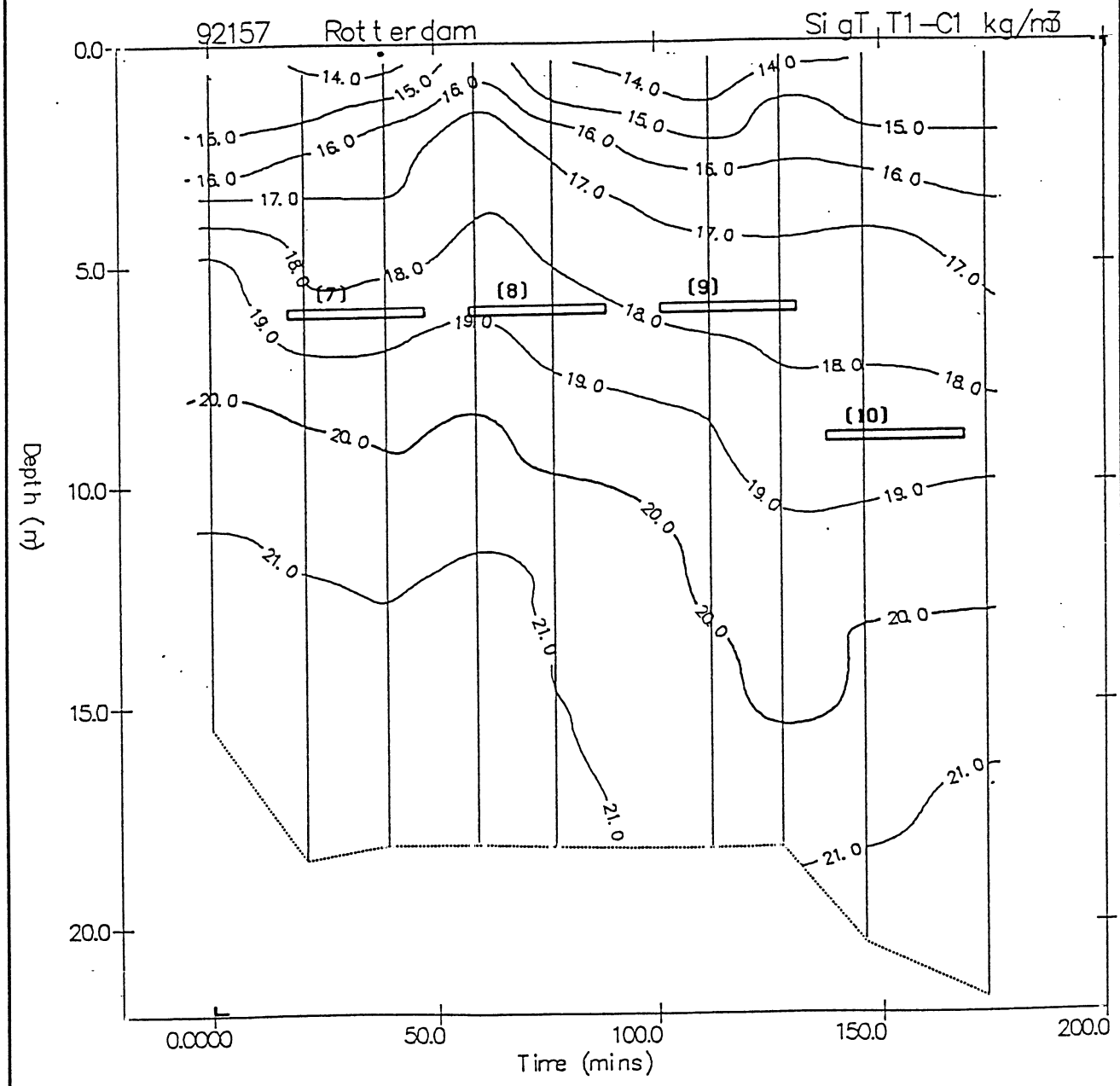

Density isolines. Calland channel (CWR) on day 157.

DELFT HYDRAULICS | Z 694 | Fig. 8

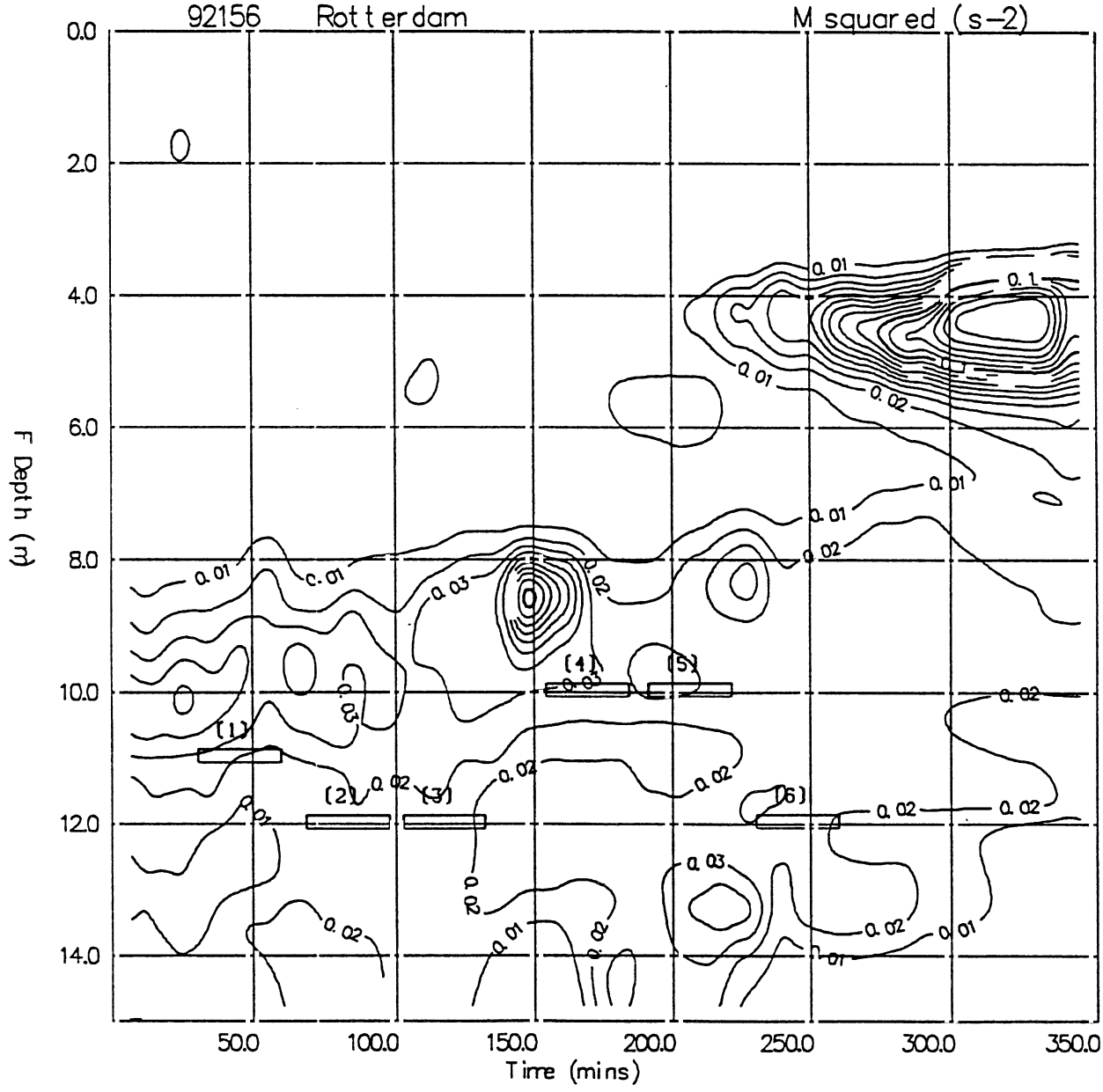

Buoyancy frequency squared. Rotterdam Waterway on day 156 [CWR].

DELFT HYDRAULICS | Z 694 | Fig.9a

Time origin: 92 yrs;156 days;746 mins.

Ri [-]

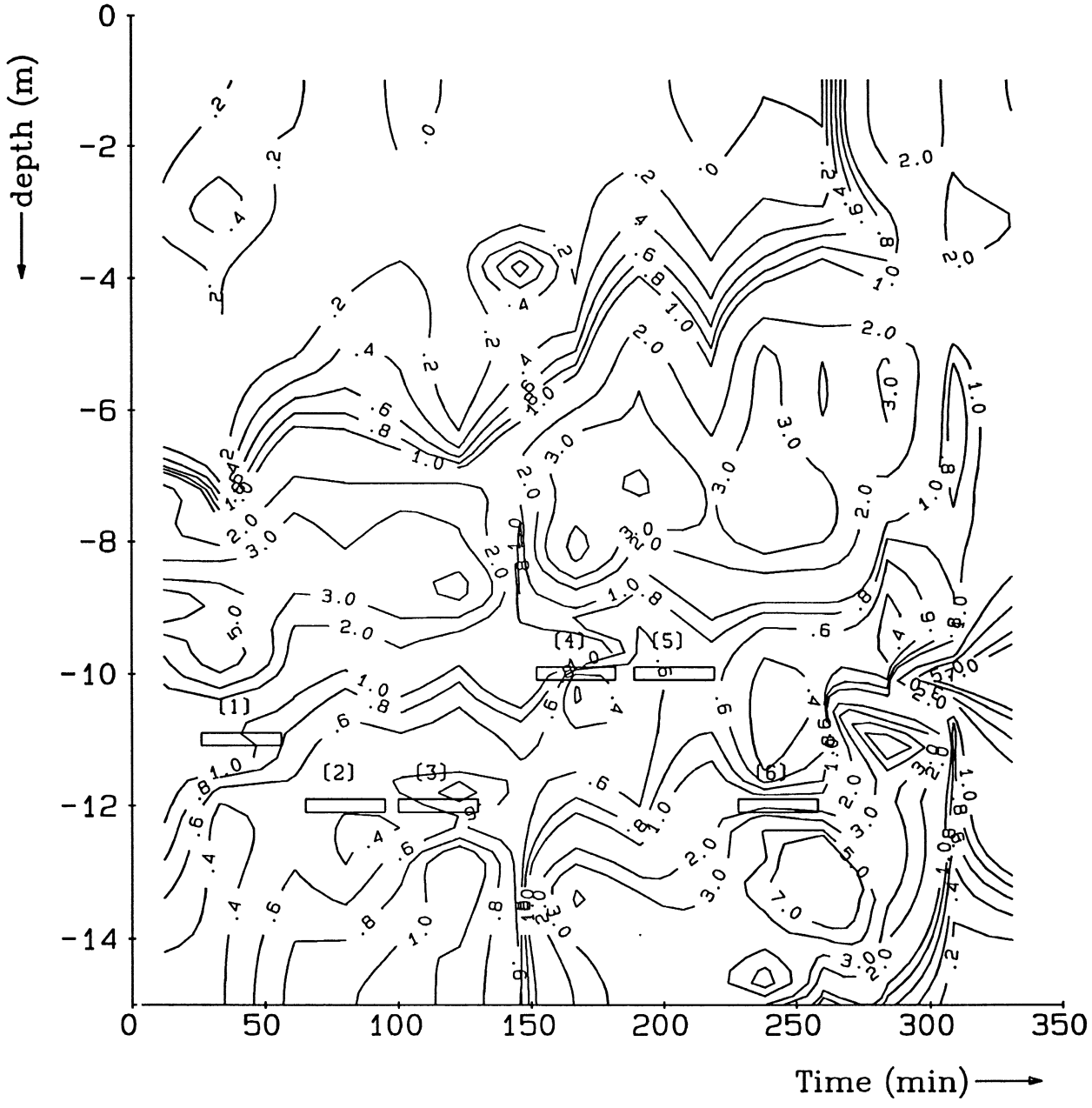

Gradient Richardson number. Rotterdam Waterway on day 156 (RWS).

ri156.iso

DELFT HYDRAULICS

Z 694

Fig.9b

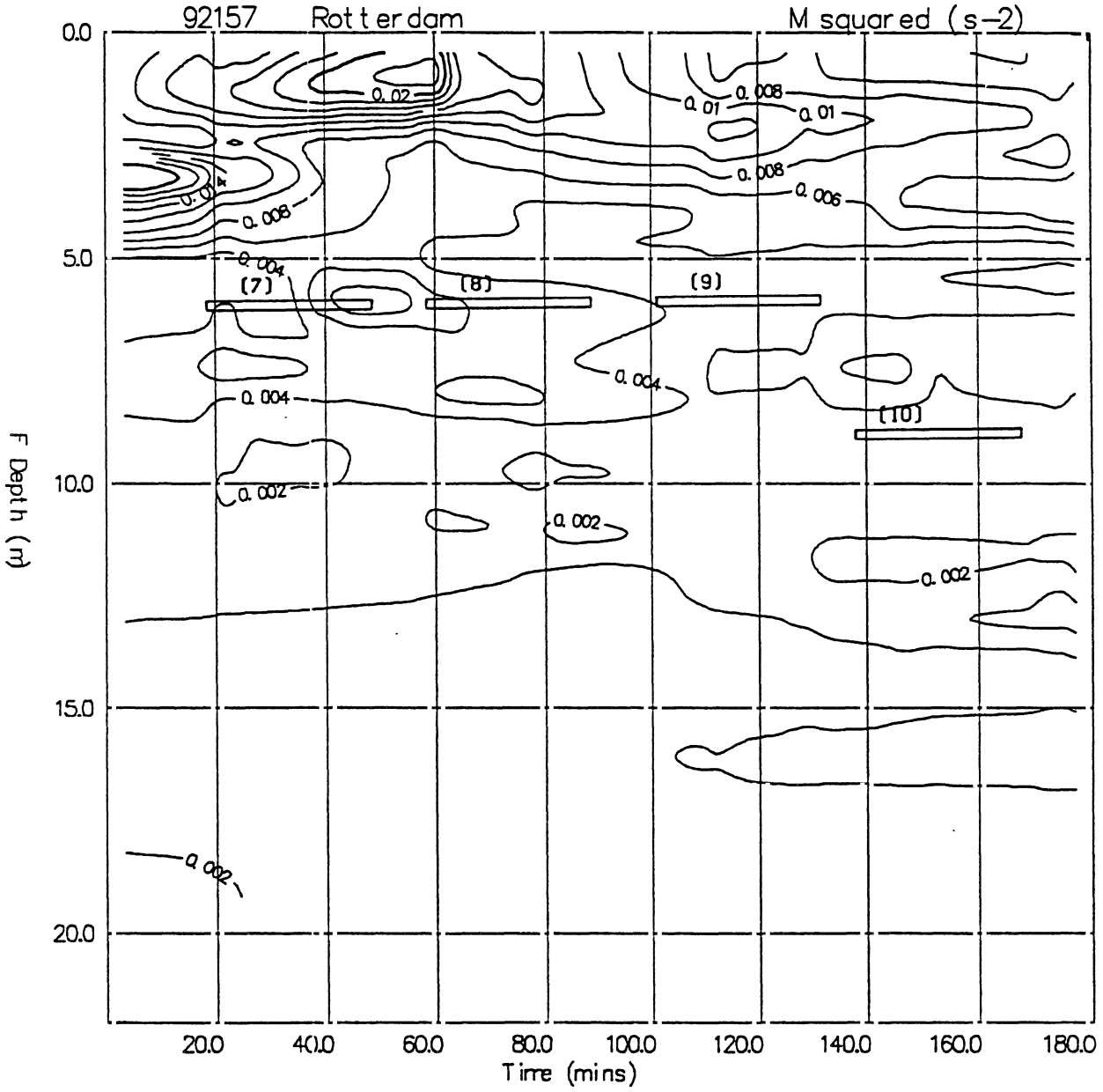

Buoyancy frequency squared. Caland channel on day 157 (CWR).

DELFT HYDRAULICS | Z 694 | Fig. 10a

time origin: 92 yrs;157 days;534 mins.

Ri [-]

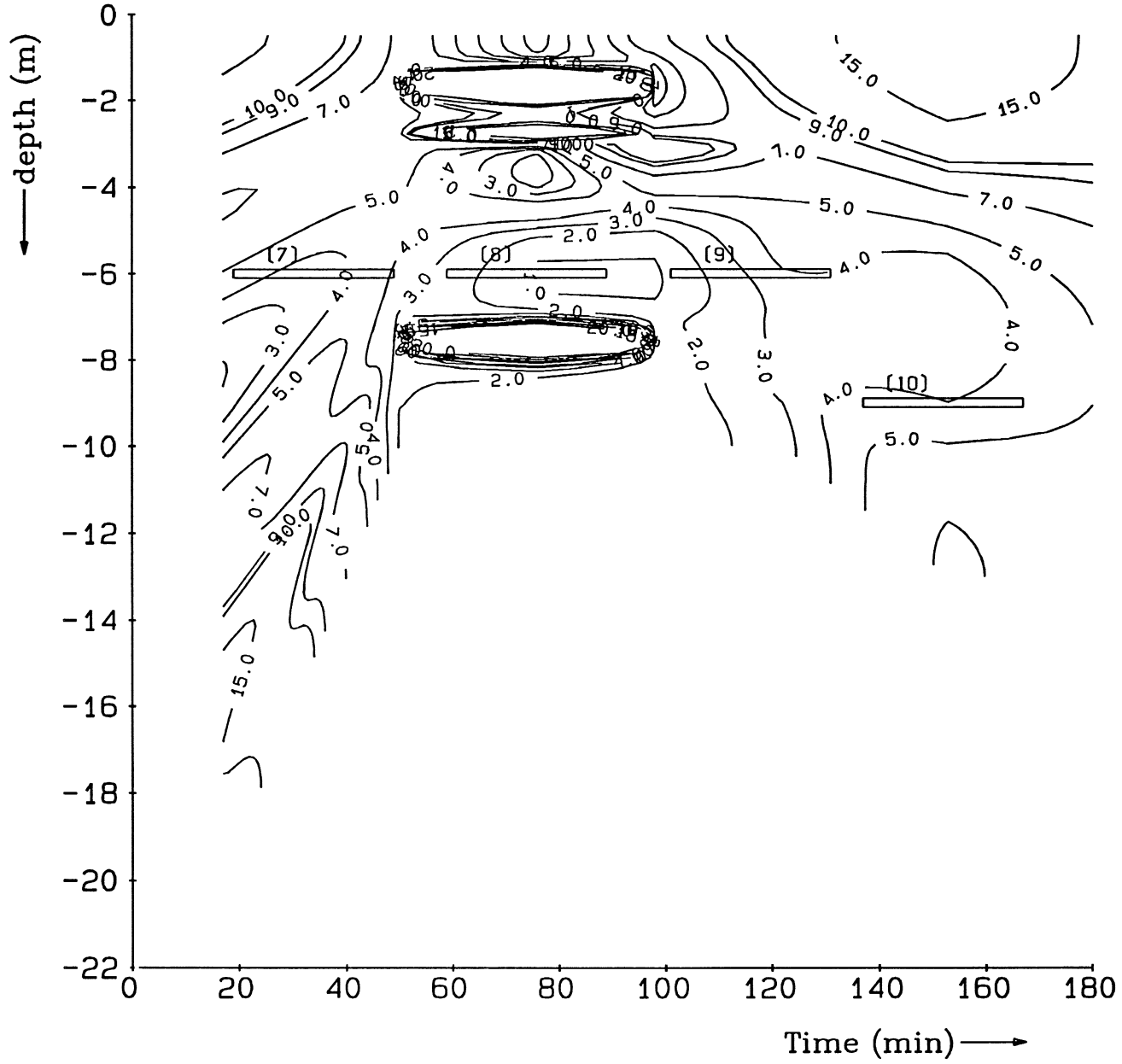

Gradient Richardson number. Caland channel on day 157 [RWS].

ri157.iso

DELFT HYDRAULICS

Z 694

Fig.10[b]

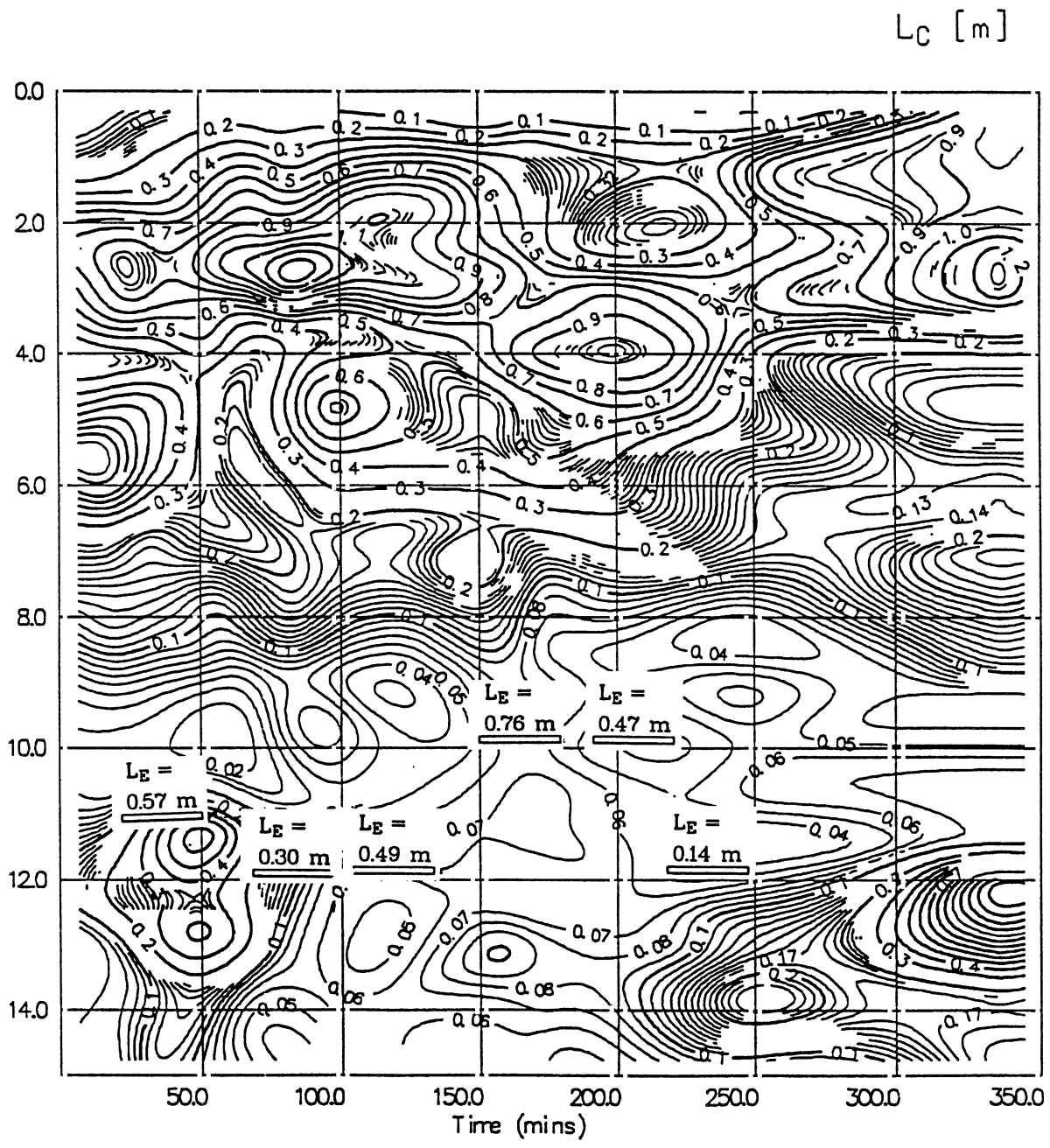

Centered displacement scale L_C. Rotterdam Waterway on day 156 (CWR).

DELFT HYDRAULICS | Z 694 | Fig.11

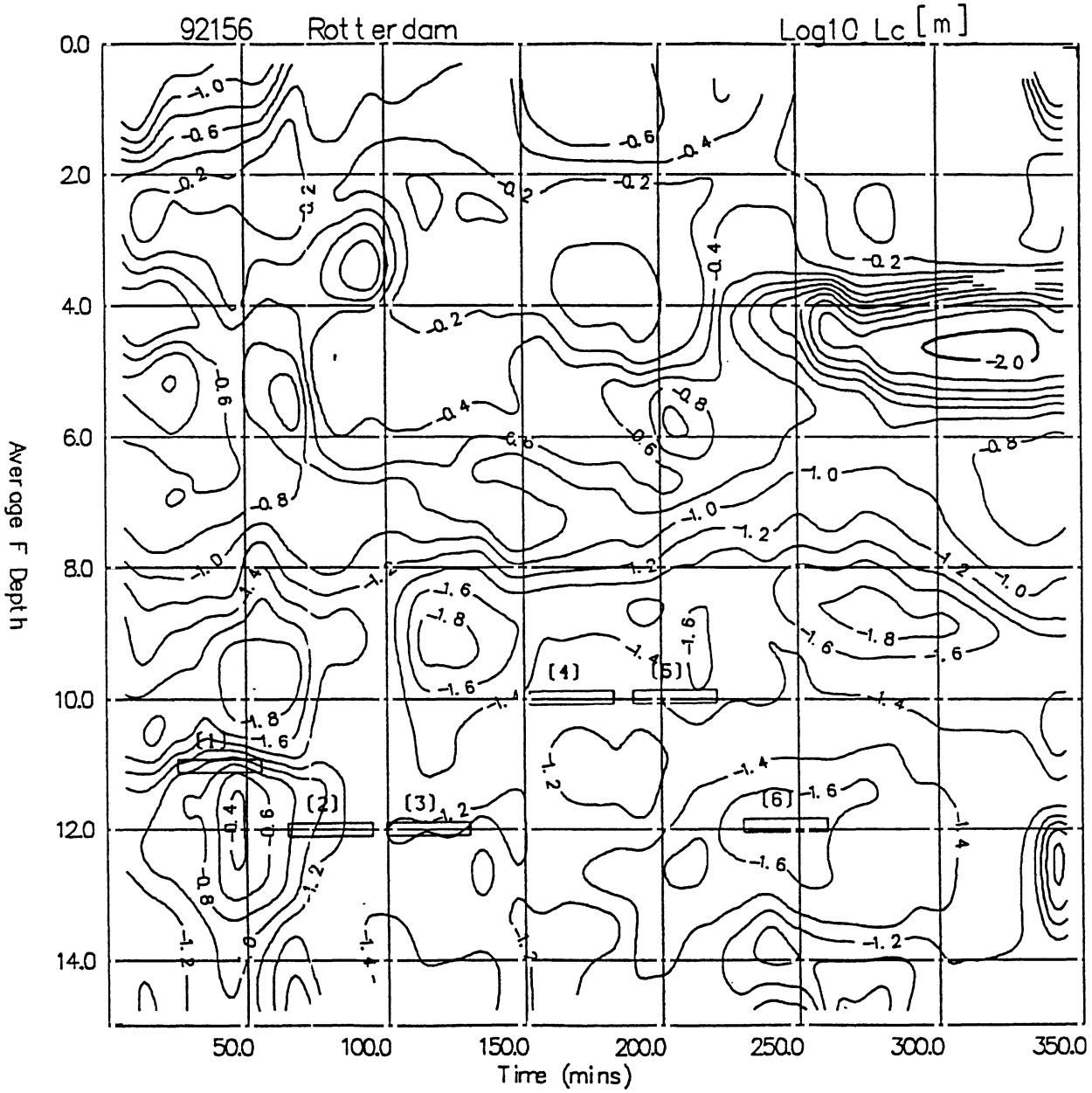

Centered displacement scale L_C. Rotterdam Waterway on day 156 (CWR).

DELFT HYDRAULICS | Z 694 | Fig.12

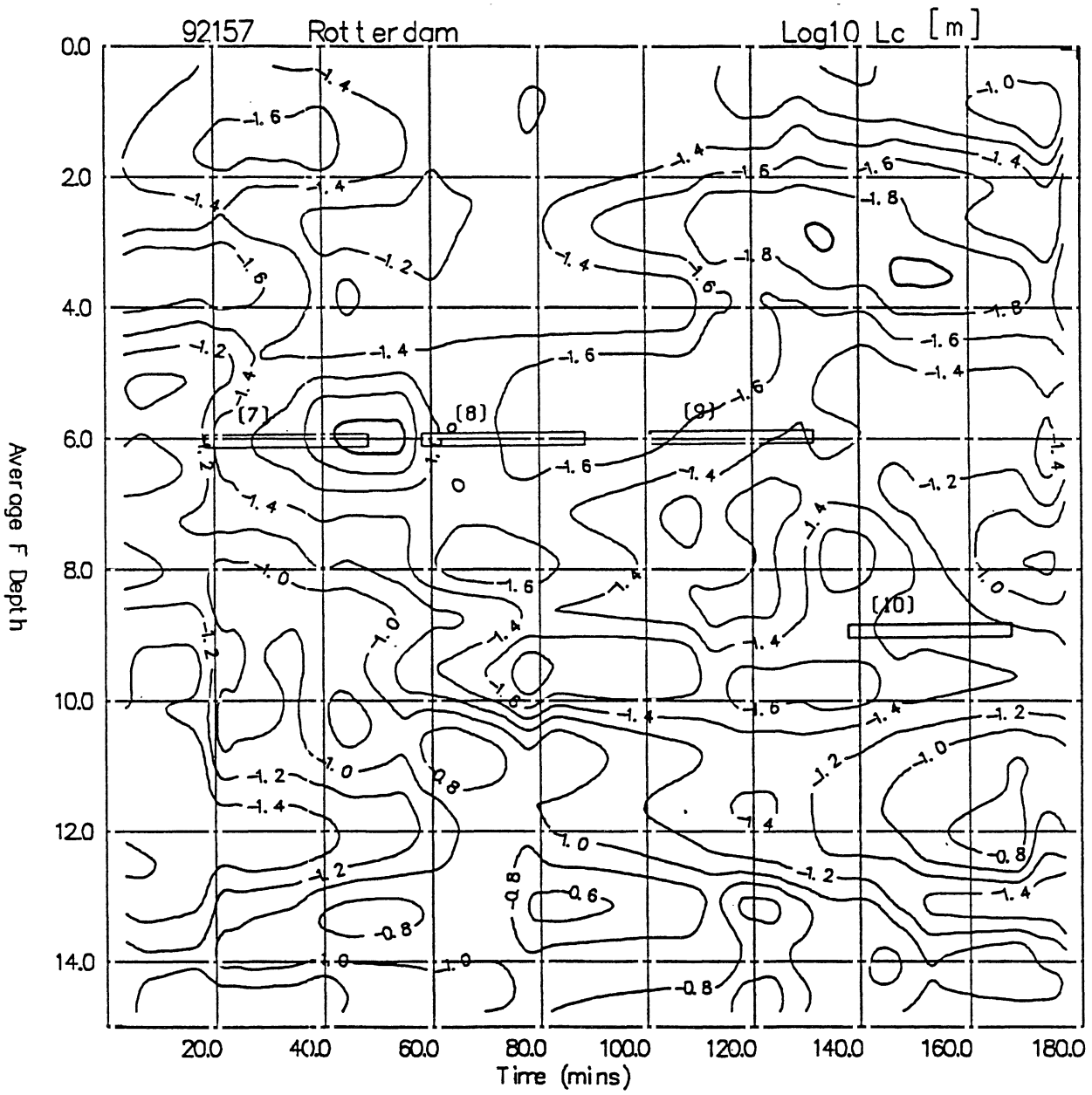

Centered displacement scale L_C. Caland channel on day 157 (CWR).

DELFT HYDRAULICS | Z 694 | Fig.13

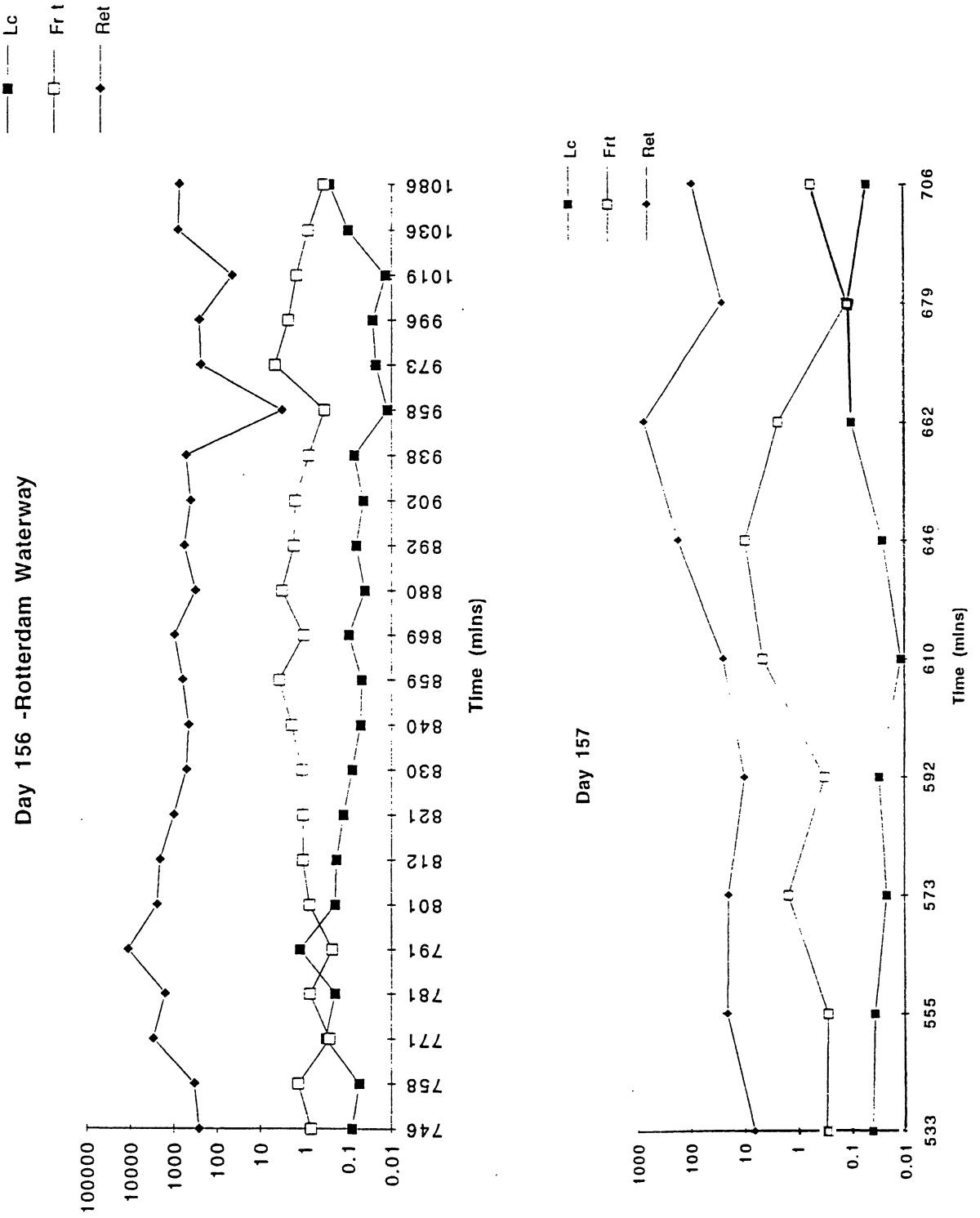

L_C, L_E, Fr_T and Re_T at or near the platform.
Rotterdam Waterway and Caland channel (CWR).

DELFT HYDRAULICS | Z 694 | Fig.14

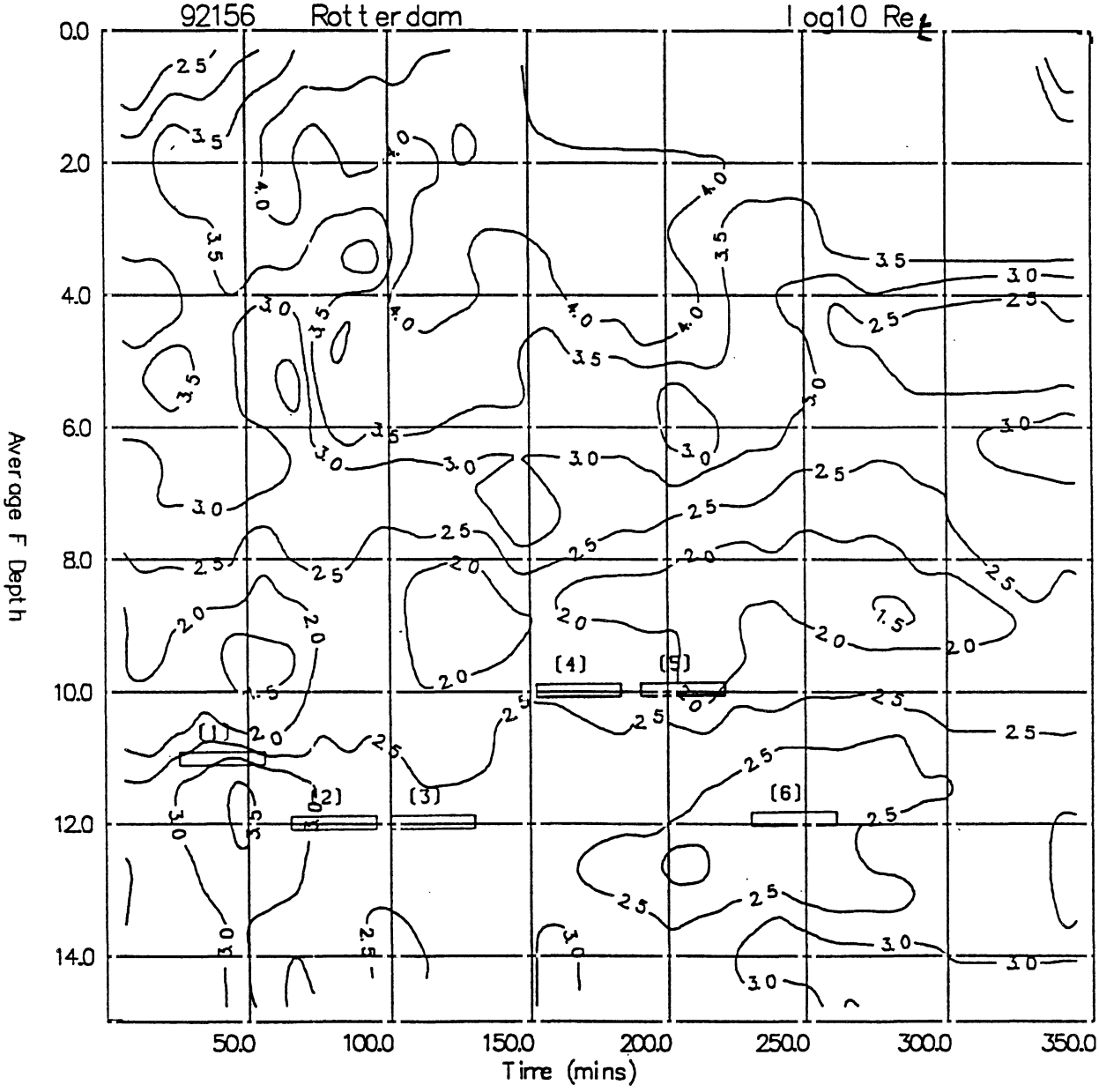

Turbulent Reynolds number Re_T.
Rotterdam Waterway (CWR).

DELFT HYDRAULICS | Z 694 | Fig.15

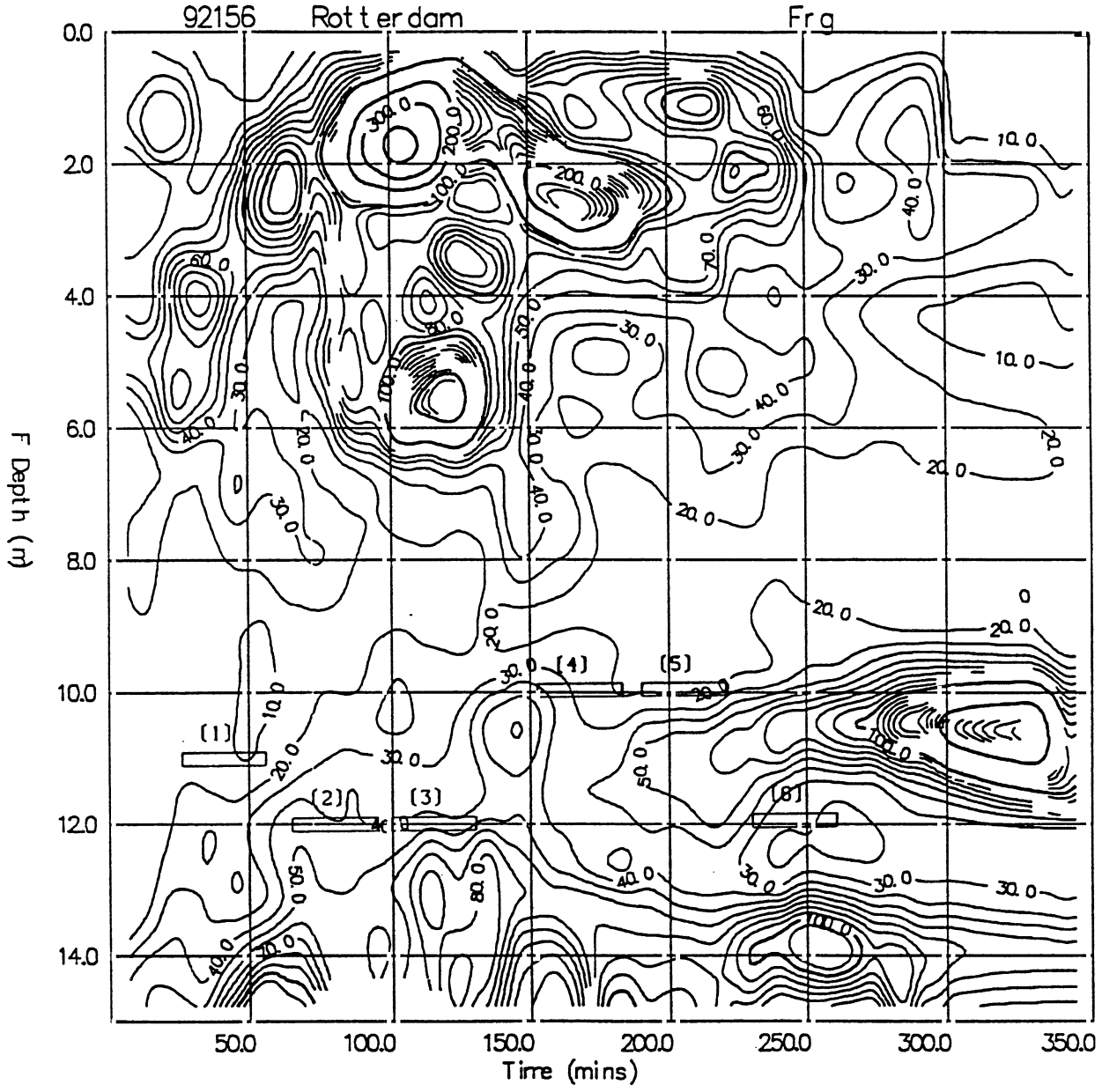

Small-scale Froude number Frg.
Rotterdam Waterway [CWR].

DELFT HYDRAULICS | Z 694 | Fig.16

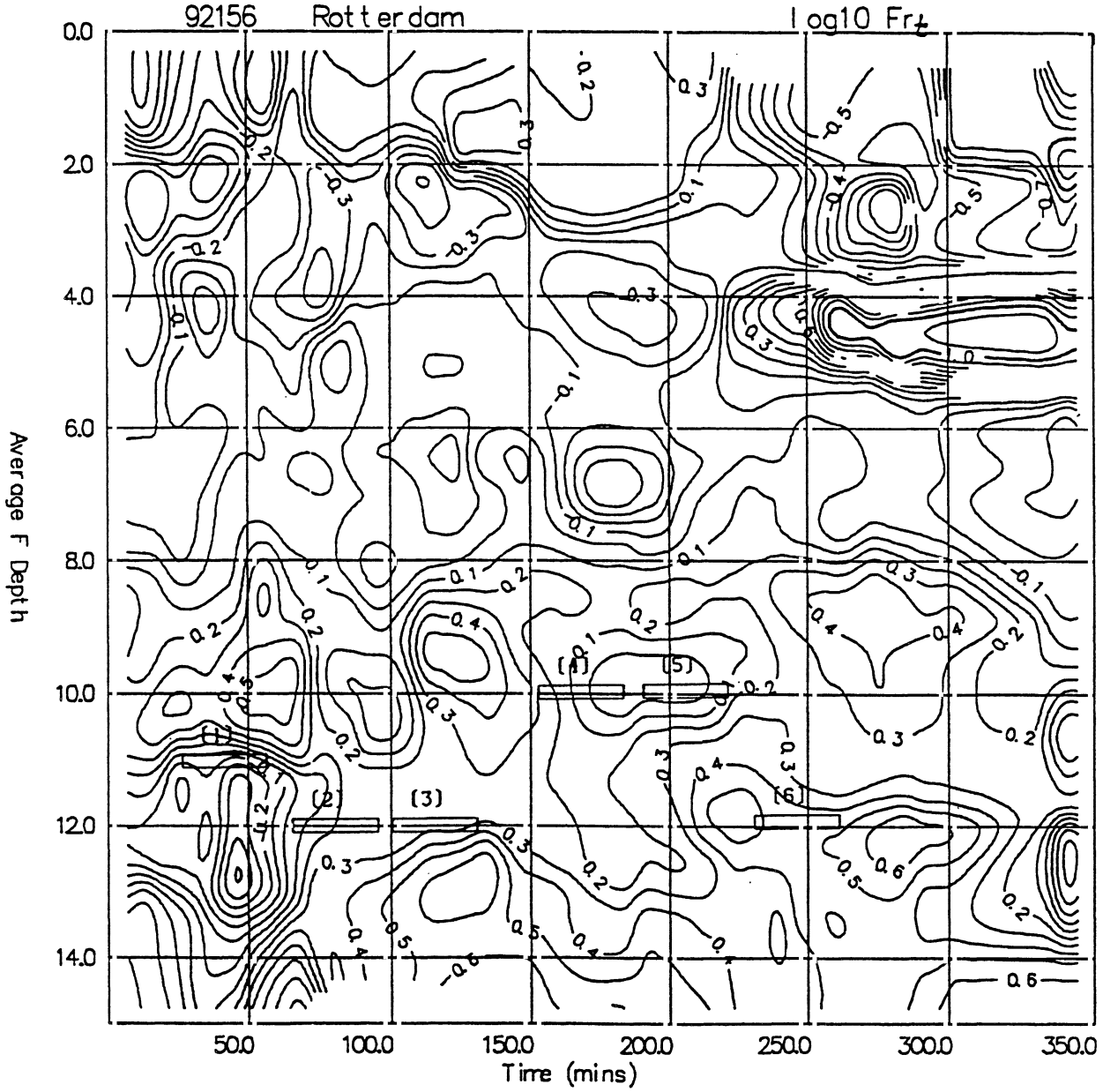

Turbulent Froude number Fr_I.
Rotterdam Waterway (CWR).

DELFT HYDRAULICS | Z 694 | Fig.17

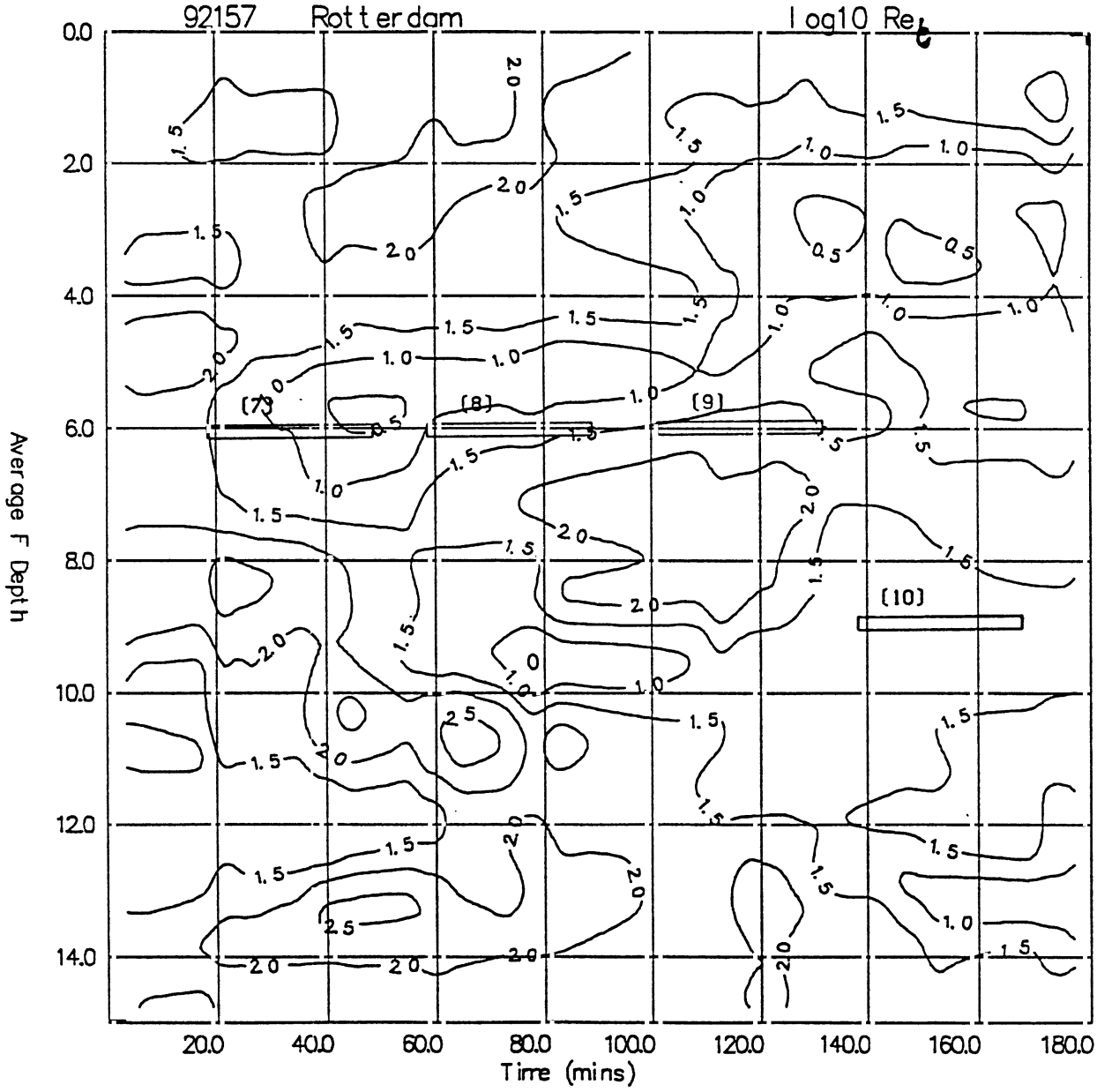

Turbulent Reynolds number Re_T.

Caland channel [CWR].

DELFT HYDRAULICS | Z 694 | Fig.18

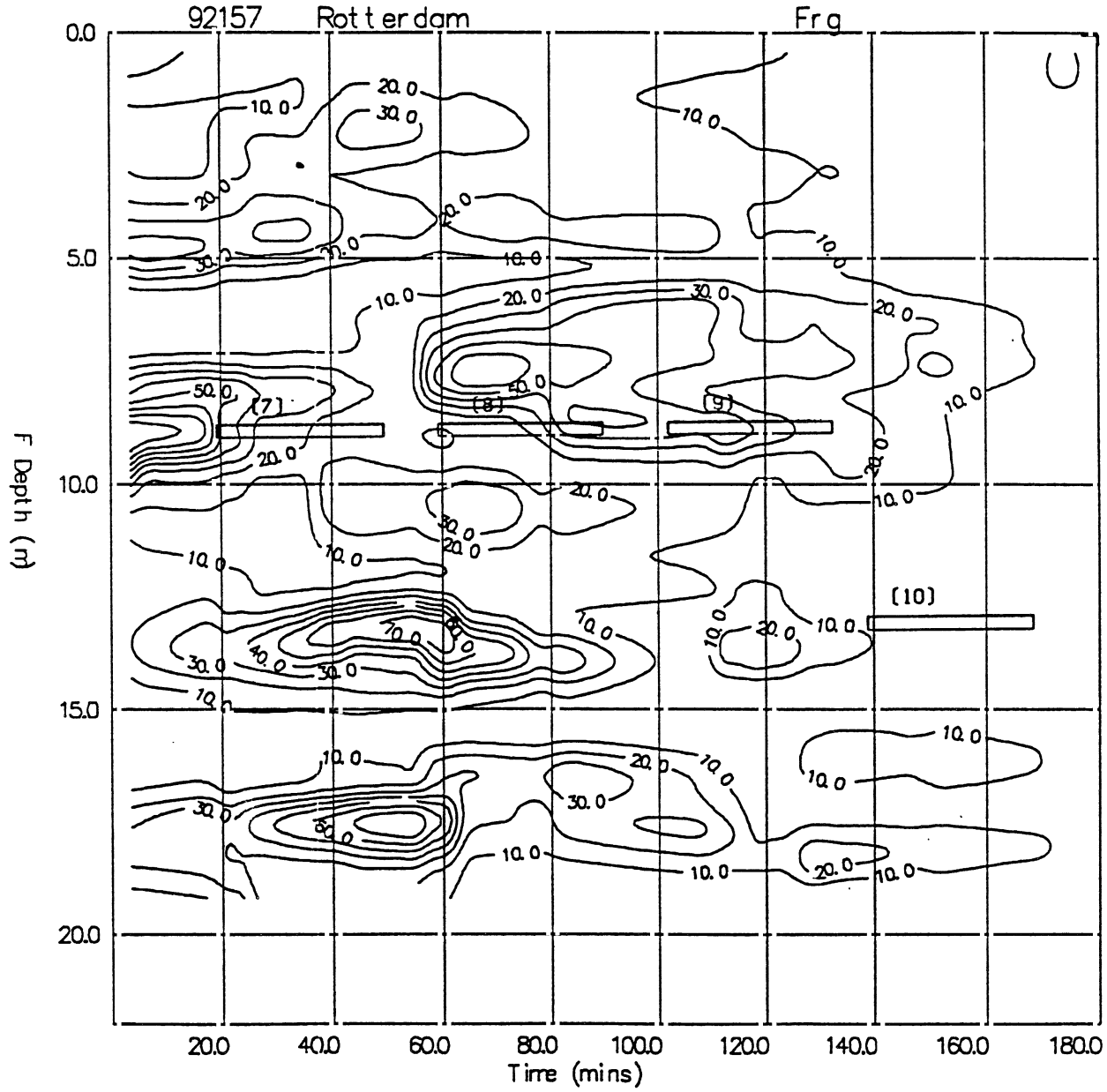

Small-scale Froude number Fr_g.
Caland channel [CWR].

DELFT HYDRAULICS | Z 694 | Fig.19

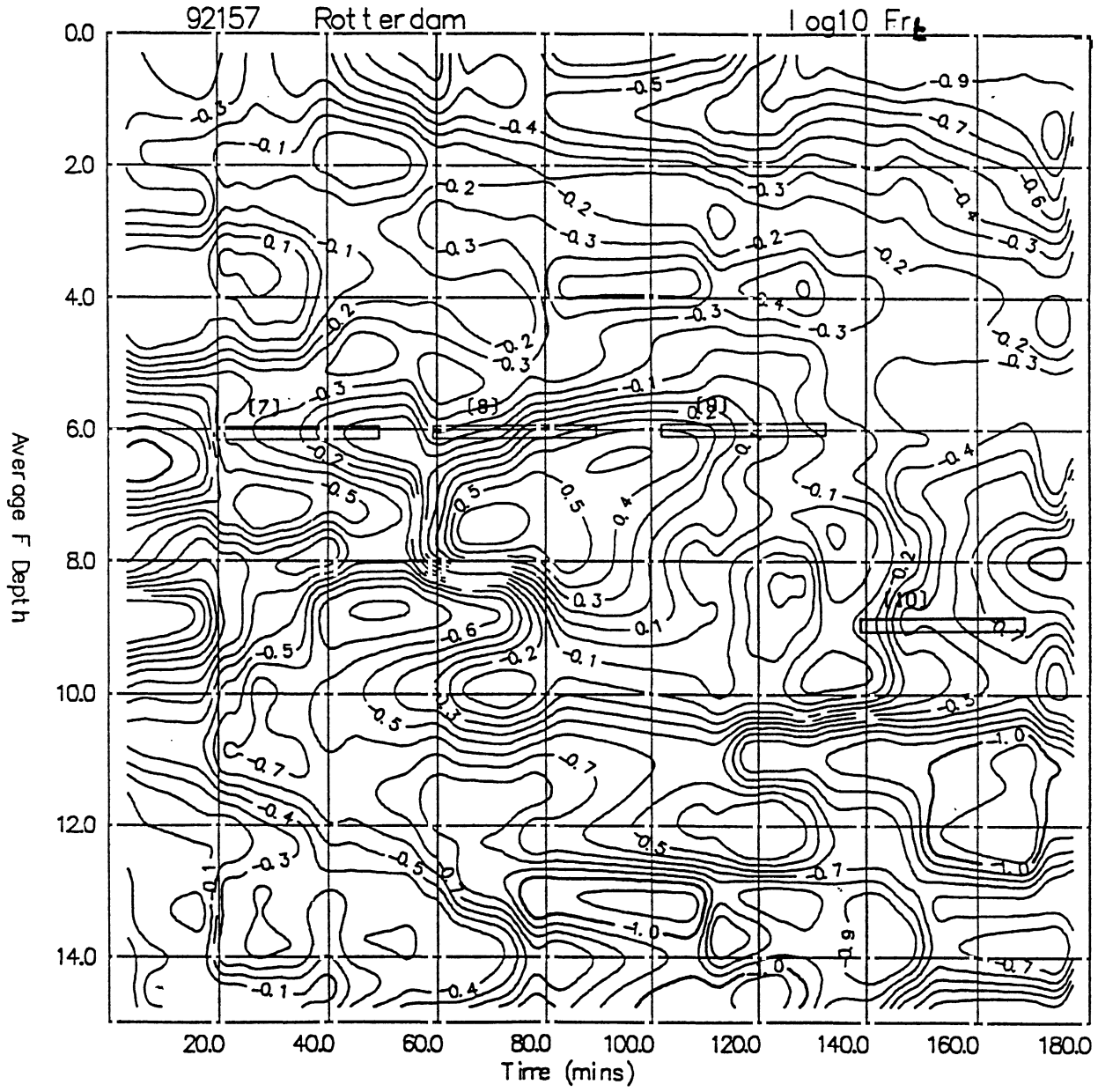

Turbulent Froude number Fr_T.

Caland channel [CWR].

DELFT HYDRAULICS | Z 694 | Fig.20

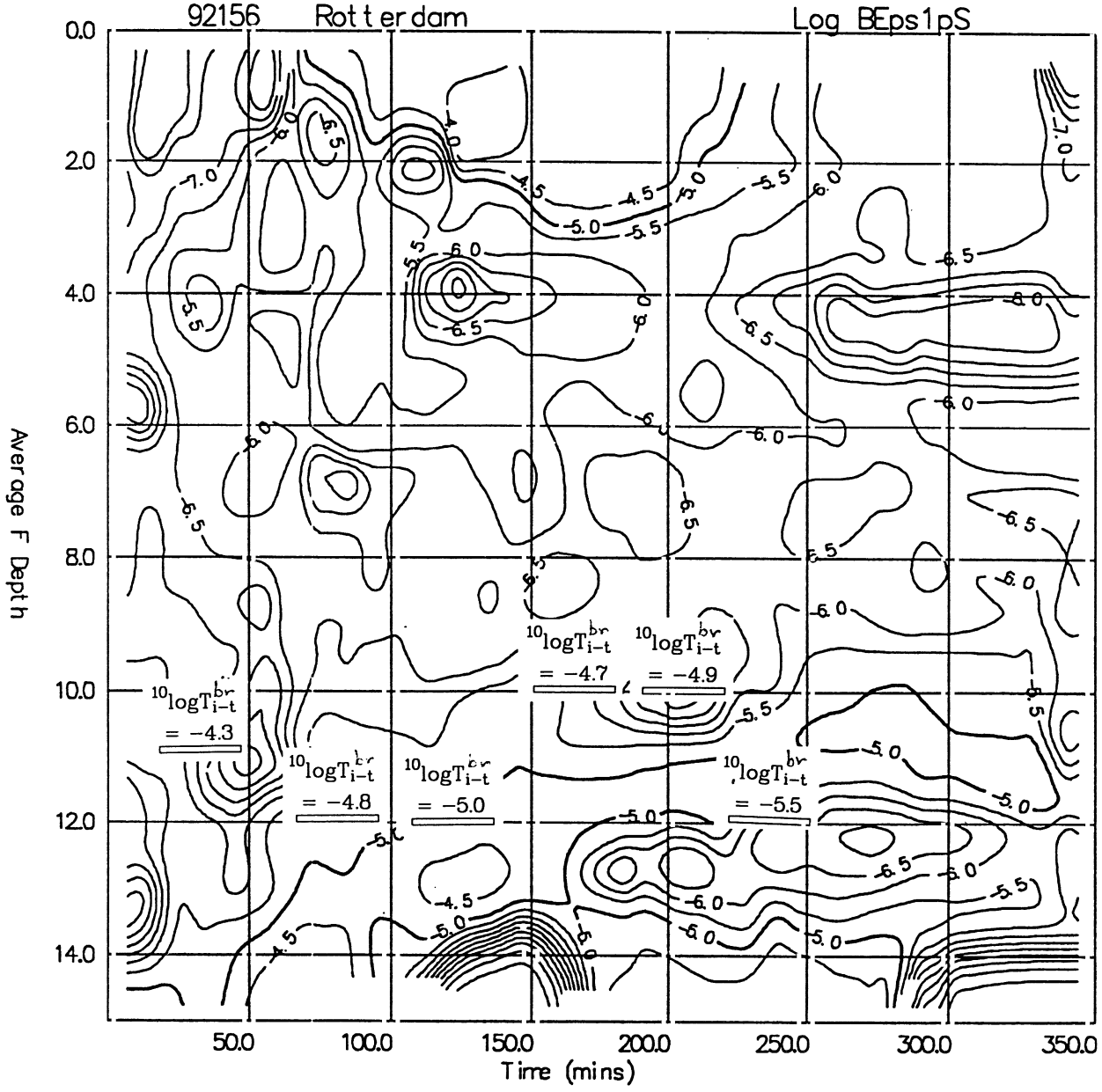

Energy dissipation rate from Batchelor spectra.
Rotterdam Waterway, day 156 (CWR).

DELFT HYDRAULICS | Z 694 | Fig.21

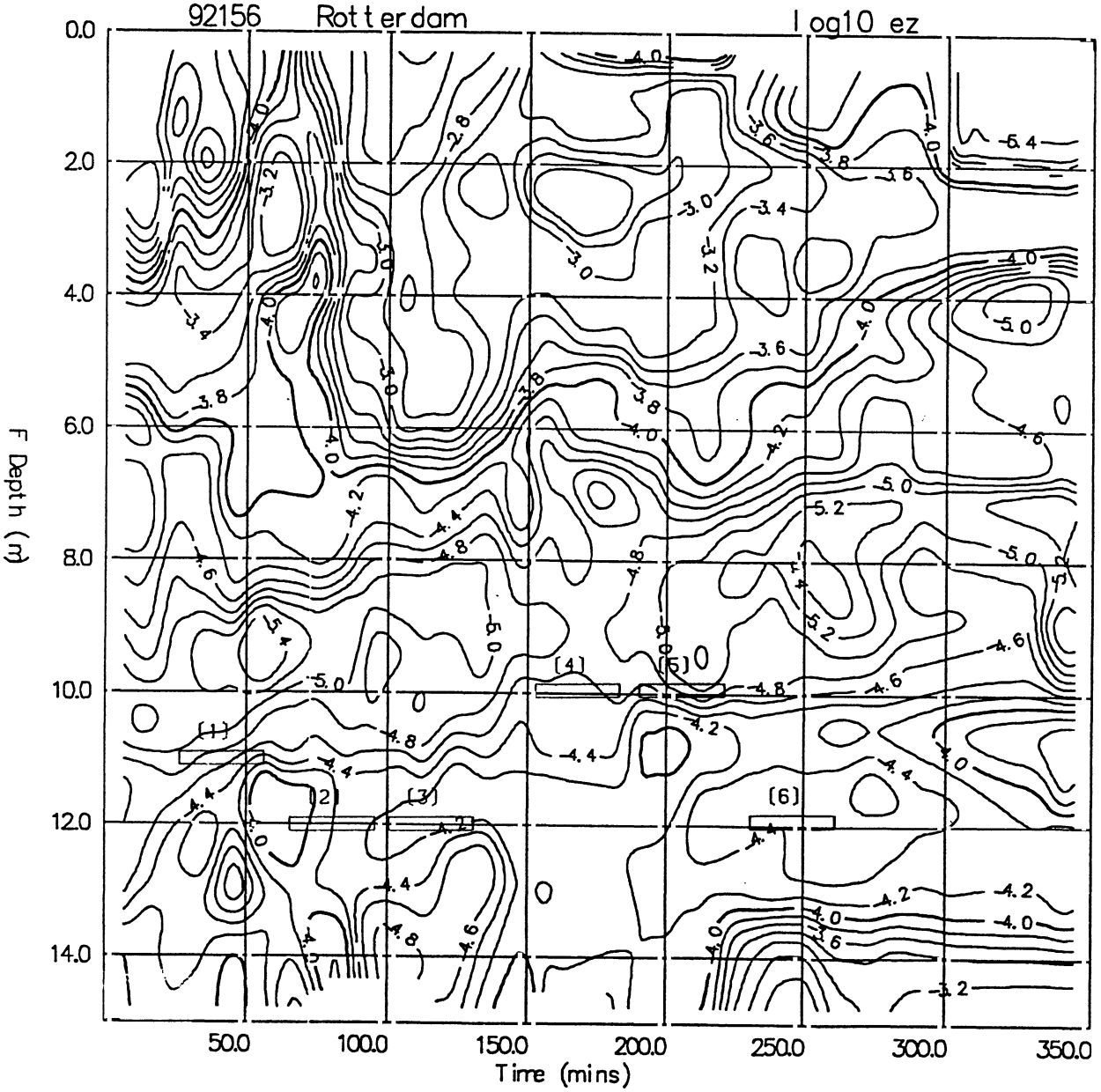

Eddy diffusivity.
Rotterdam Waterway, day 156 (CWR).

DELFT HYDRAULICS | Z 694 | Fig.22

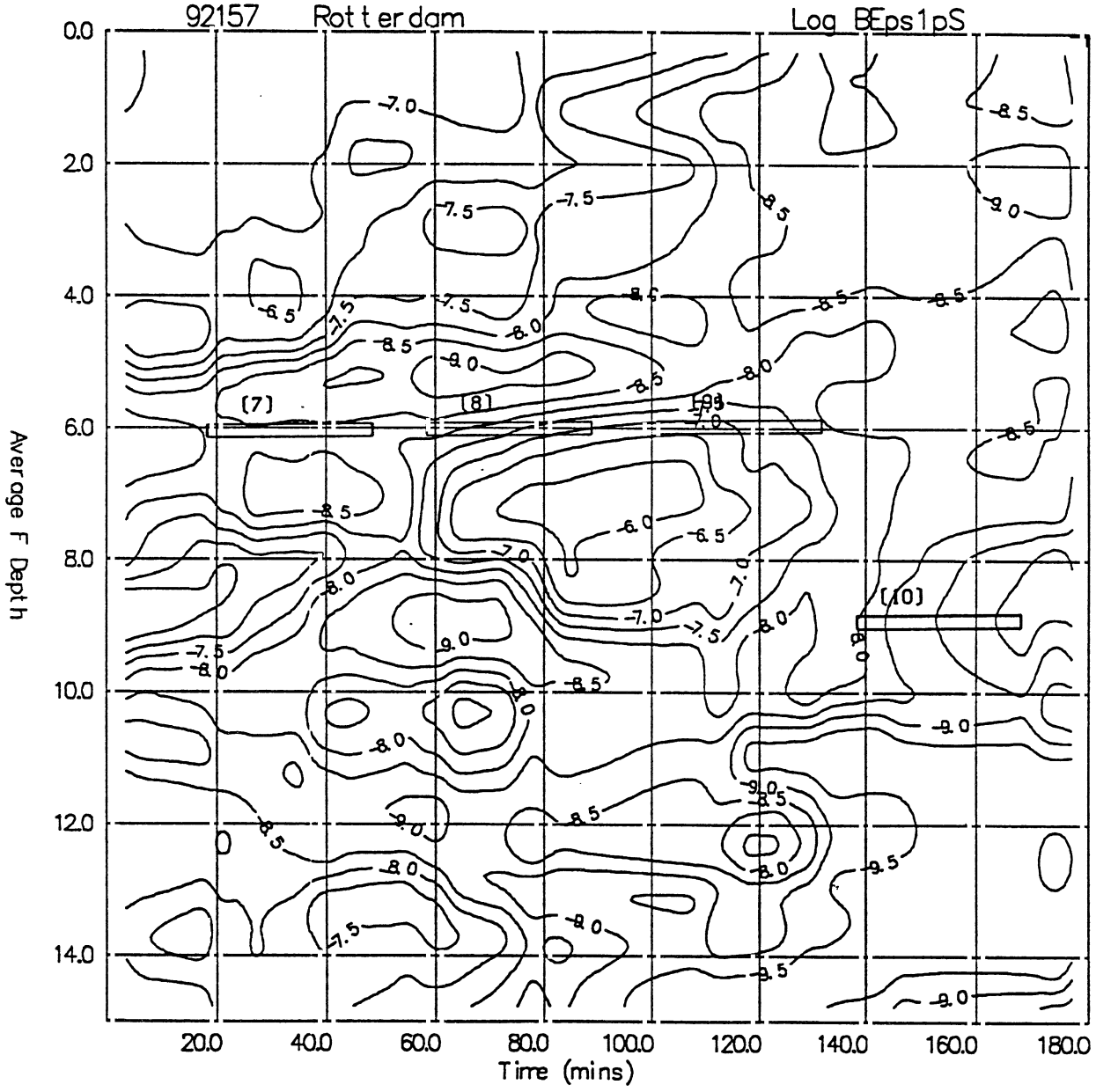

Energy dissipation rate from Batchelor spectra.
Caland channel, day 157 [CWR].

DELFT HYDRAULICS | Z 694 | Fig.23

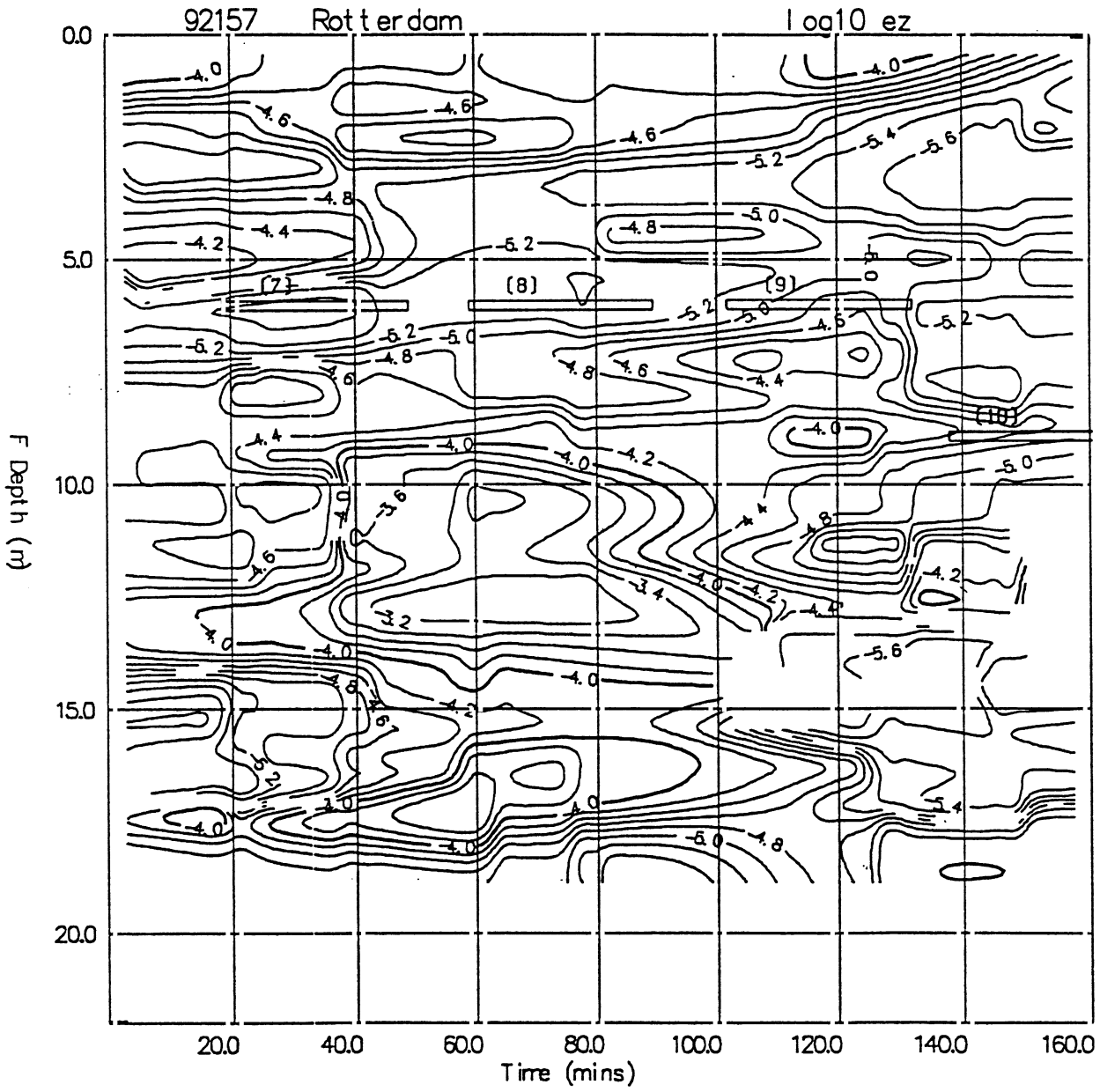

Eddy diffusivity.
Caland channel, day 157 [CWR].

DELFT HYDRAULICS | Z 694 | Fig.24

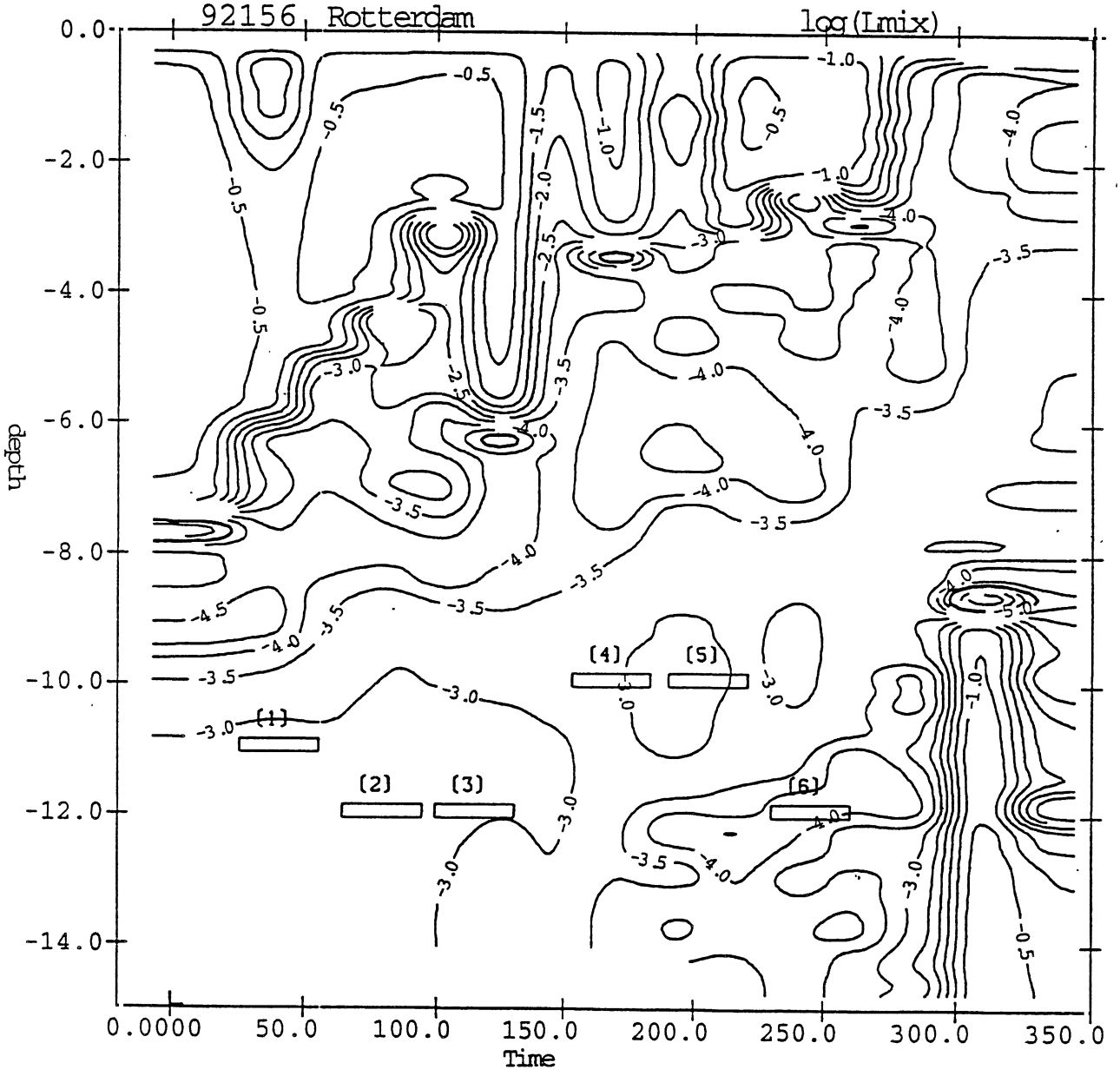

Mixing length ; 1DV q^2-ε turbulence model.
Rotterdam Waterway, day 156.

DELFT HYDRAULICS | Z 694 | Fig.25

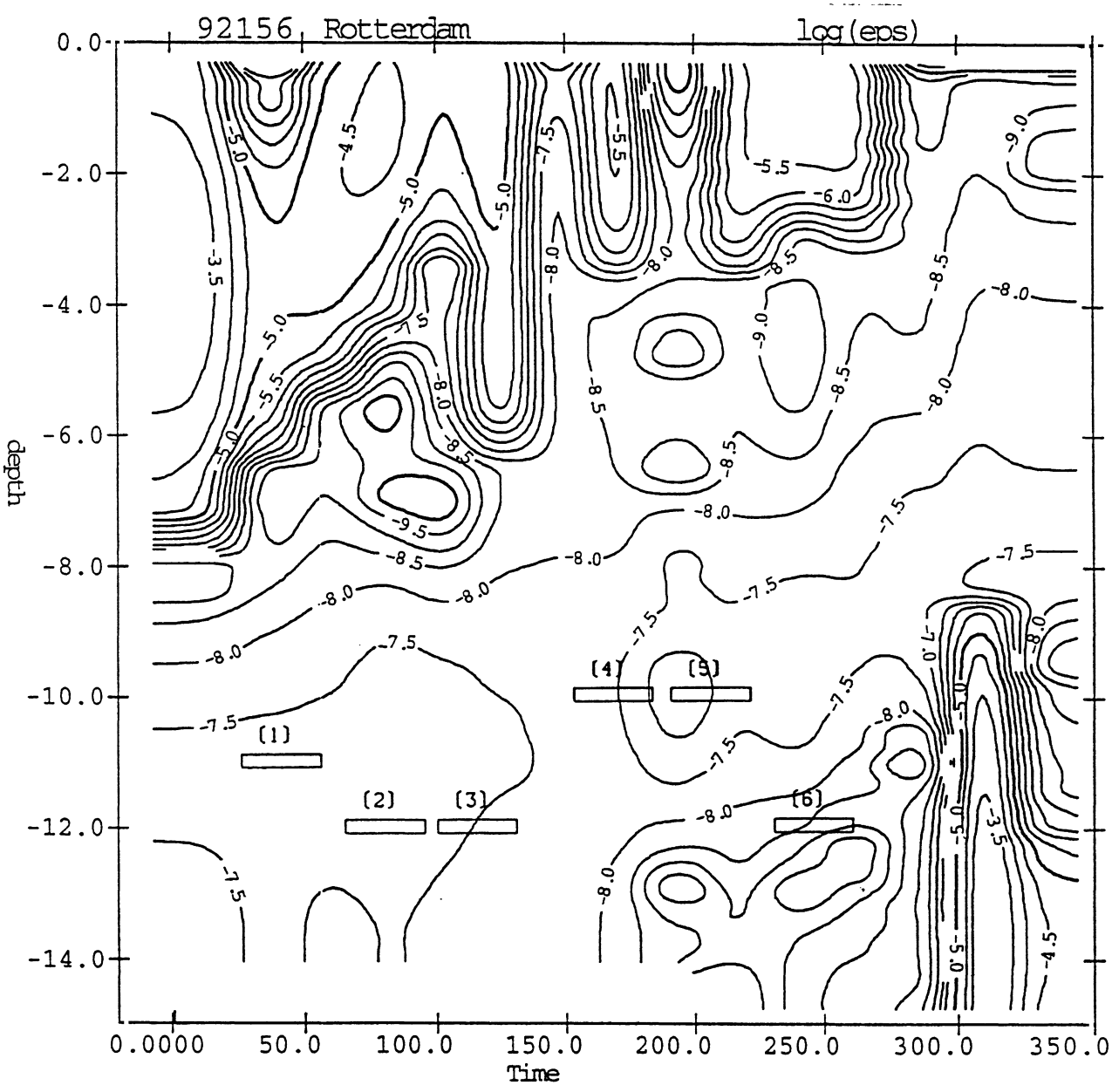

Energy dissipation ; 1DV q^2-ε turbulence model.
Rotterdam Waterway, day 156.

DELFT HYDRAULICS | Z 694 | Fig.26

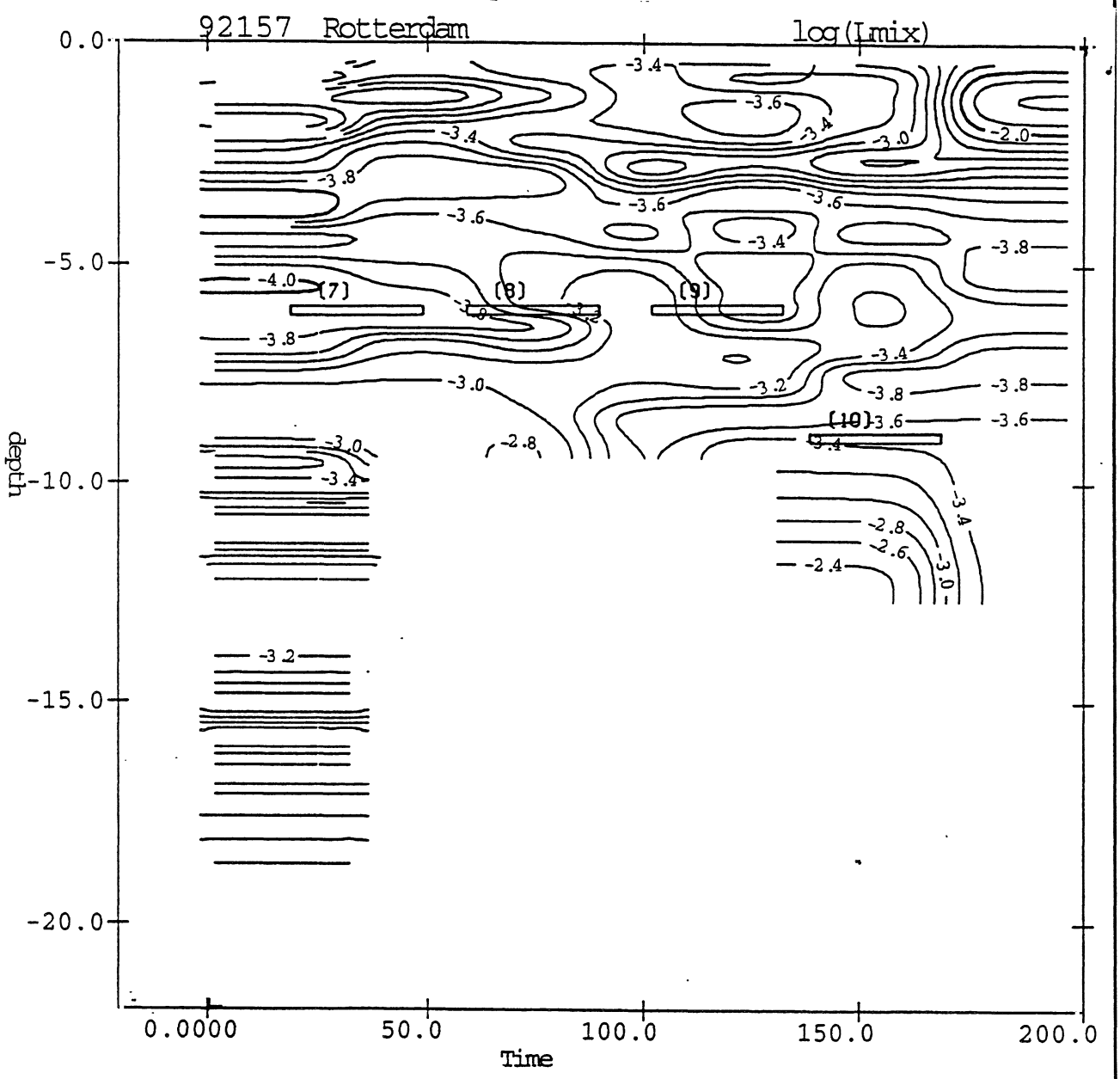

Mixing length ; 1DV q^2-ε turbulence model.
Caland channel, day 157.

DELFT HYDRAULICS | Z 694 | Fig.27

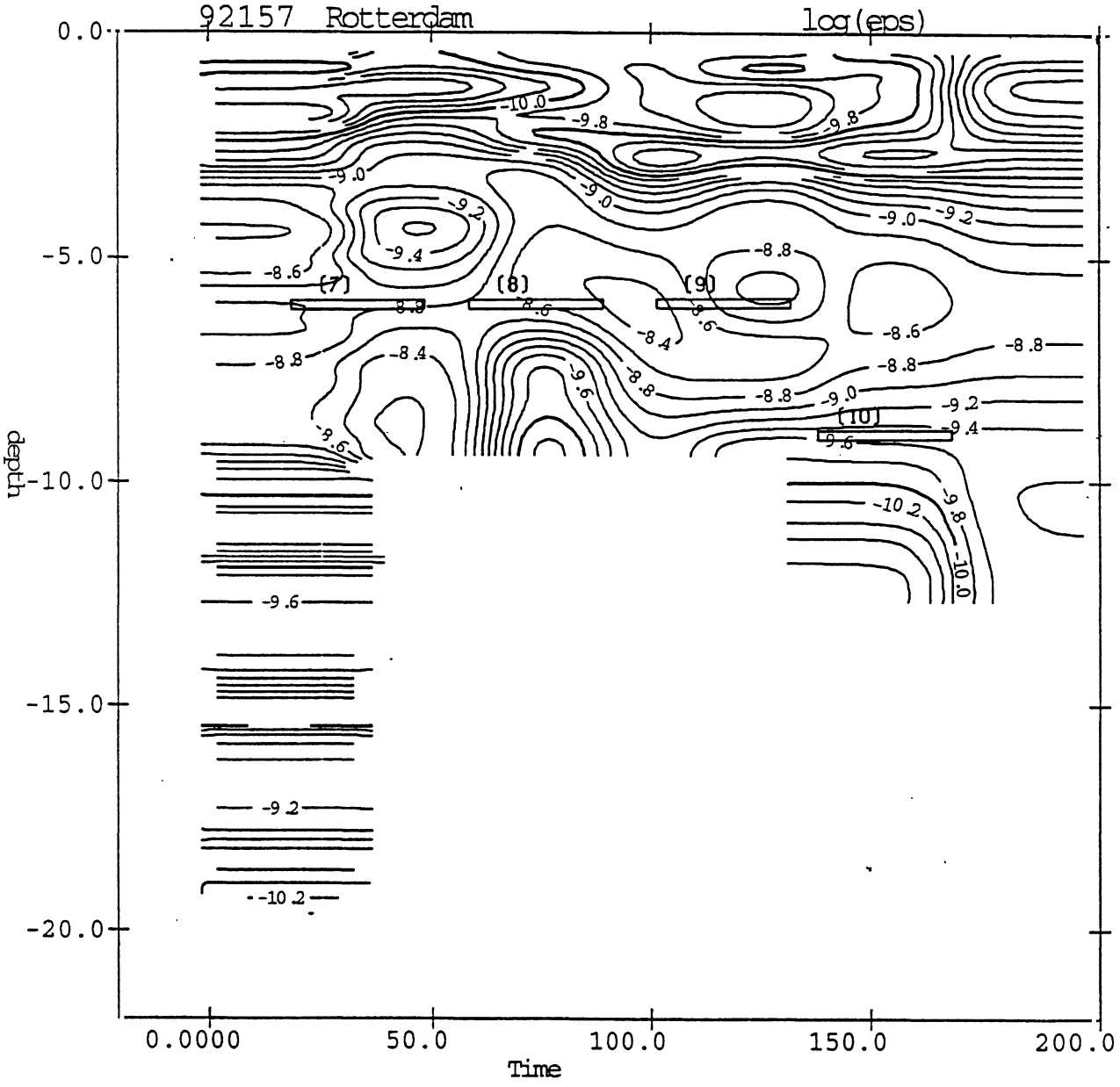

Energy dissipation ; 1DV q^2-ε turbulence model.
Caland channel, day 157.

DELFT HYDRAULICS | Z 694 | Fig.28

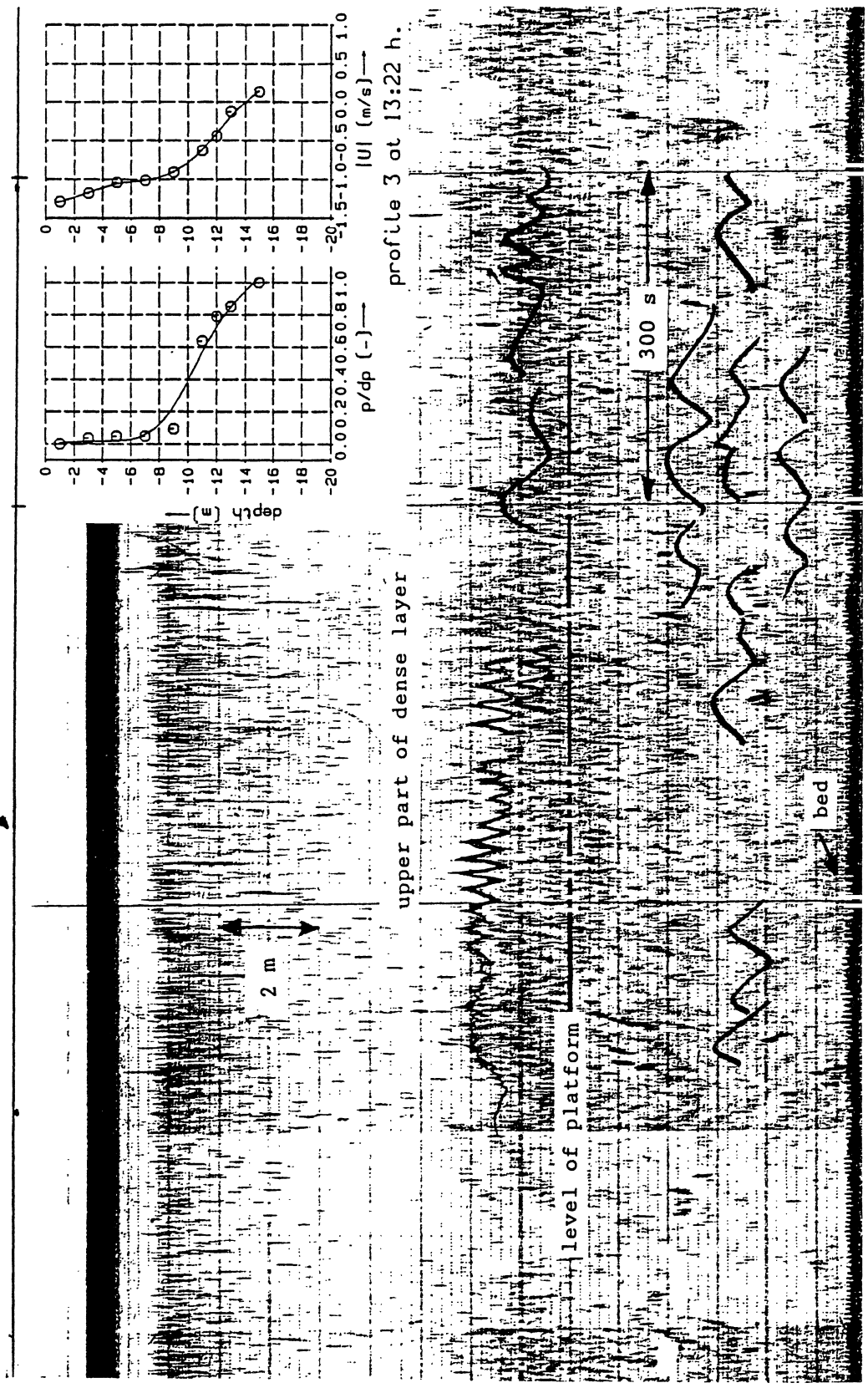

Echosounder observations from the anchored Pavo. Rotterdam Waterway on day 156.

DELFT HYDRAULICS | Z 694 | Fig.29

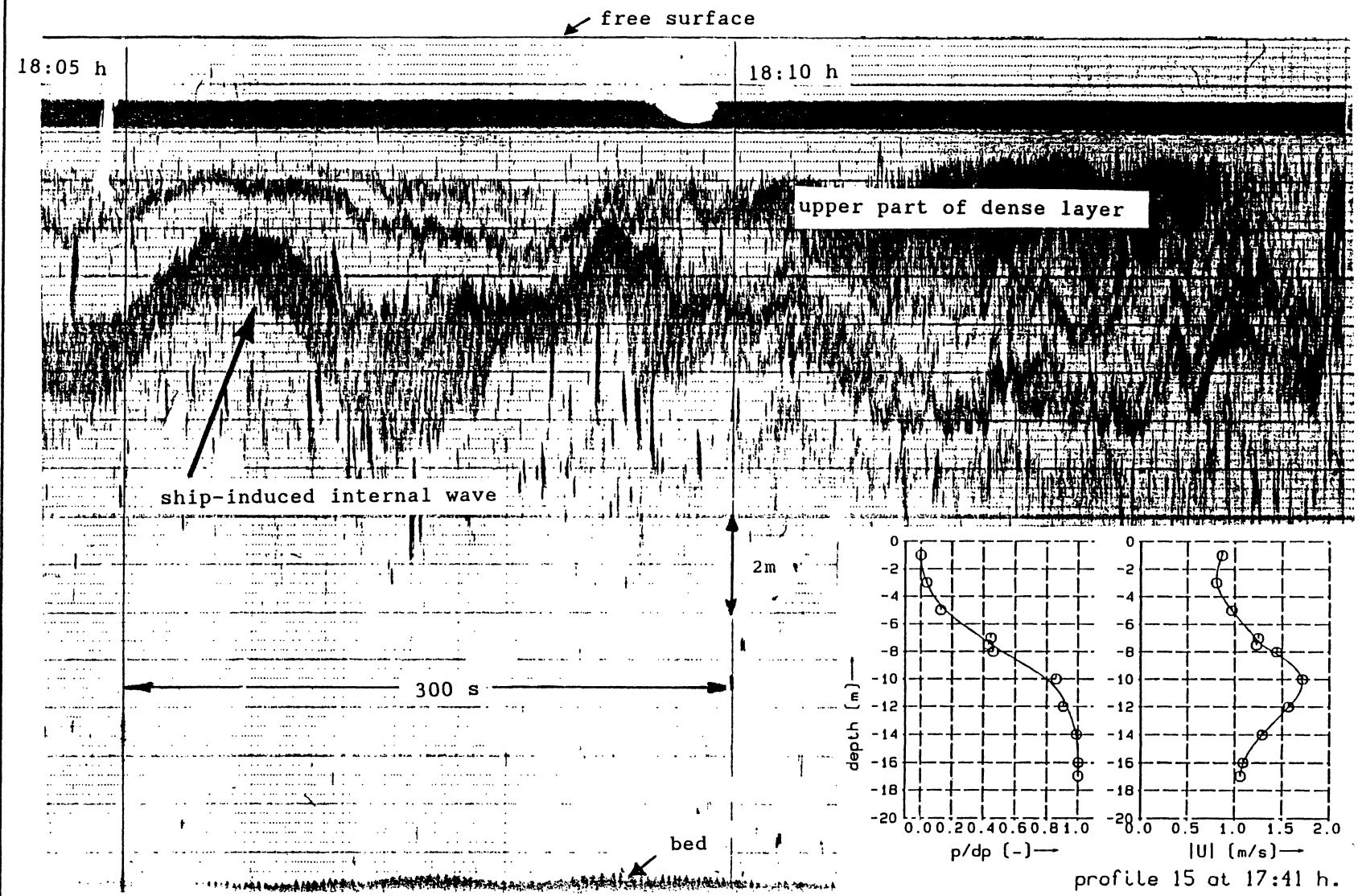

Echosounder recording of a ship-induced internal wave. Rotterdam Waterway on day 156.

DELFT HYDRAULICS

Z 694

Fig.30

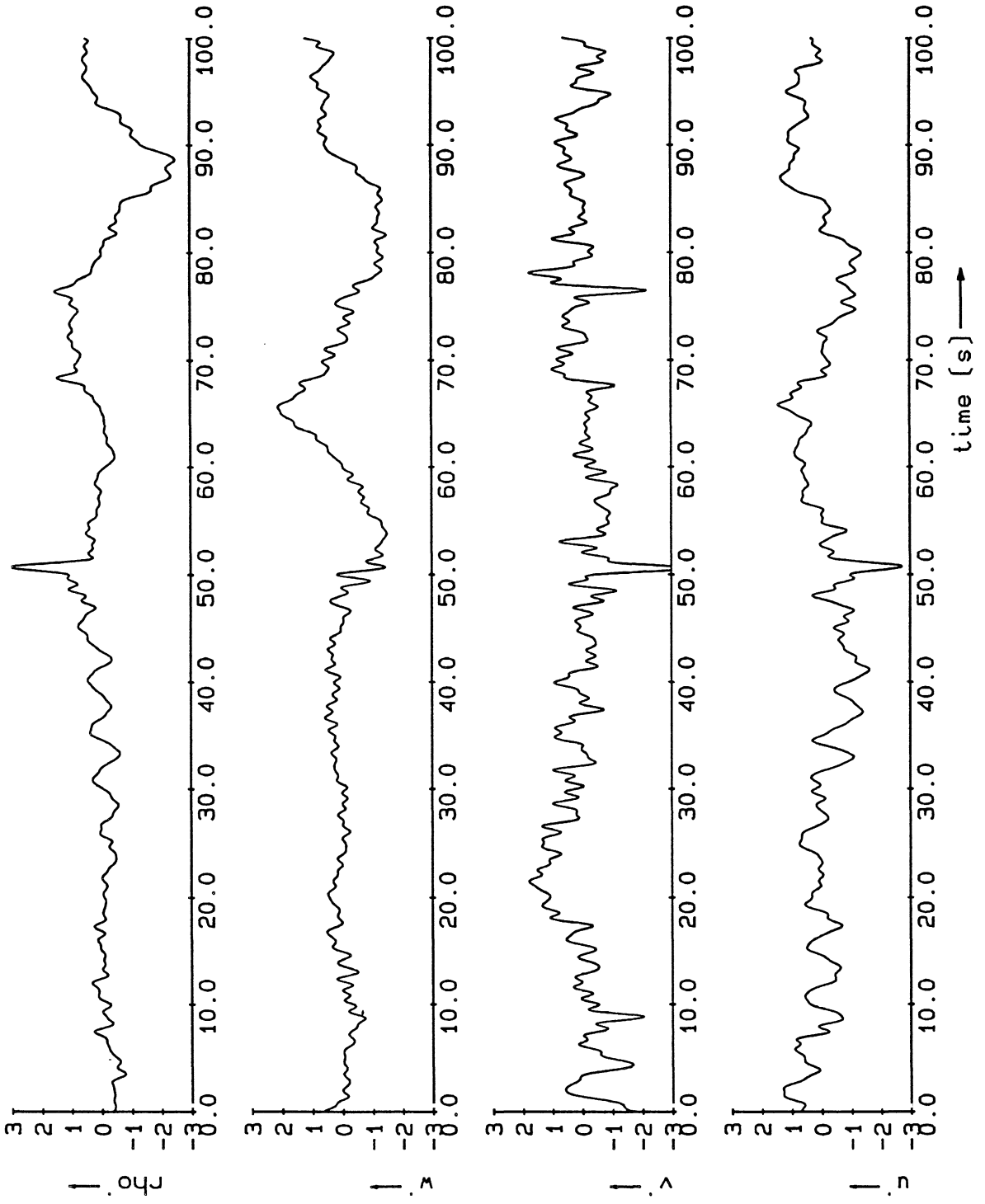

Filtered velocity and density signals; normalised, corrected for trend and for platform motions.

12:53/156 [0;100]

inspct.inv

DELFT HYDRAULICS

Z 694

Fig.31

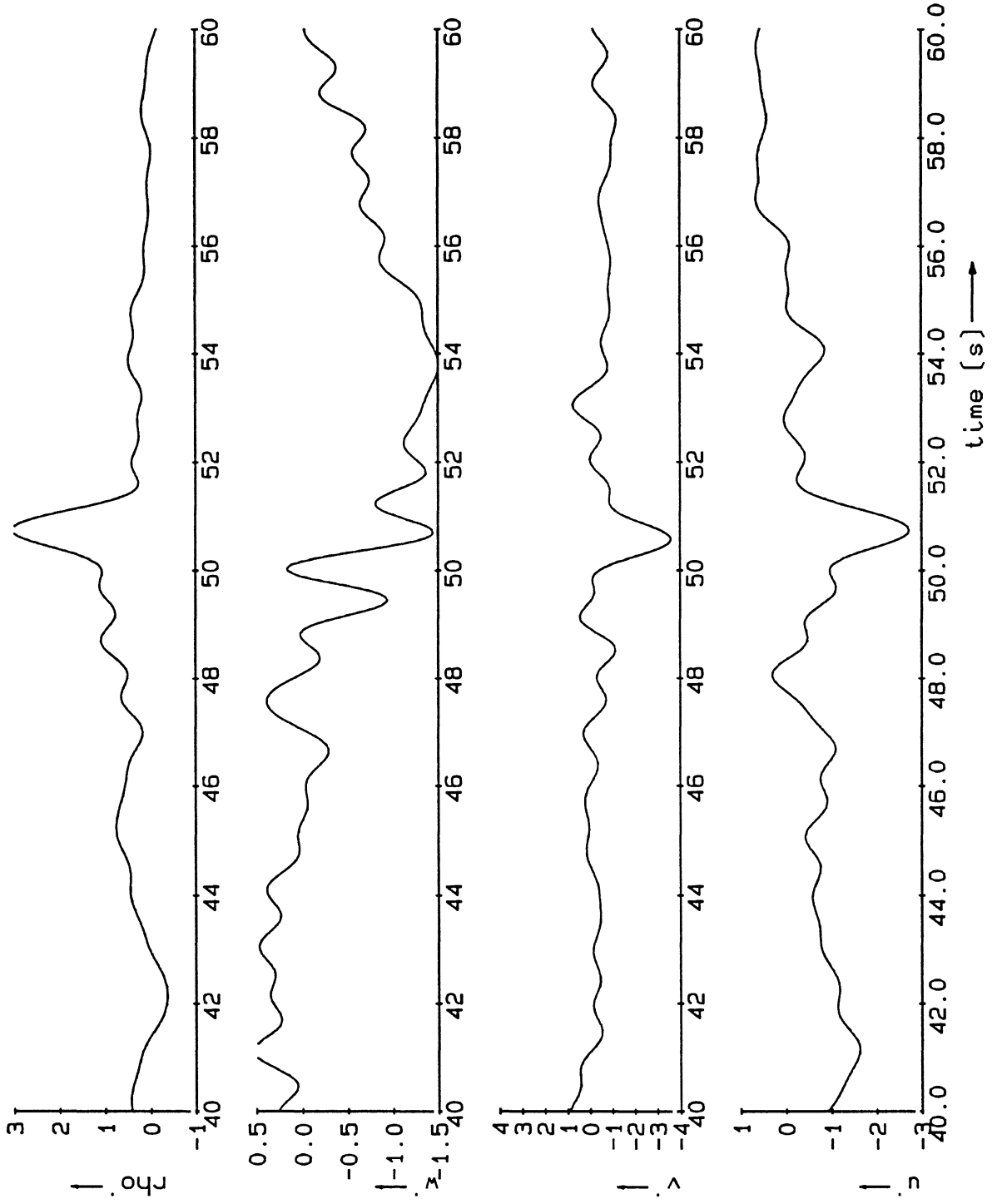

Filtered velocity and density signals; normalised, corrected for linear trend and for platform motions.

12:53/156 [0;100]

break.inv

DELFT HYDRAULICS

Z 694

Fig.32

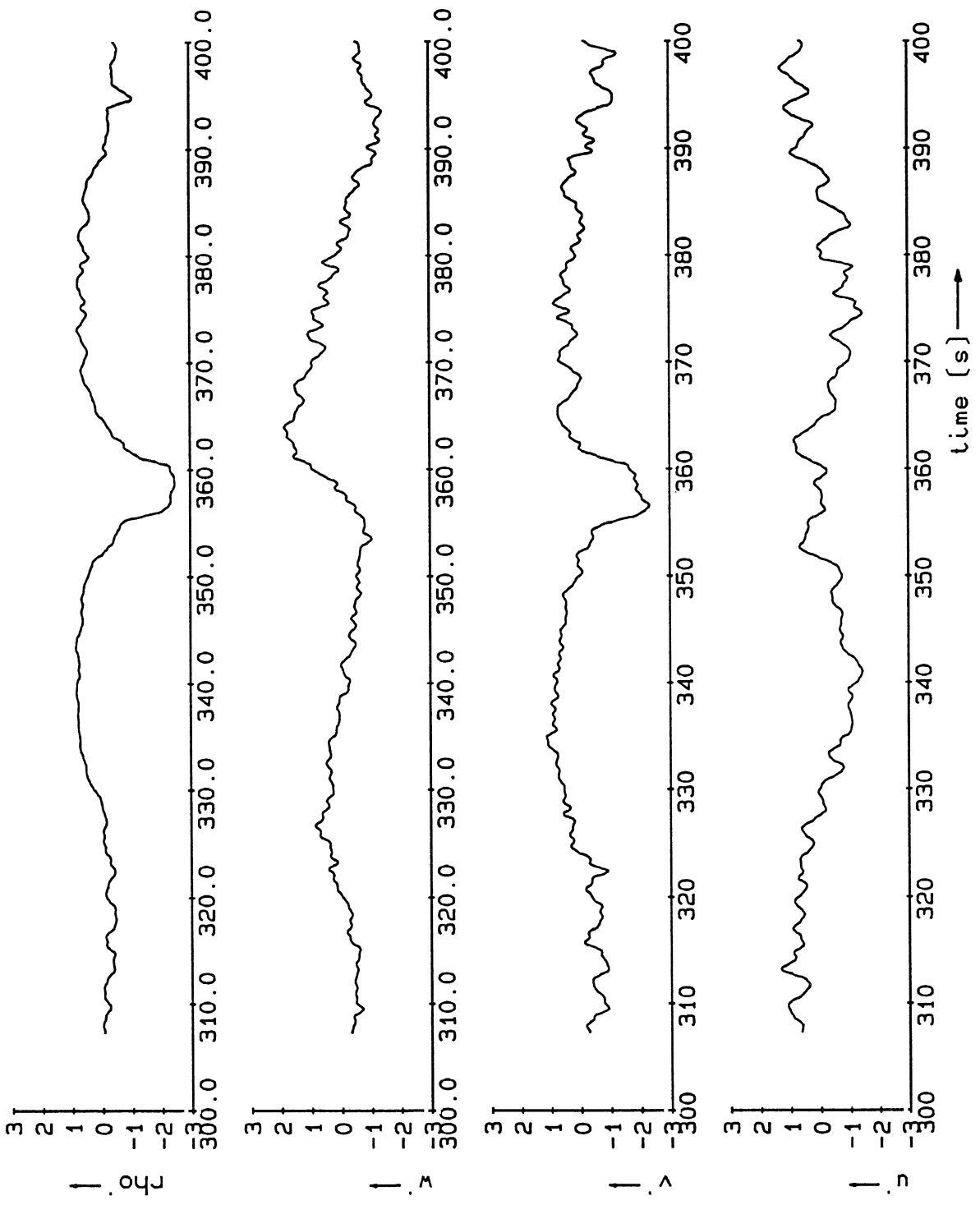

Filtered velocity and density signals; normalised, corrected for trend and for platform motions.

12:53/156 [0;100]

inspct.inv

DELFT HYDRAULICS

Z 694

Fig.33

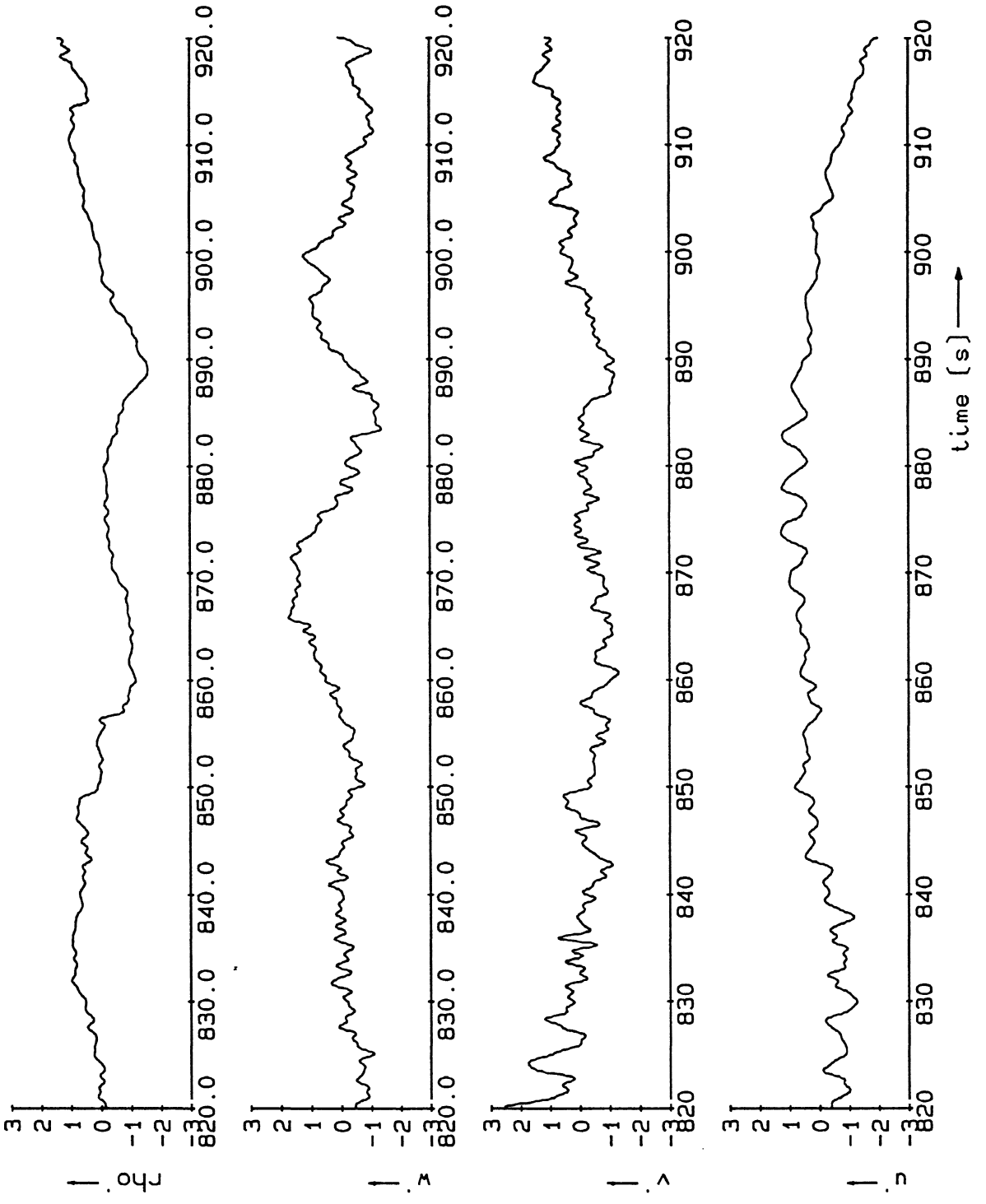

Filtered velocity and density signals; normalised, corrected for trend and for platform motions.

12:53/156 [0;100]

inspct.inv

DELFT HYDRAULICS

Z 694

Fig.34

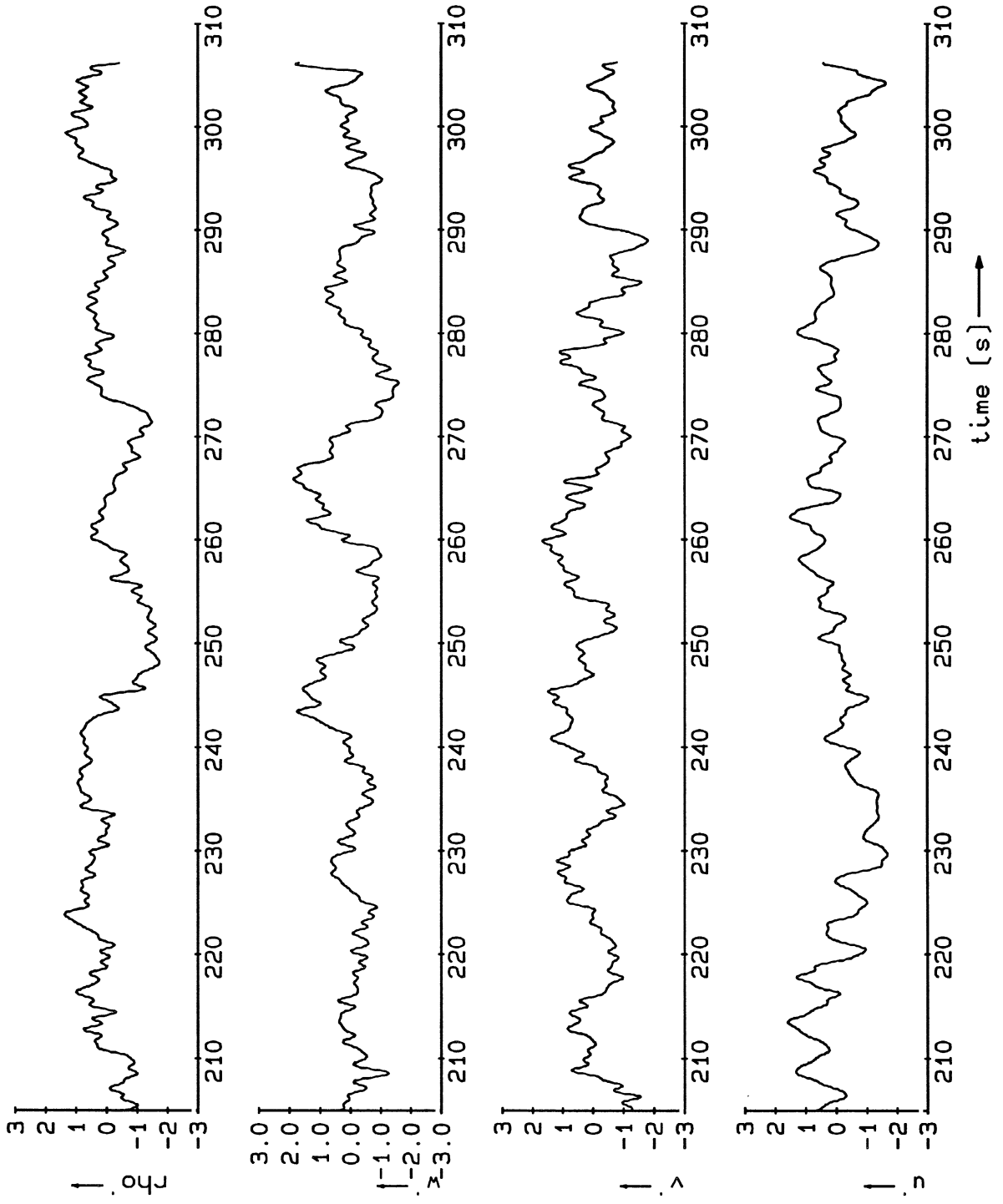

Filtered velocity and density signals; normalised, corrected for trend and for platform motions.

13:32/156 [0;100]

inspct.inv

DELFT HYDRAULICS

Z 694

Fig.35

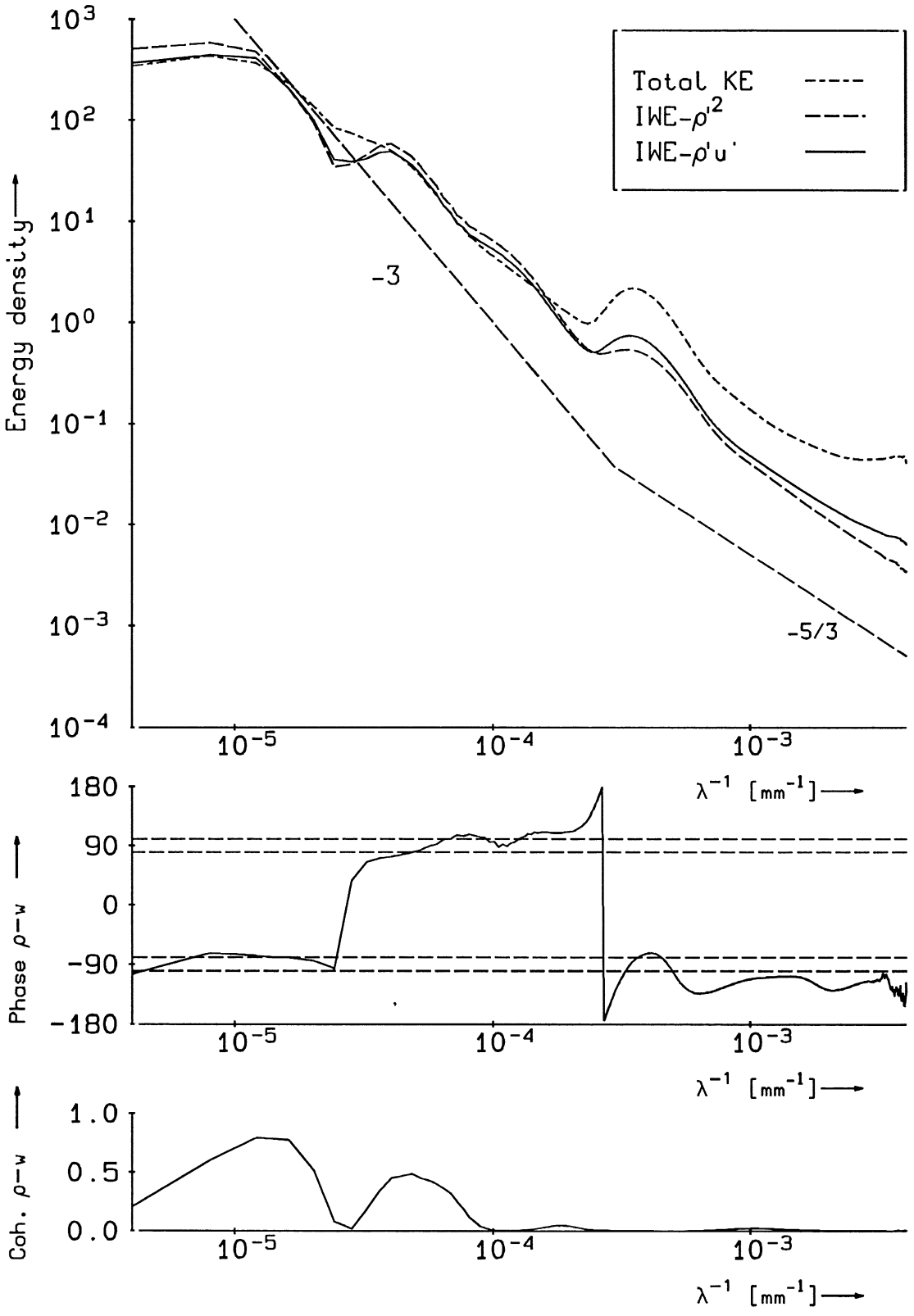

TKE-IWE decomposition. Field measurements in Rotterdam Waterway (Ri=1.2;N=0.17 rad/s).

06.04.12:53|25-56 min

iwefield.125

DELFT HYDRAULICS

Z 722

Fig.36

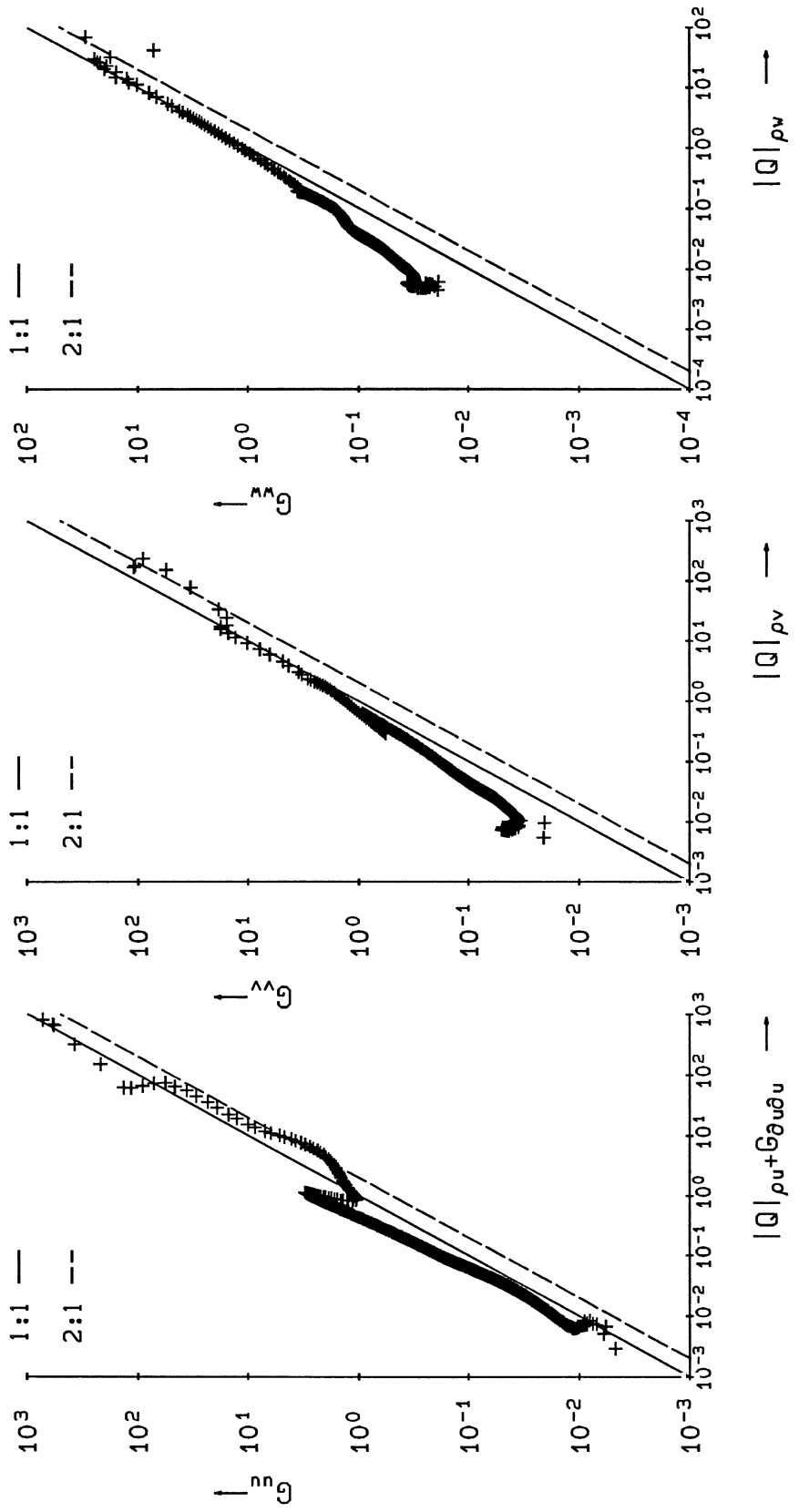

Absolute quad spectra compared with power spectra of velocity components u, v, and w.	06.04.12:53|26-56 min	
	tet125.inv	
DELFT HYDRAULICS	Z 722	Fig.36[b]

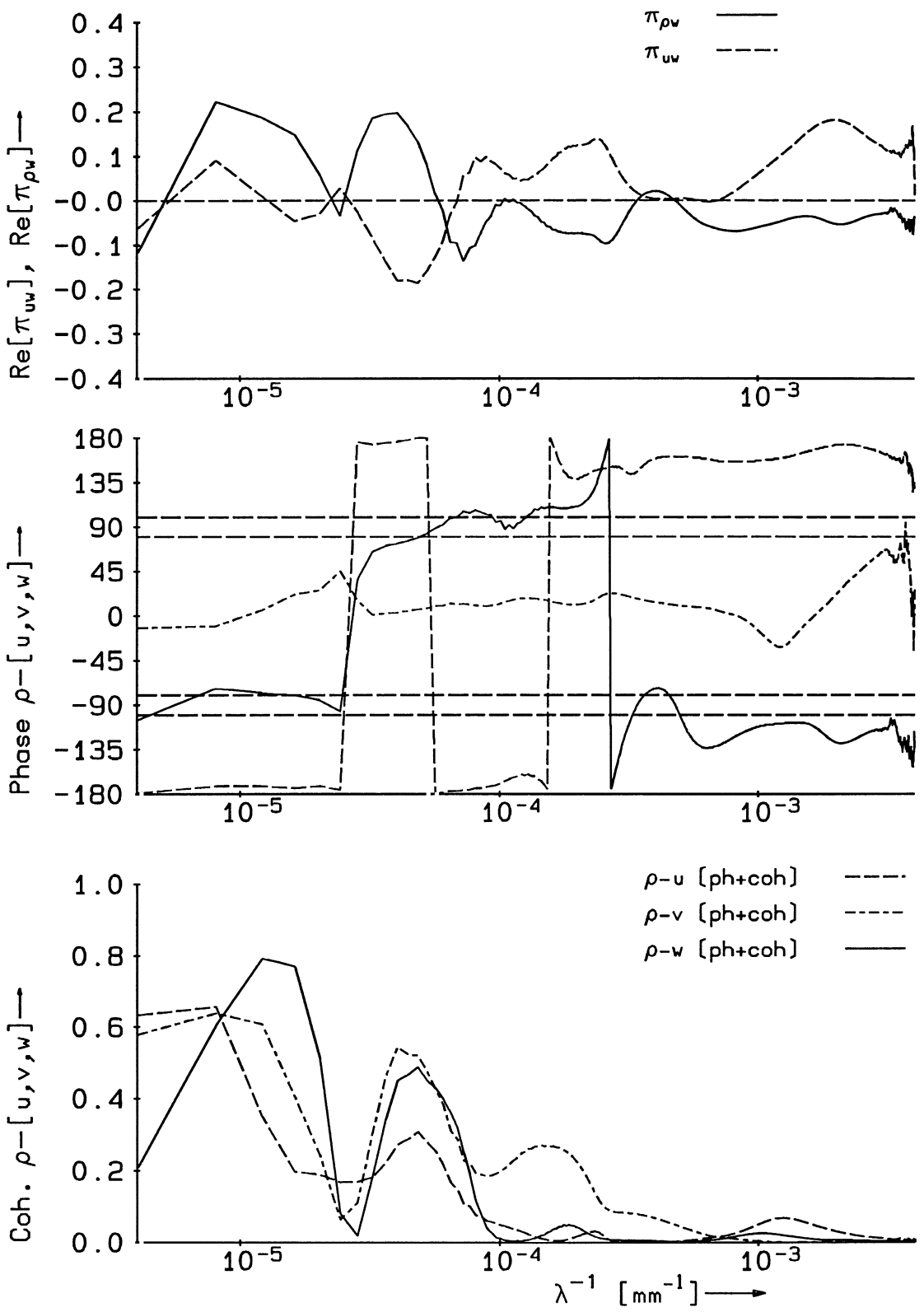

Phase, coherence, momentum and buoyancy fluxes. Rotterdam Waterway (Ri=1.2;N=0.17 rad/s).	06.04.12:53|26-56 min iwe125.inv	
DELFT HYDRAULICS	Z 722	Fig.36[c]

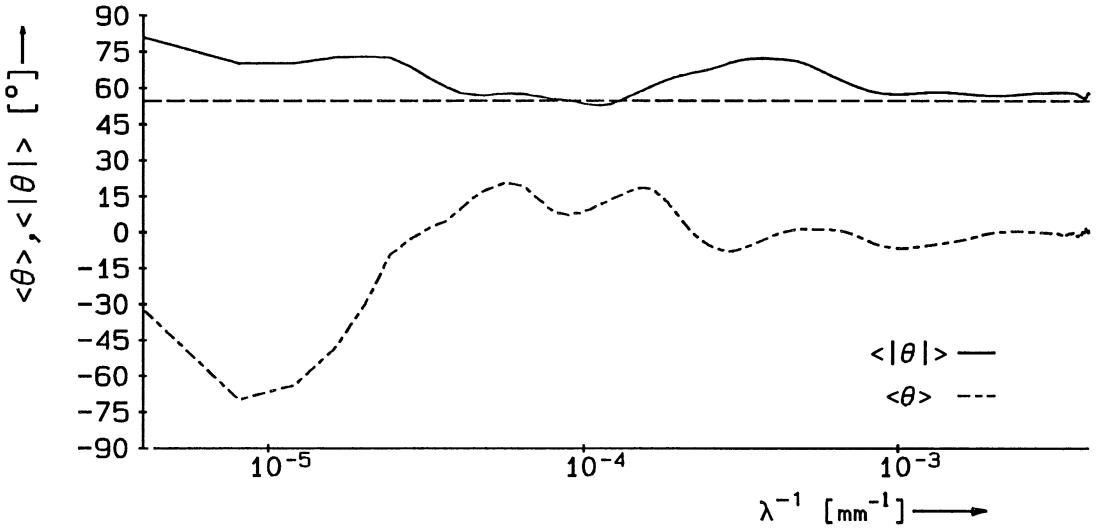

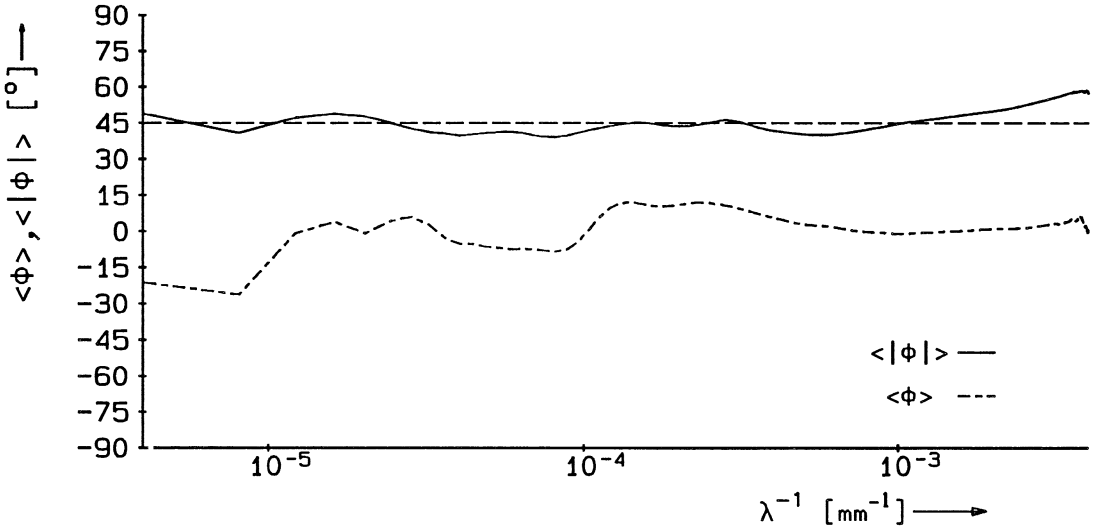

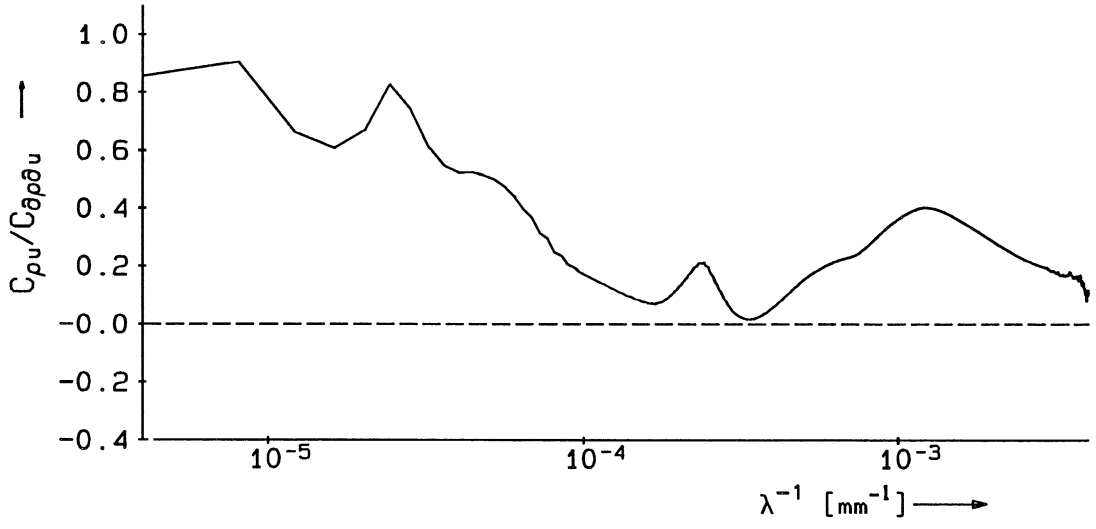

Normalized Stokes mass drift and IW angles.	06.04.12:53|26-56 min	
Rotterdam Waterway (Ri=1.2;N=0.17 rad/s).	stok125.inv	
DELFT HYDRAULICS	Z 722	Fig.36d

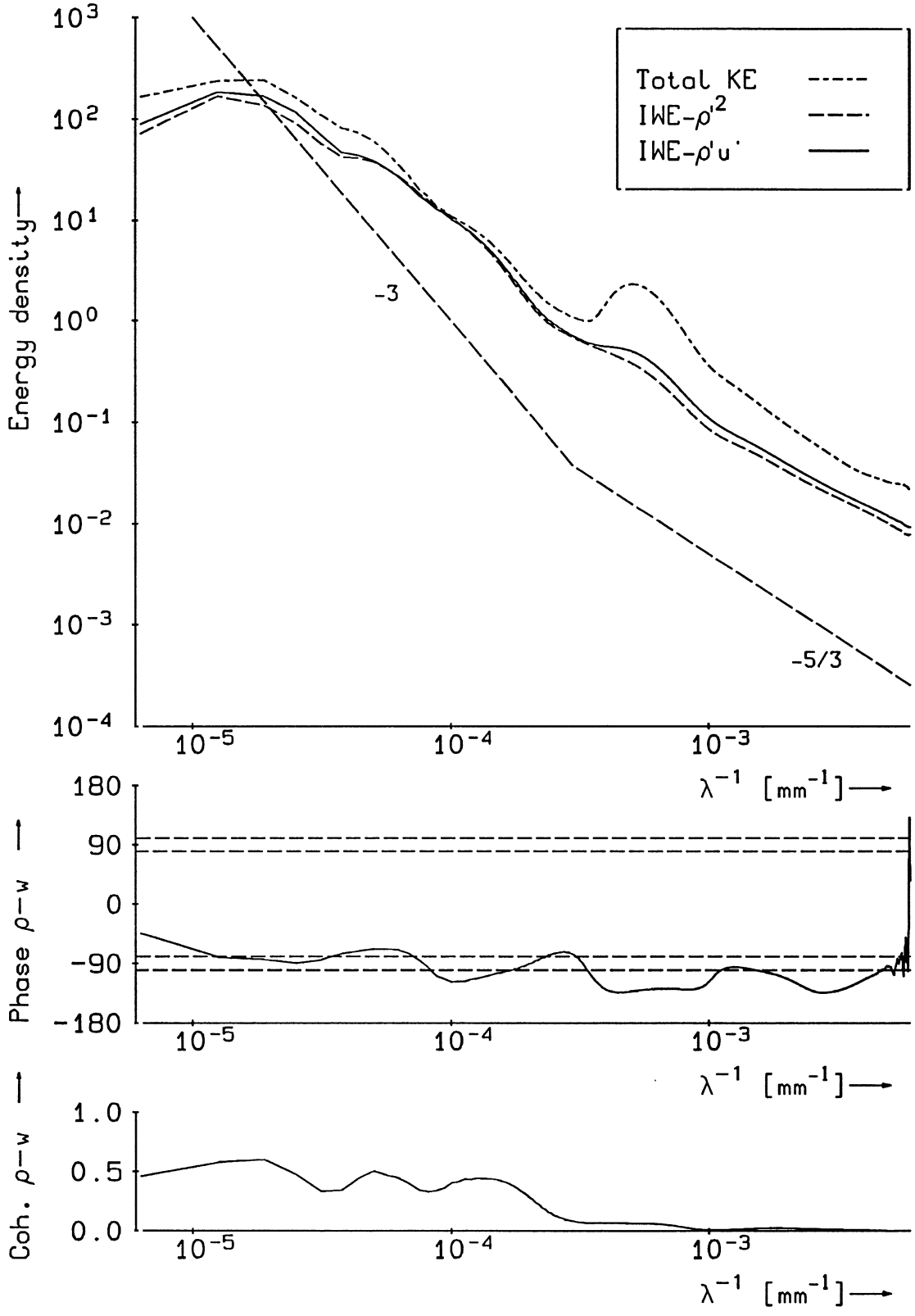

TKE-IWE decomposition. Field measurements in Rotterdam Waterway (Ri=0.43;N=0.15 rad/s).

06.04.13:32|65-95 min

iwefield.133

DELFT HYDRAULICS

Z 722

Fig.37

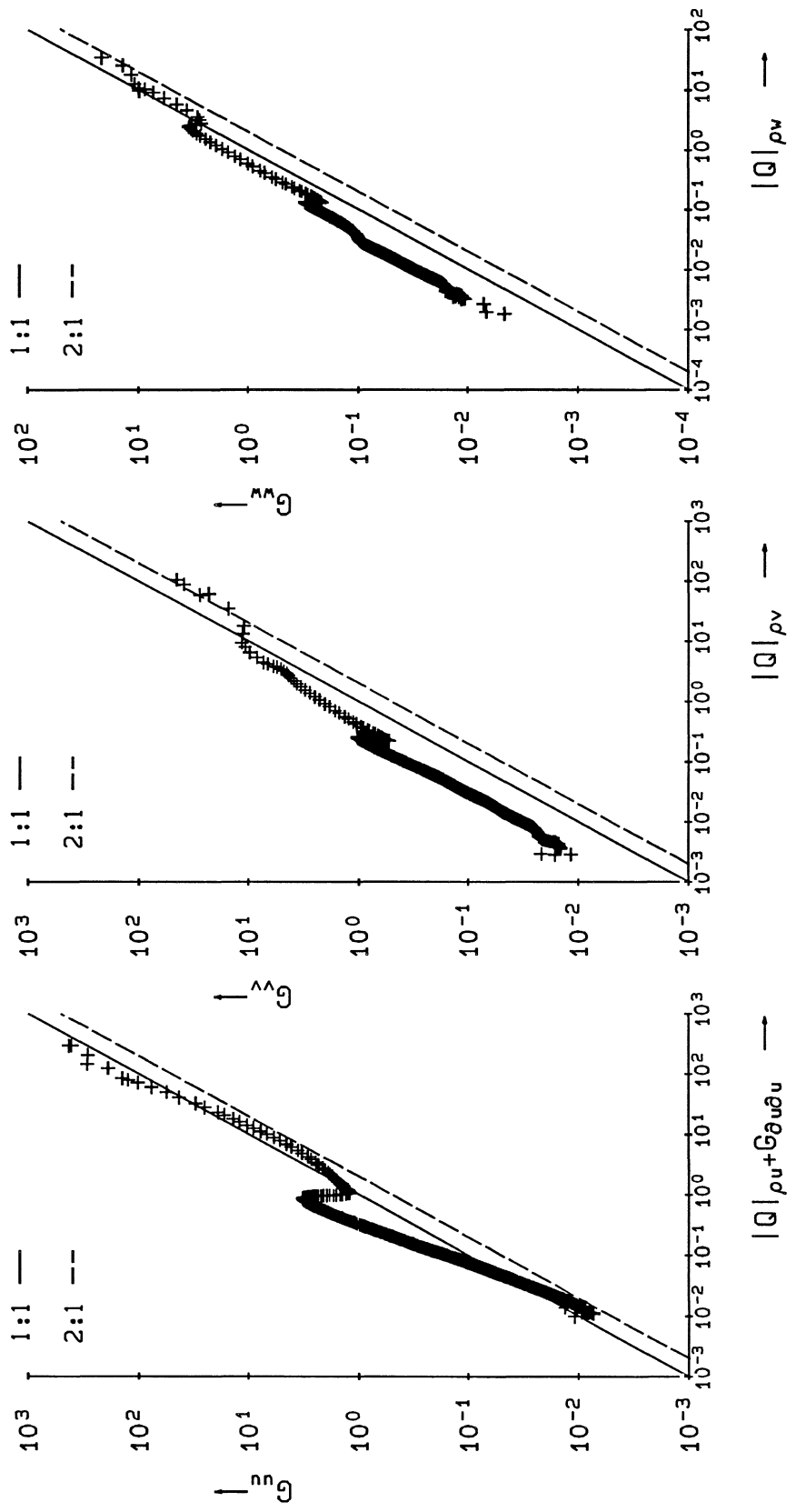

Absolute quad spectra compared with power spectra of velocity components u, v, and w.	06.04.13:32|65-95 min	
	tet133.inv	
DELFT HYDRAULICS	Z 722	Fig.37[b]

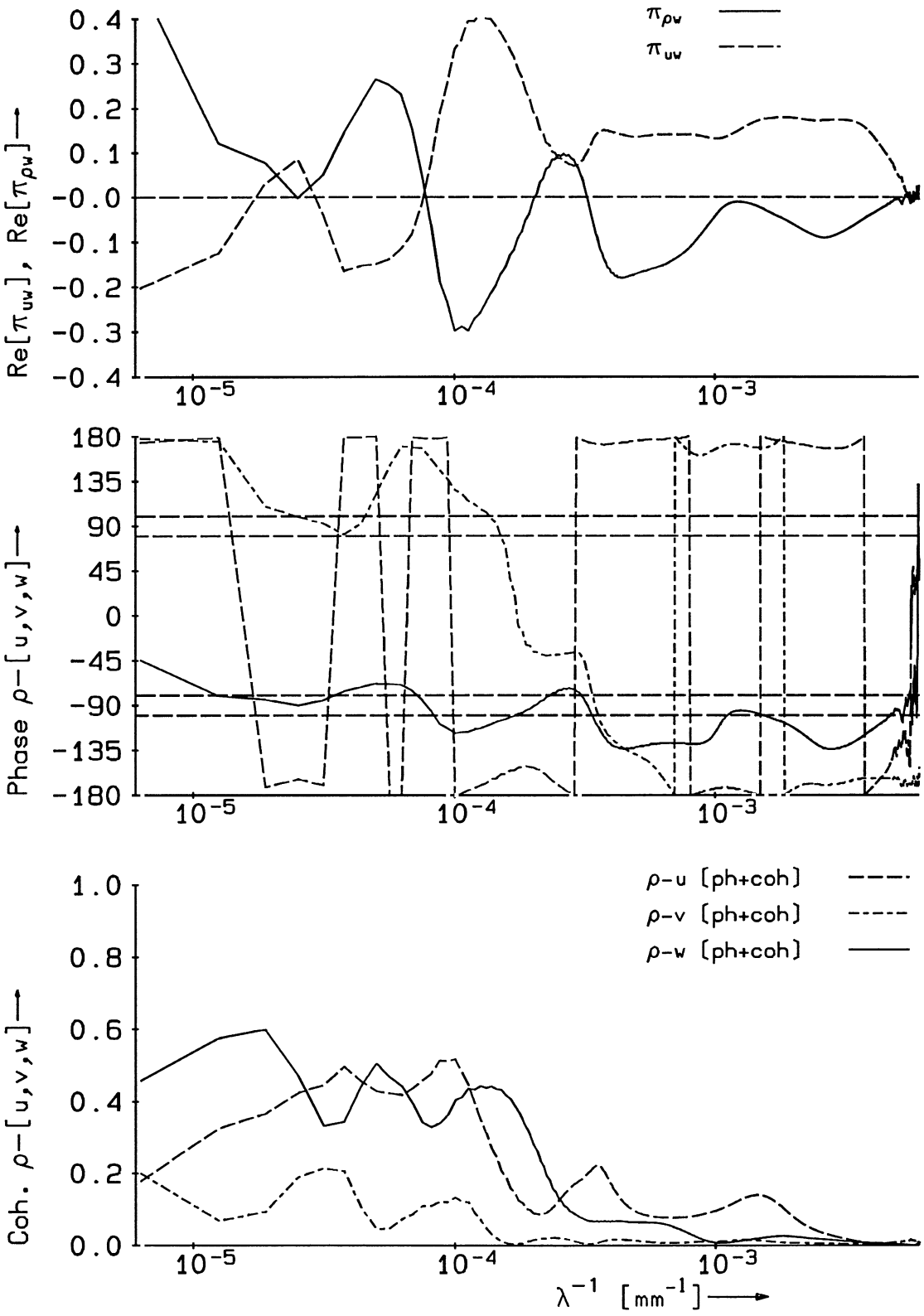

Phase, coherence, momentum and buoyancy fluxes.	06.04.13:32|65-95 min	
Rotterdam Waterway (Ri=0.43;N=0.15 rad/s).	iwe133.inv	
DELFT HYDRAULICS	Z 722	Fig.37c

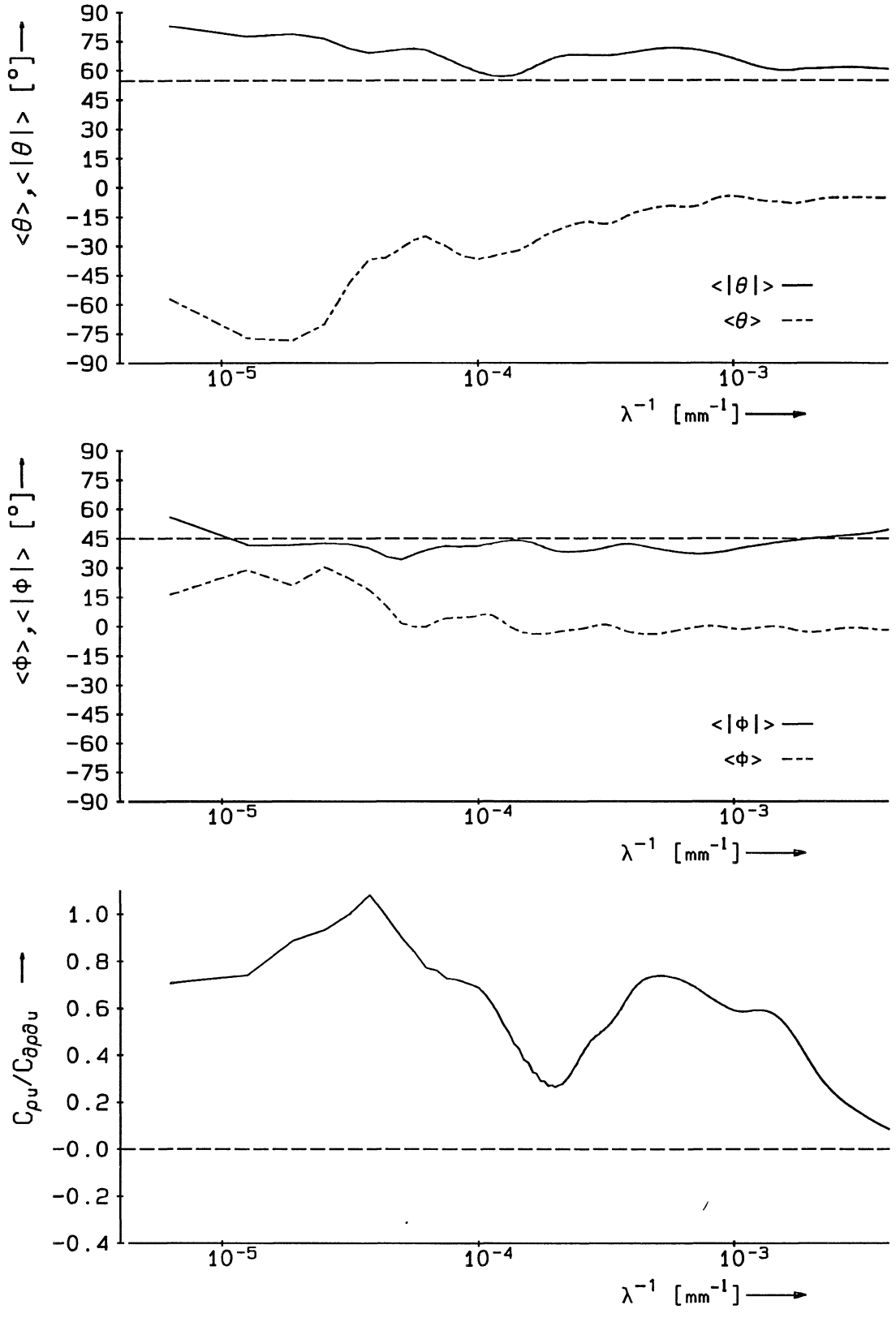

Normalized Stokes mass drift and IW angles.	06.04.13:32|65-95 min	
Rotterdam Waterway (Ri=0.43;N=0.15 rad/s).	stok133.inv	
DELFT HYDRAULICS	Z 722	Fig.37d

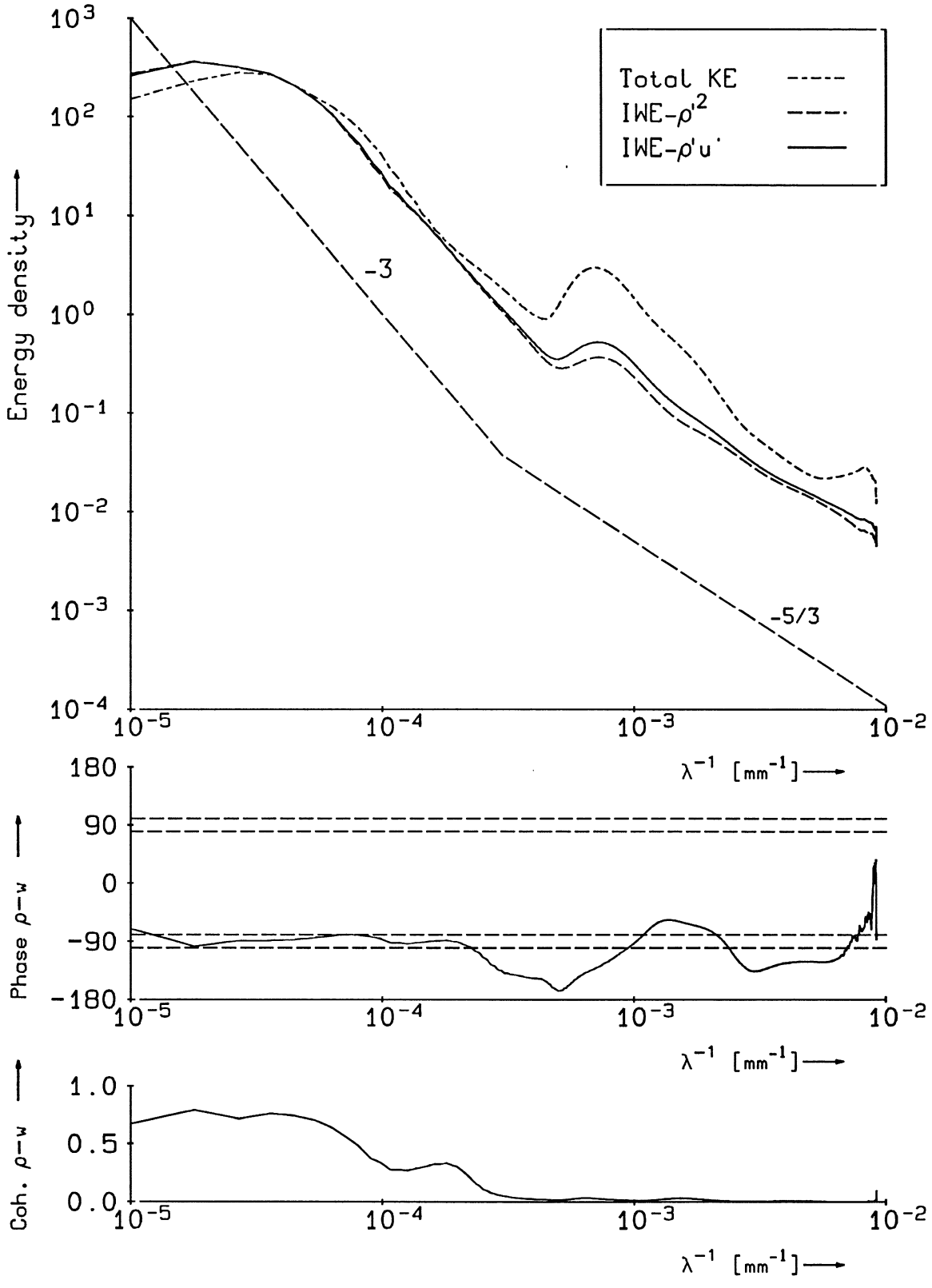

TKE-IWE decomposition. Field measurements in Rotterdam Waterway (Ri=0.55;N=0.12 rad/s).

06.04.14:07|100-130 min

iwefield.140

DELFT HYDRAULICS

Z 722

Fig.38

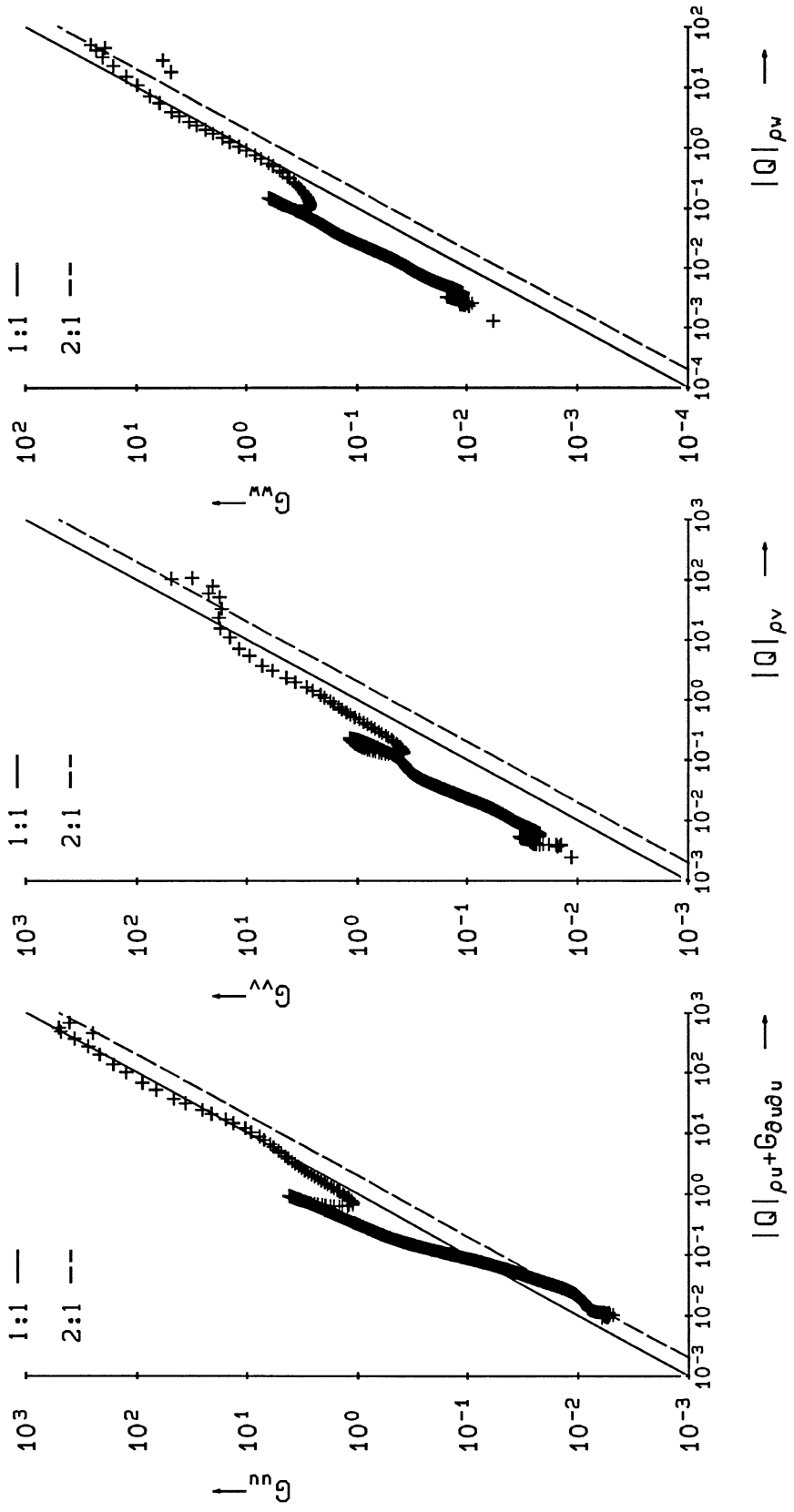

Absolute quad spectra compared with power spectra of velocity components u, v, and w.

06.04.14:07|100-130 min

tet140.inv

DELFT HYDRAULICS

Z 722

Fig.38b

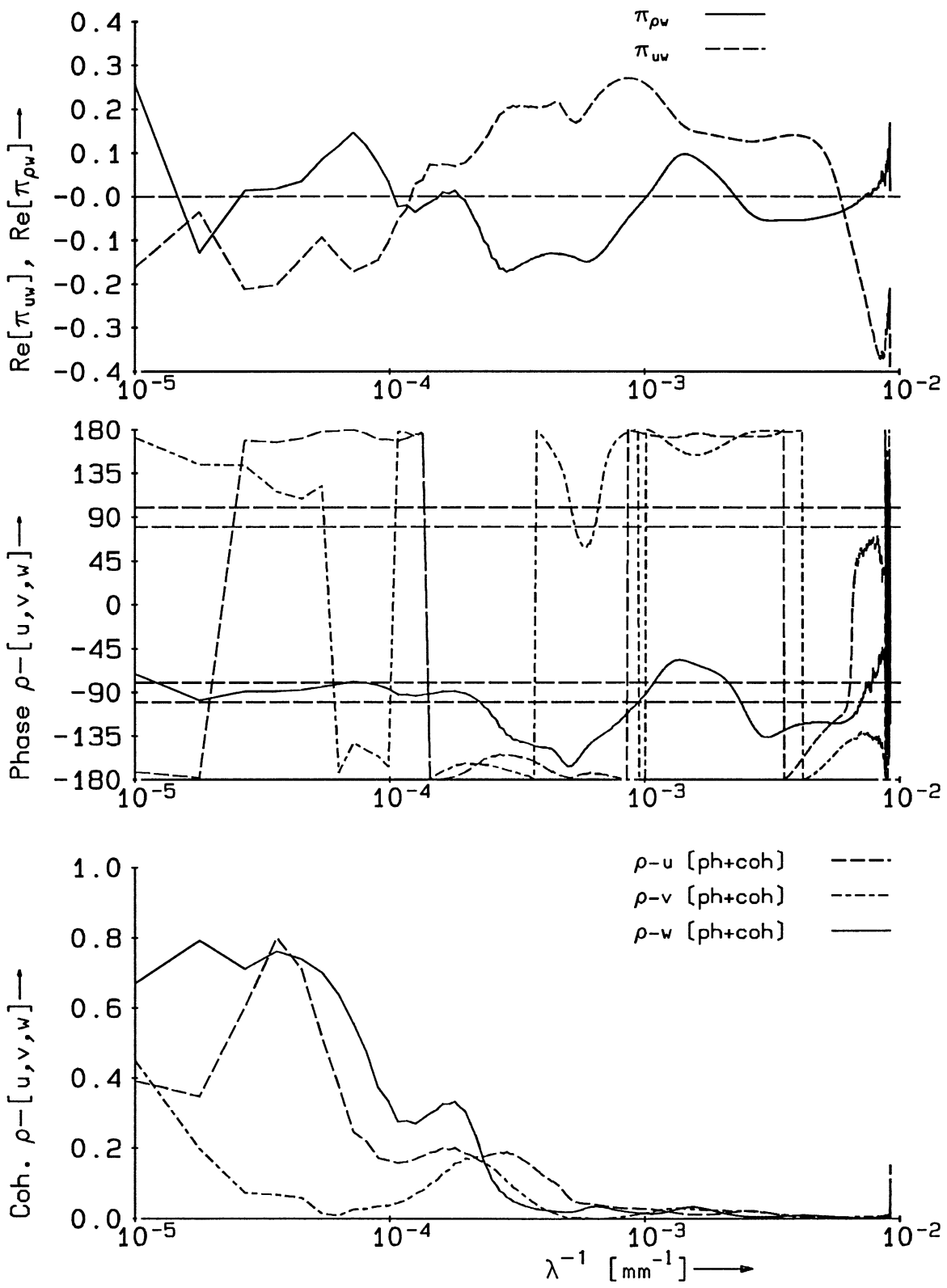

Phase, coherence, momentum and buoyancy fluxes.	06.04.14:071100-130 mir	
Rotterdam Waterway (Ri=0.55;N=0.12 rad/s).	iwe140.inv	
DELFT HYDRAULICS	Z 722	Fig.38c

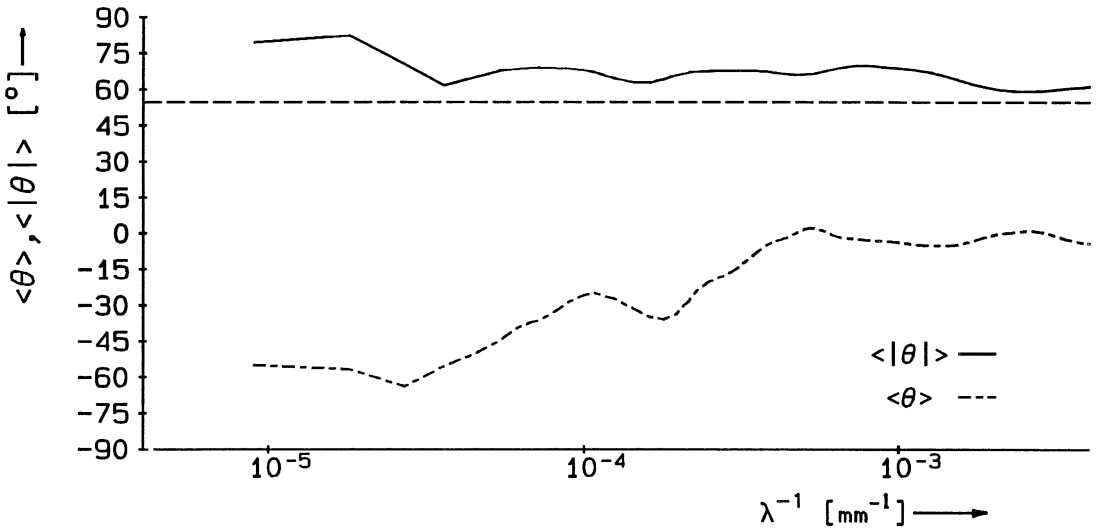

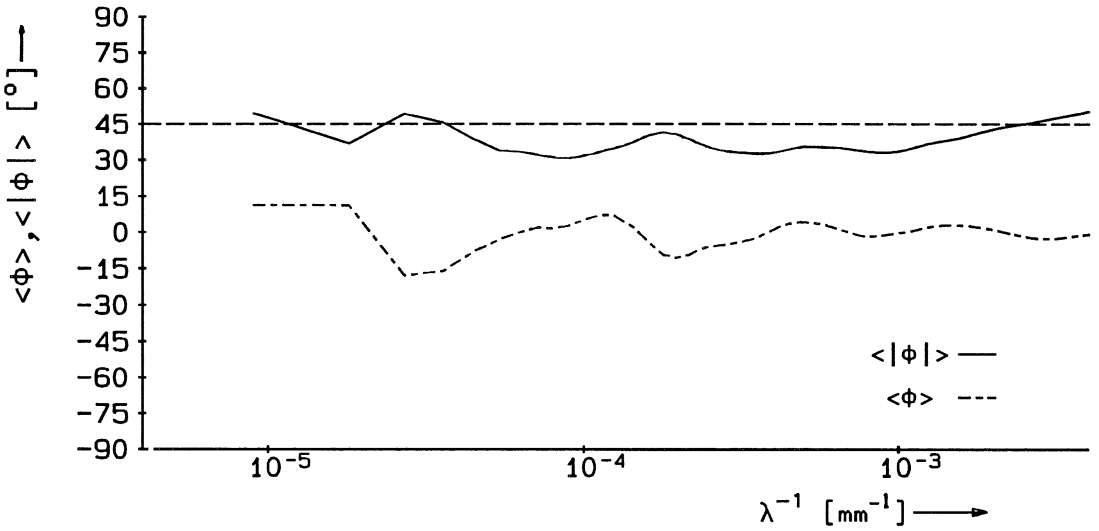

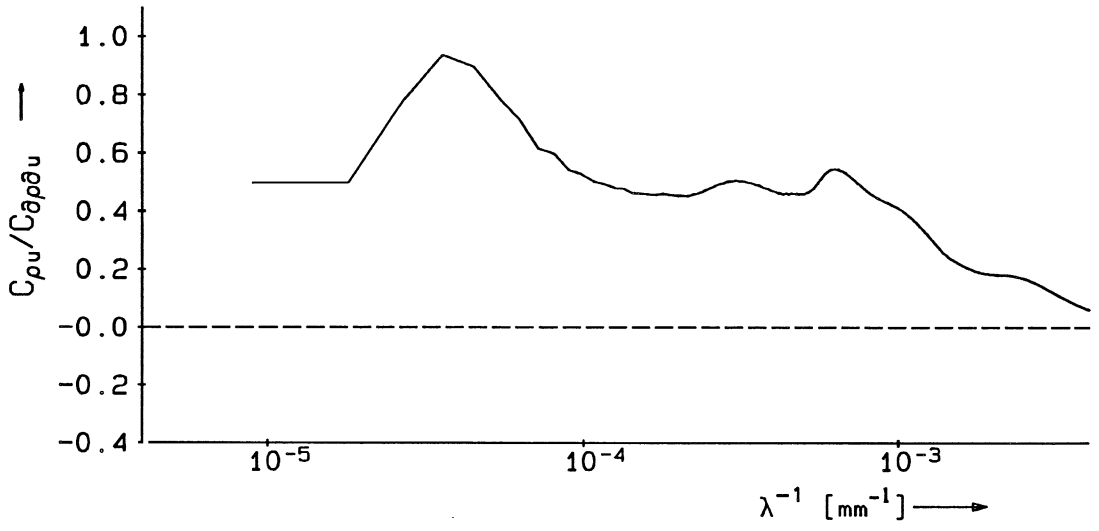

Normalized Stokes mass drift and IW angles.	06.04.14:07|100-130 mir	
Rotterdam Waterway (Ri=0.55;N=0.12 rad/s).	stok140.inv	
DELFT HYDRAULICS	Z 722	Fig.38d

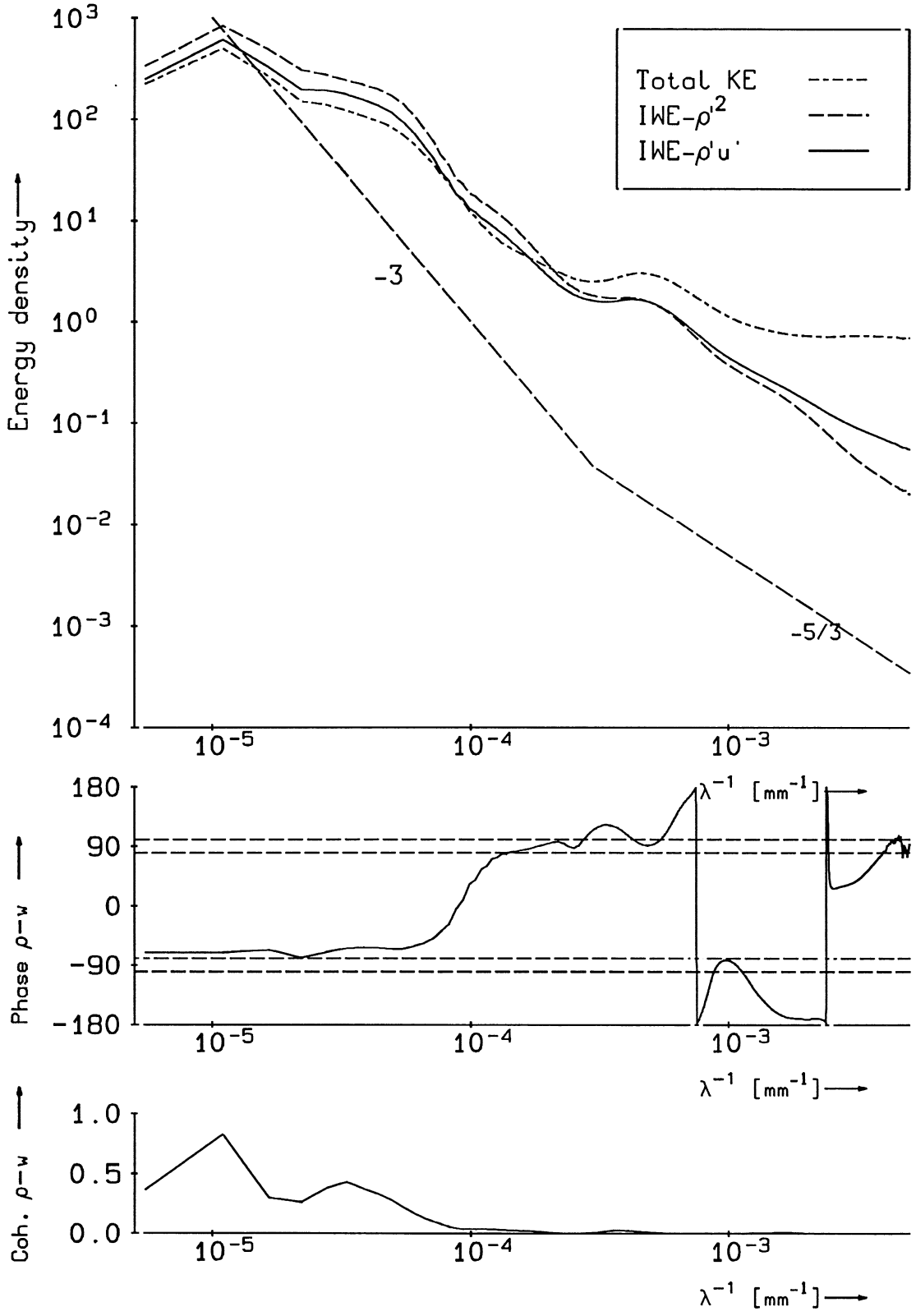

TKE-IWE decomposition. Field measurements in Rotterdam Waterway (Ri=0.48;N=0.17 rad/s).

06.04.14:59|152-182 mir

iwefield.145

DELFT HYDRAULICS

Z 722

Fig.39

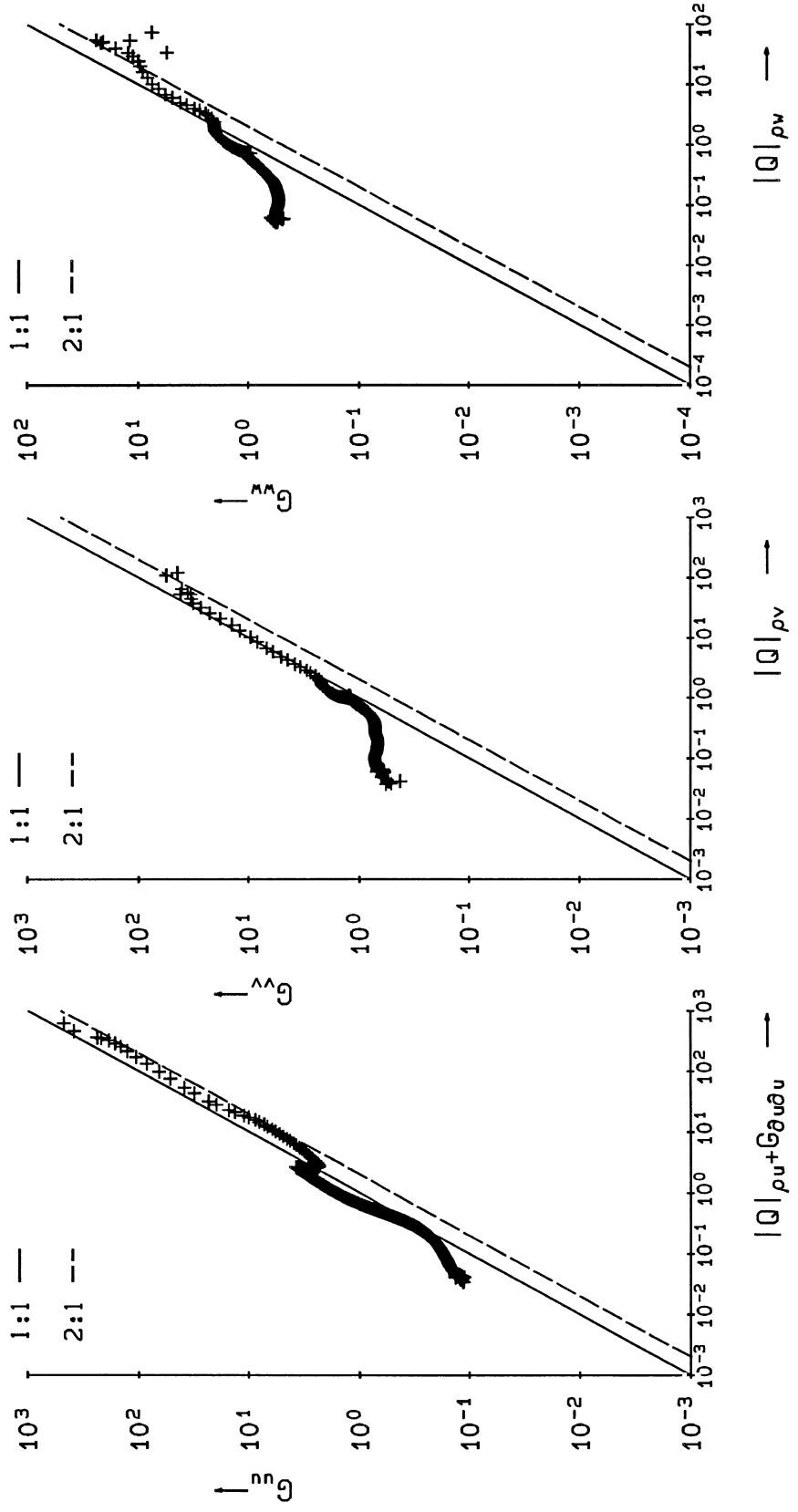

Absolute quad spectra compared with power spectra of velocity components u, v, and w.

06.04.14:59|152-182 mih

tet145.inv

DELFT HYDRAULICS

Z 722

Fig.39[b]

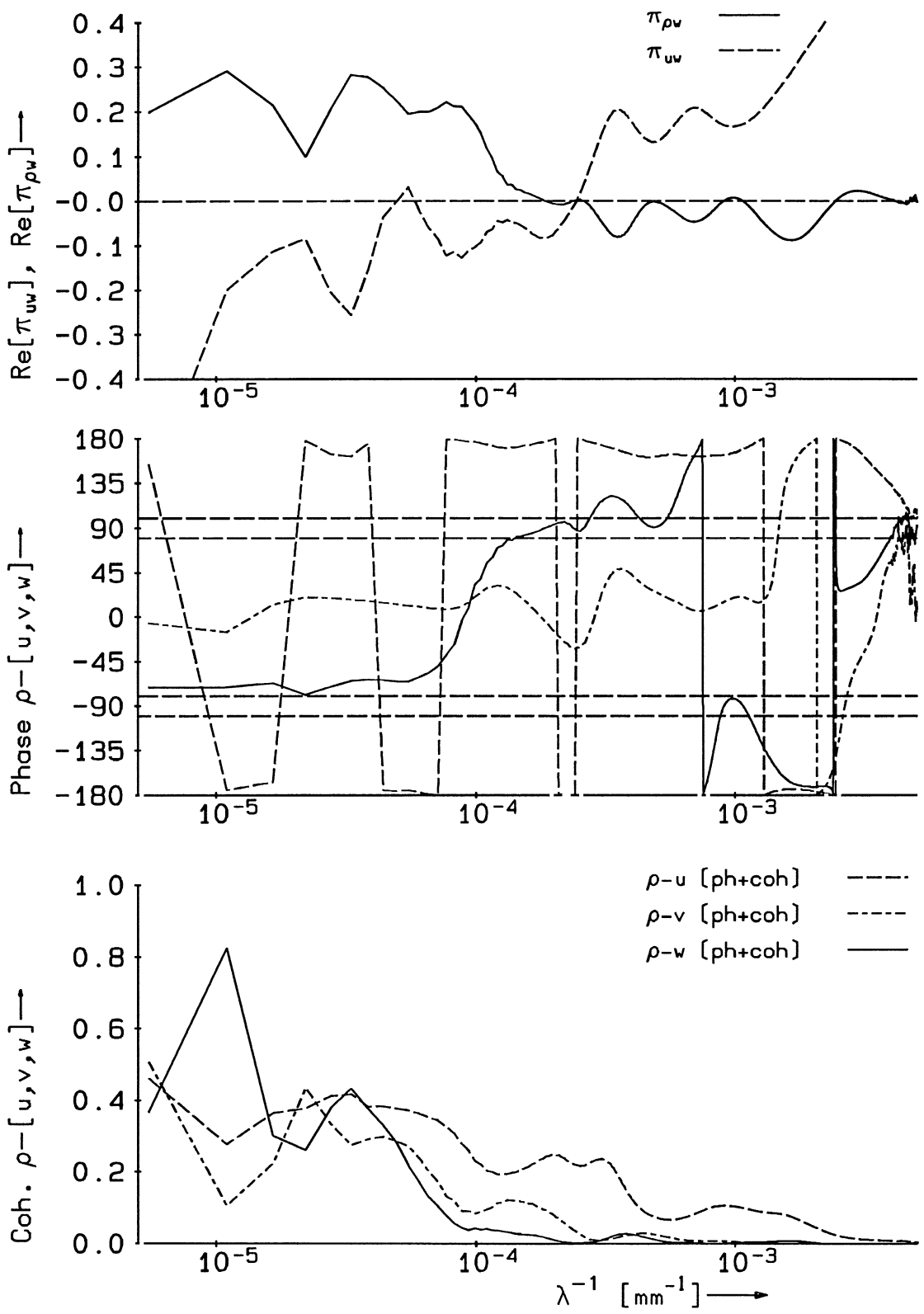

Phase, coherence, momentum and buoyancy fluxes.	06.04.14:59|152-182 min	
Rotterdam Waterway (Ri=0.48;N=0.17 rad/s).	iwe145.inv	
DELFT HYDRAULICS	Z 722	Fig.39c

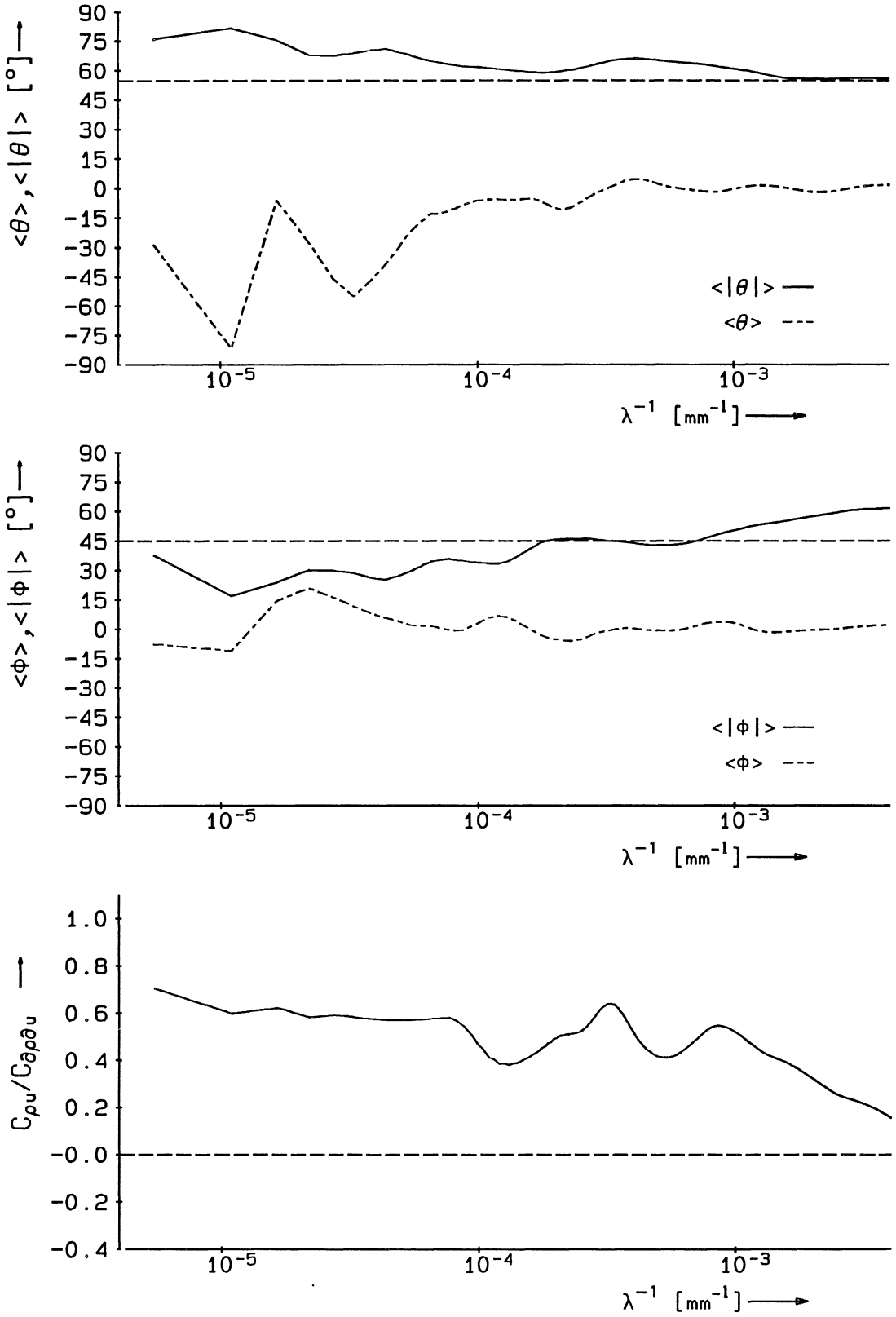

Normalized Stokes mass drift and IW angles.	06.04.14:59|152-182 mir	
Rotterdam Waterway (Ri=0.48;N=0.17 rad/s).	stok145.inv	
DELFT HYDRAULICS	Z 722	Fig.39[d]

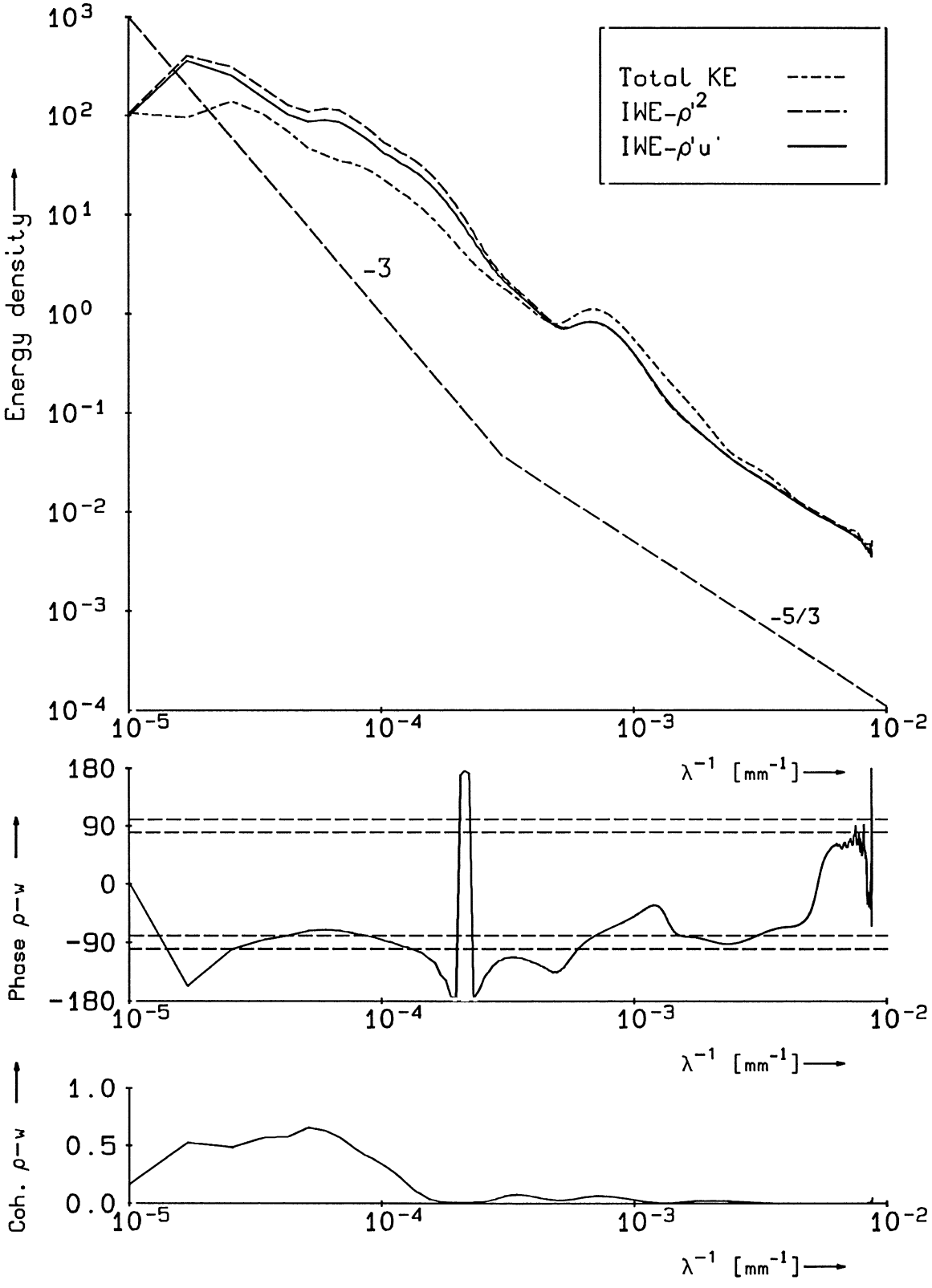

TKE-IWE decomposition. Field measurements in Rotterdam Waterway (Ri=0.63;N=0.17 rad/s).	06.04.15:36|189-219 min	
	iwefield.153	
DELFT HYDRAULICS	Z 722	Fig.40

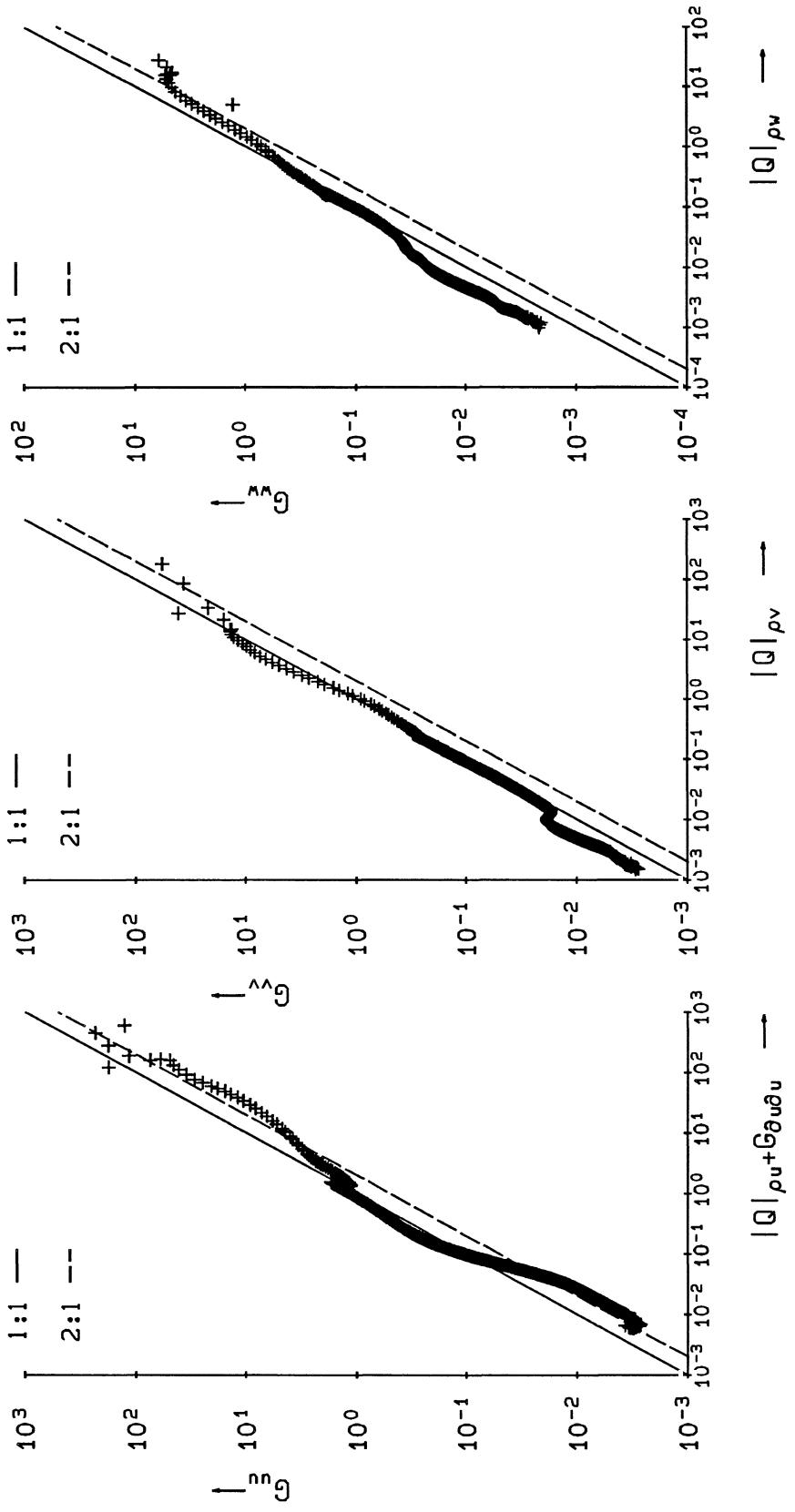

Absolute quad spectra compared with power spectra of velocity components u, v, and w.

06.04.15:36|189-219 mi

tet153.inv

DELFT HYDRAULICS

Z 722

Fig.40[b]

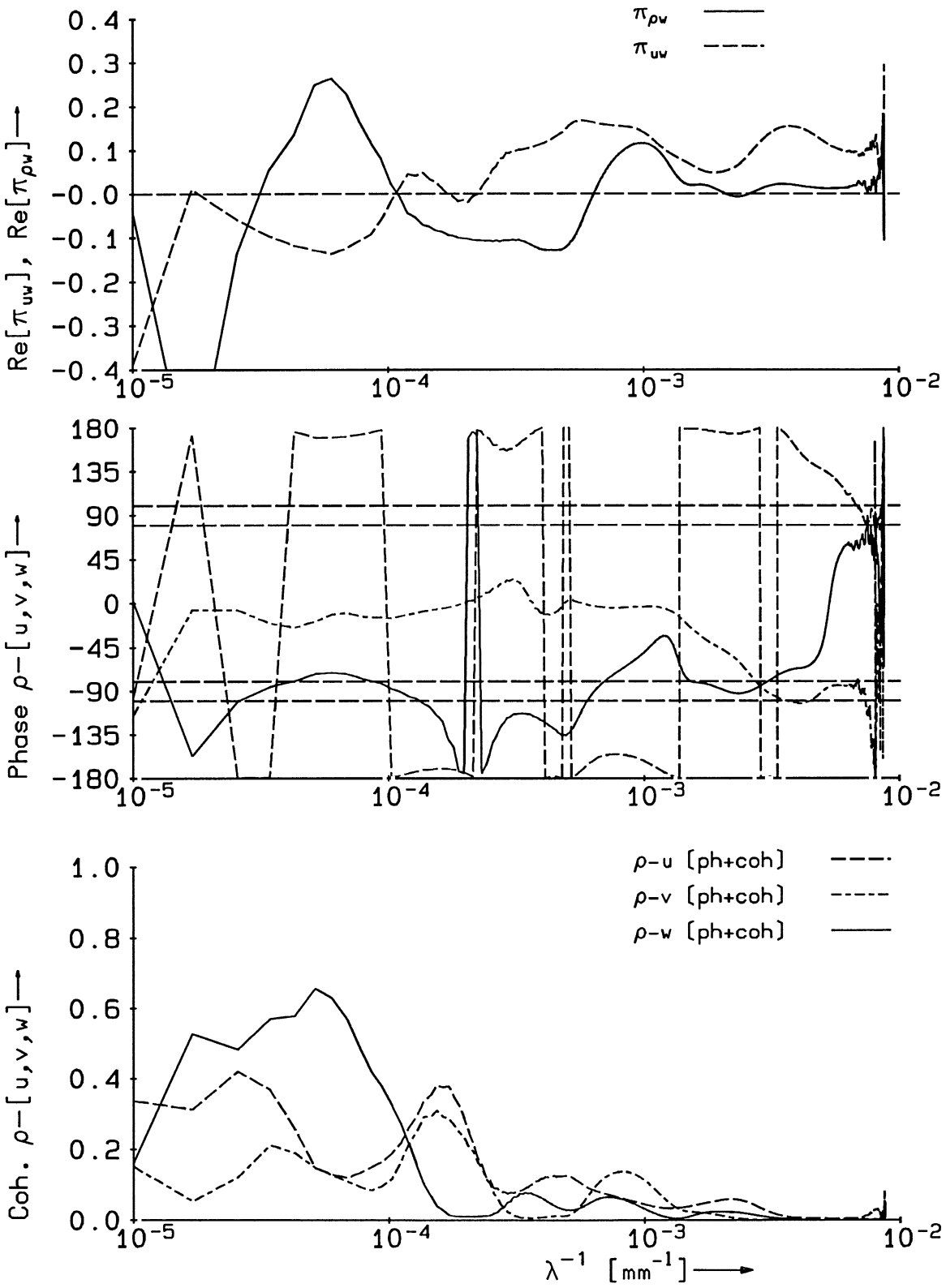

Phase, coherence, momentum and buoyancy fluxes.	06.04.15:36|189-219 mir	
Rotterdam Waterway (Ri=0.63;N=0.17 rad/s).	iwe153.inv	
DELFT HYDRAULICS	Z 722	Fig.40c

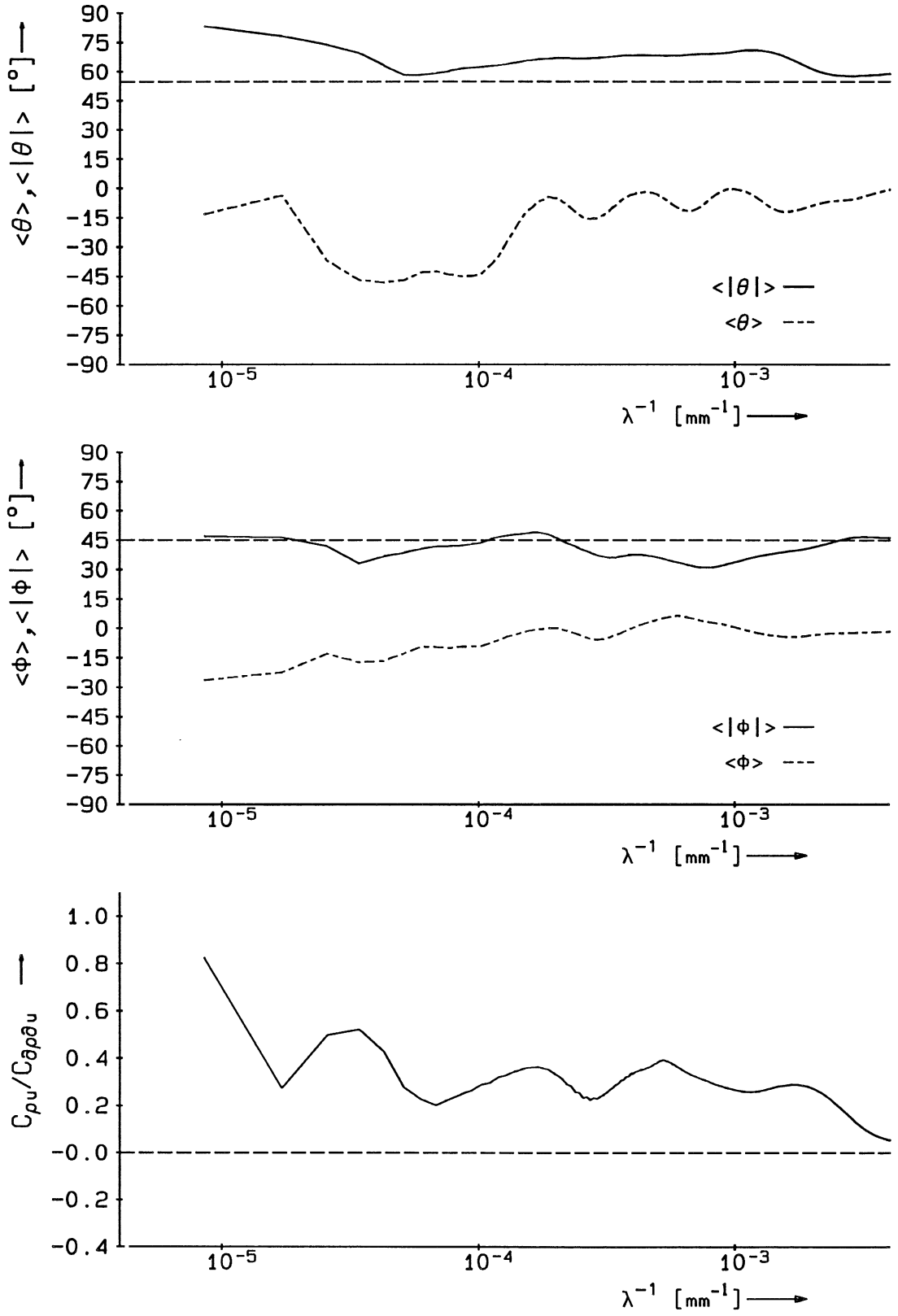

Normalized Stokes mass drift and IW angles.	06.04.15:36|189-219 mir	
Rotterdam Waterway (Ri=0.63;N=0.17 rad/s).	stok153.inv	
DELFT HYDRAULICS	Z 722	Fig.40[d]

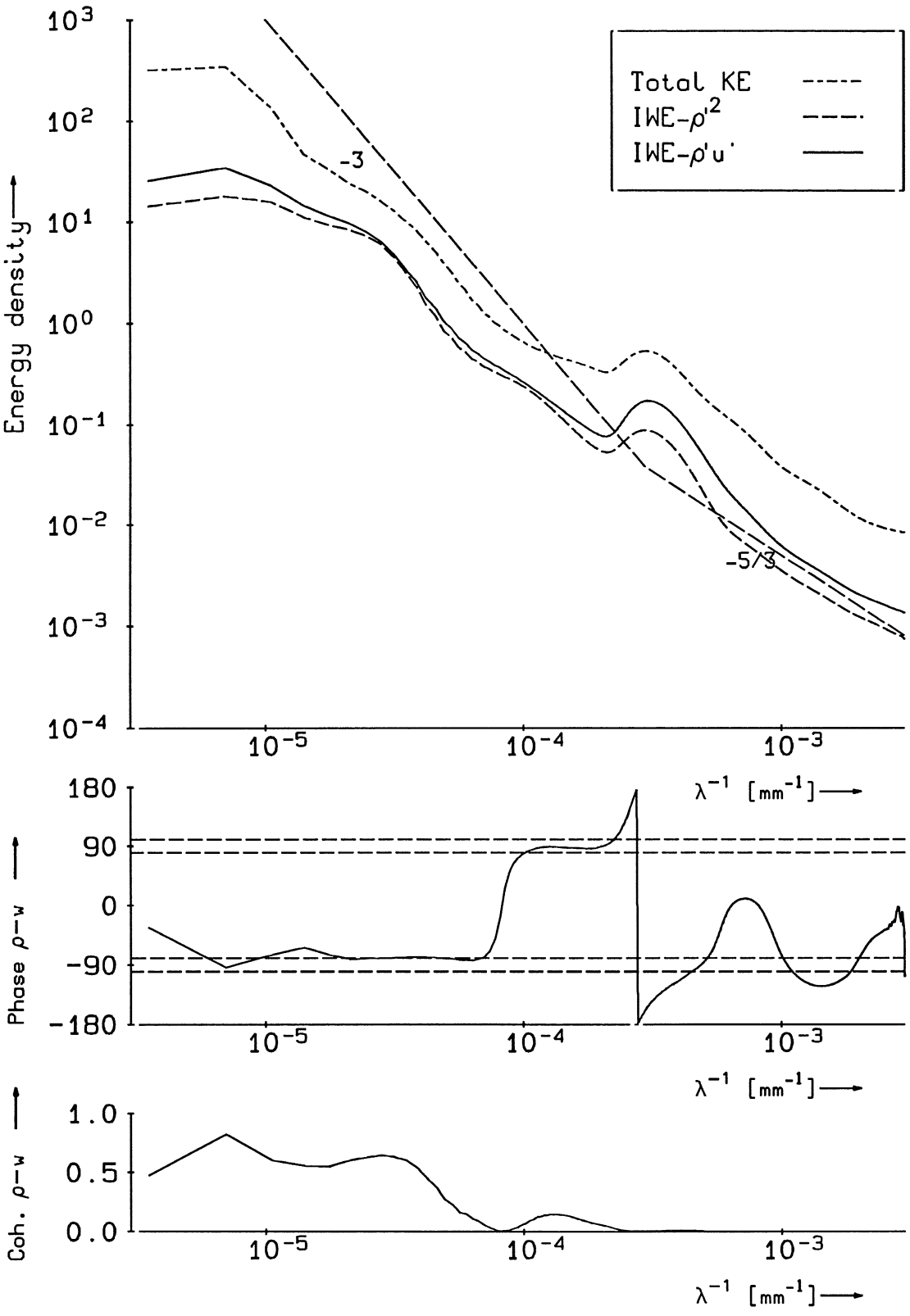

TKE-IWE decomposition. Field measurements in Rotterdam Waterway (Ri=2.2;N=0.18 rad/s).

06.04.16:15|228-258 min

iwefield.161

DELFT HYDRAULICS

Z 722

Fig.41

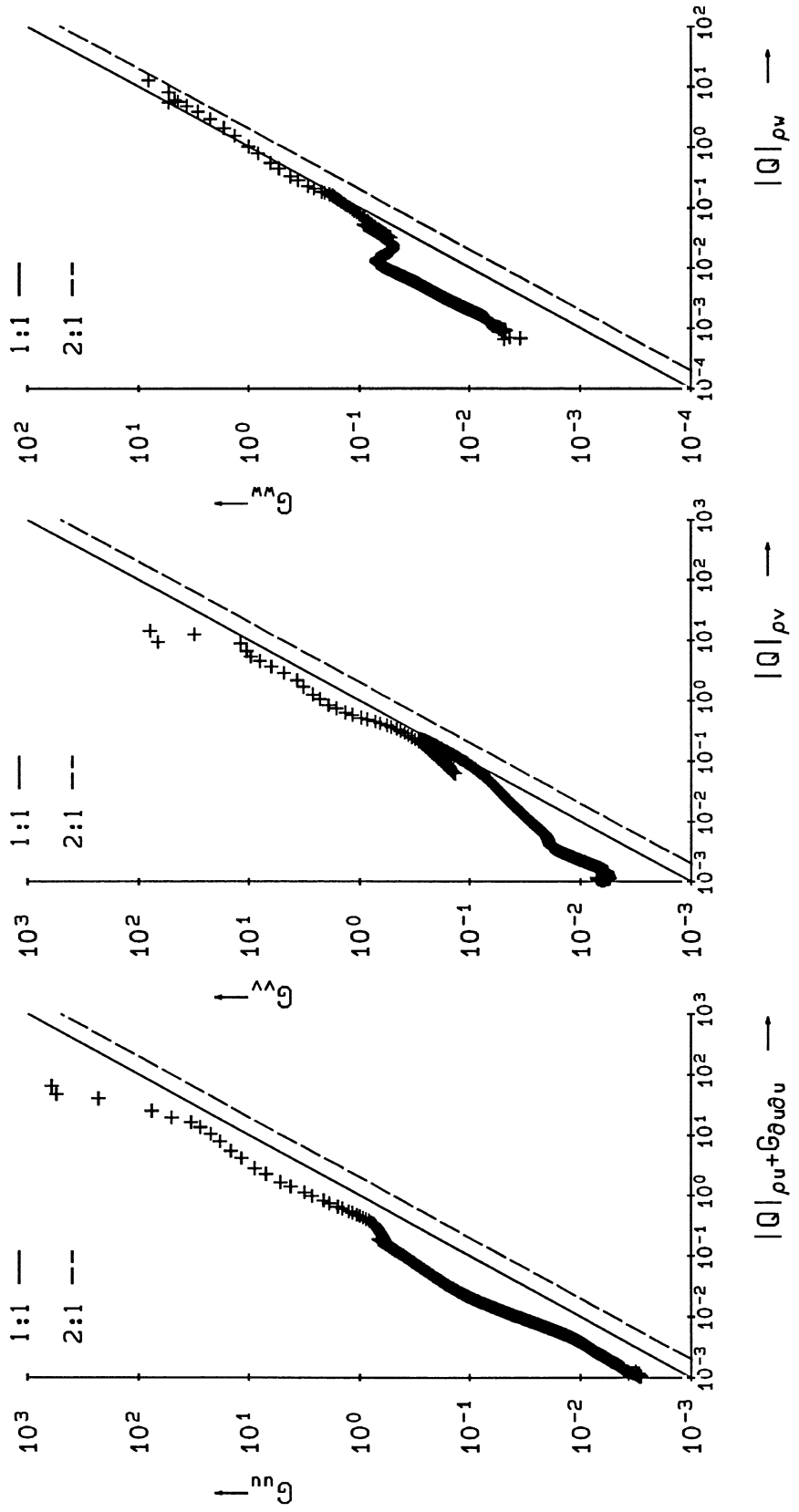

Absolute quad spectra compared with power spectra of velocity components u, v, and w.	06.04.16:15|228-258 mi	
	tet161.inv	
DELFT HYDRAULICS	Z 722	Fig.41[b]

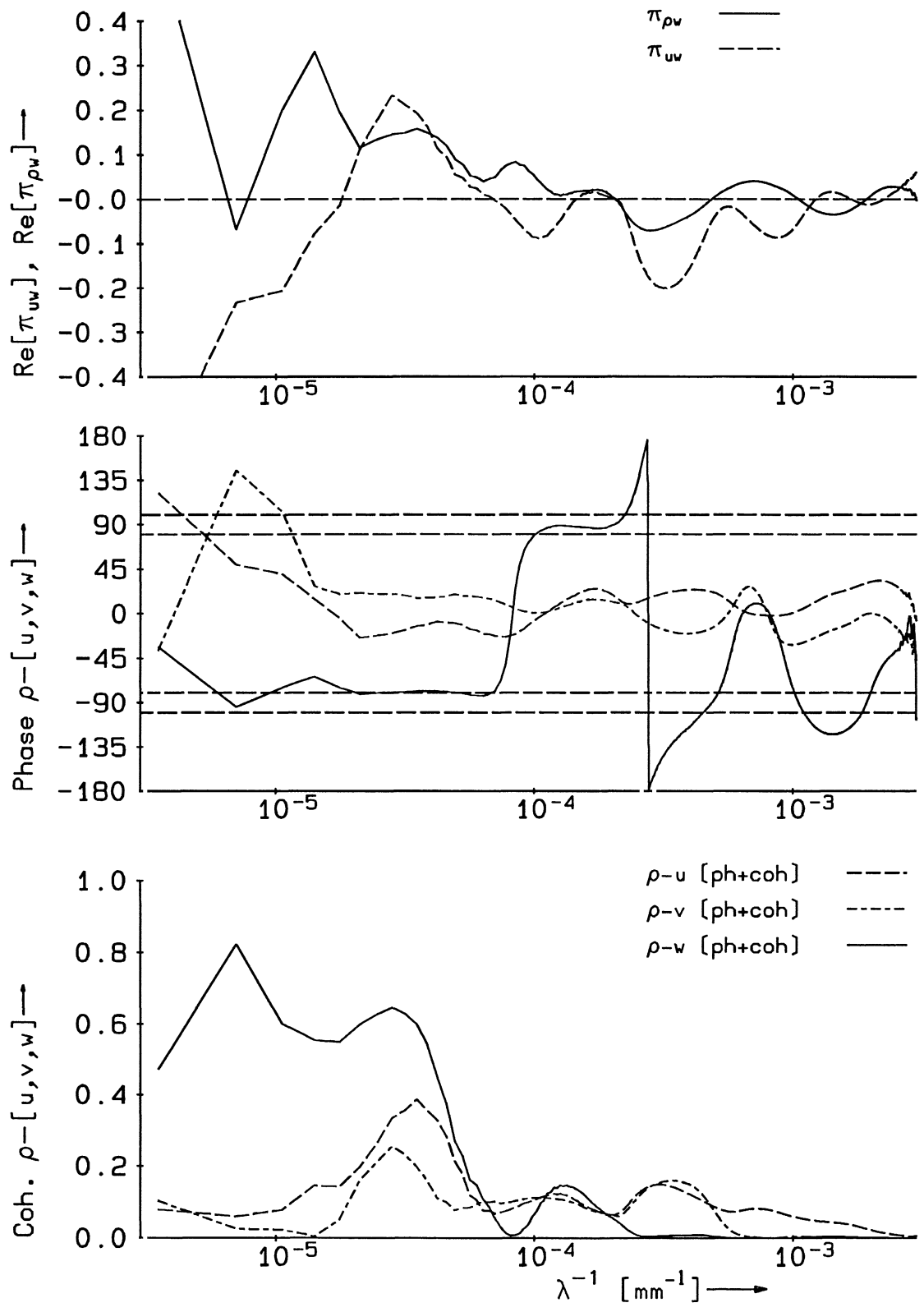

Phase, coherence, momentum and buoyancy fluxes. Rotterdam Waterway (Ri=2.2;N=0.18 rad/s).	06.04.16:151228-258 mir iwe161.inv	
DELFT HYDRAULICS	Z 722	Fig.41c

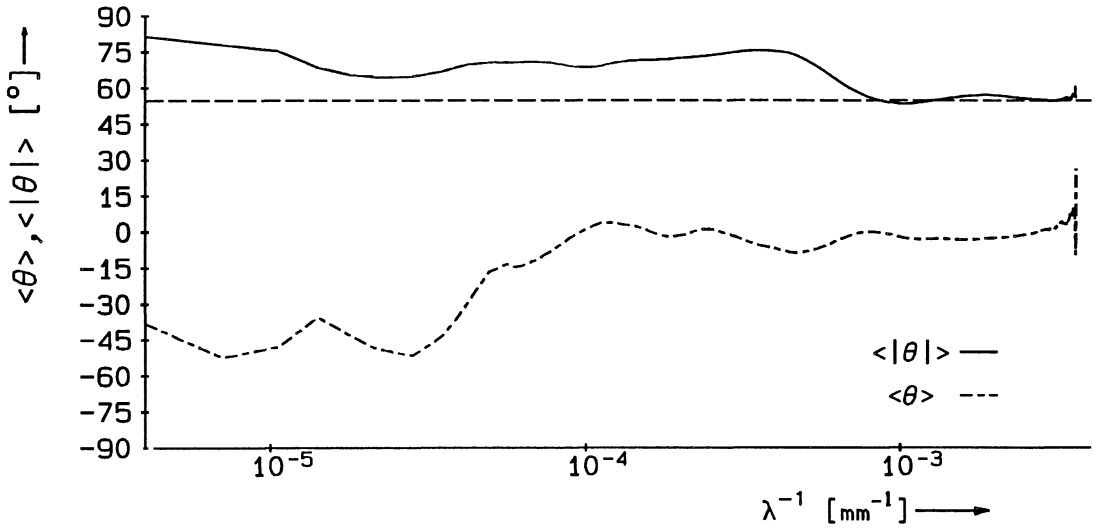

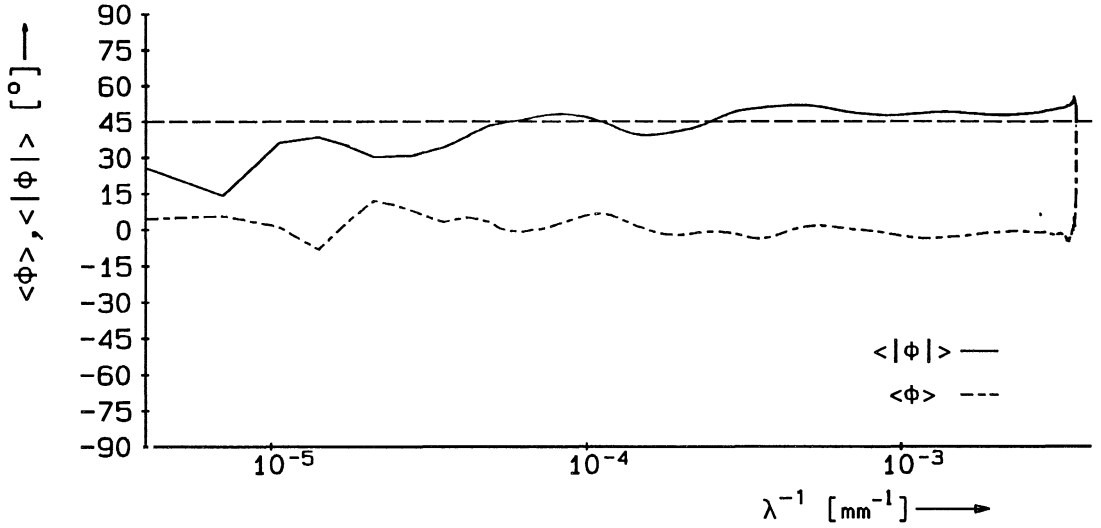

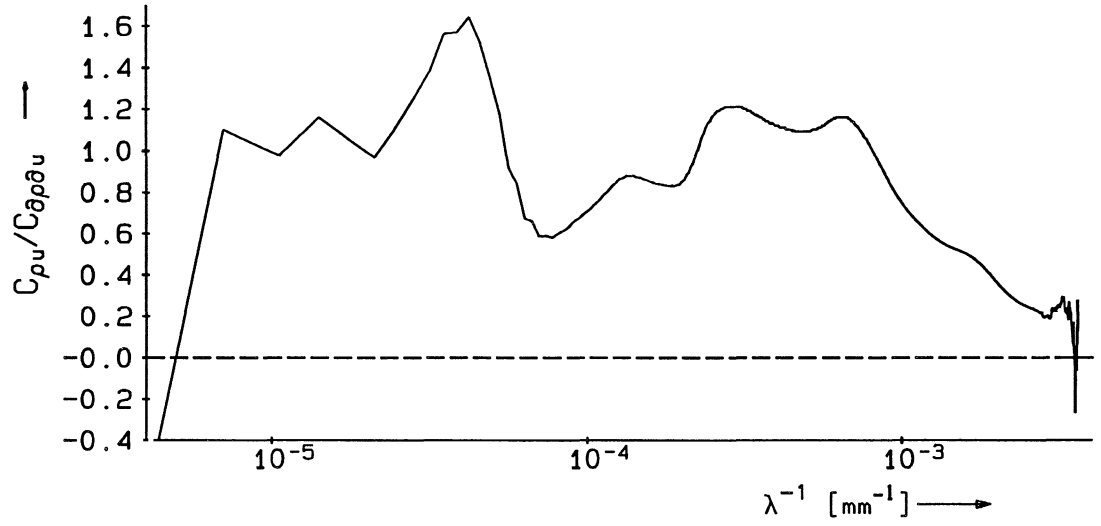

Normalized Stokes mass drift and IW angles.

Rotterdam Waterway (Ri=2.2;N=0.18 rad/s).

06.04.16:15|228-258 mir

stok161.inv

DELFT HYDRAULICS

Z 722

Fig.41d

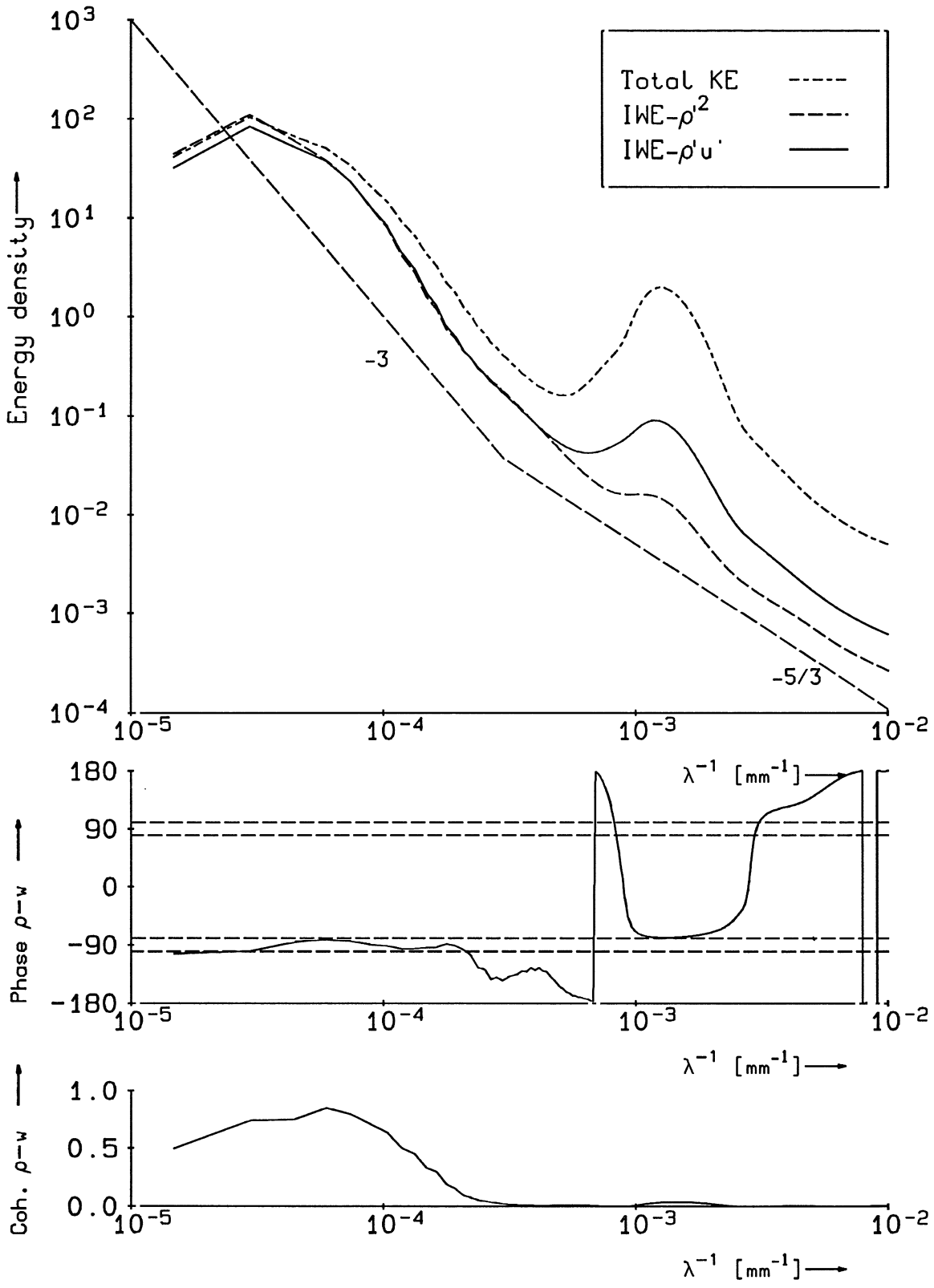

TKE-IWE decomposition. Field measurements in Caland channel (Ri=4.9;N=0.082 rad/s).

06.05.09:13|19-49 min

iwefield.913

DELFT HYDRAULICS

Z 722

Fig.42

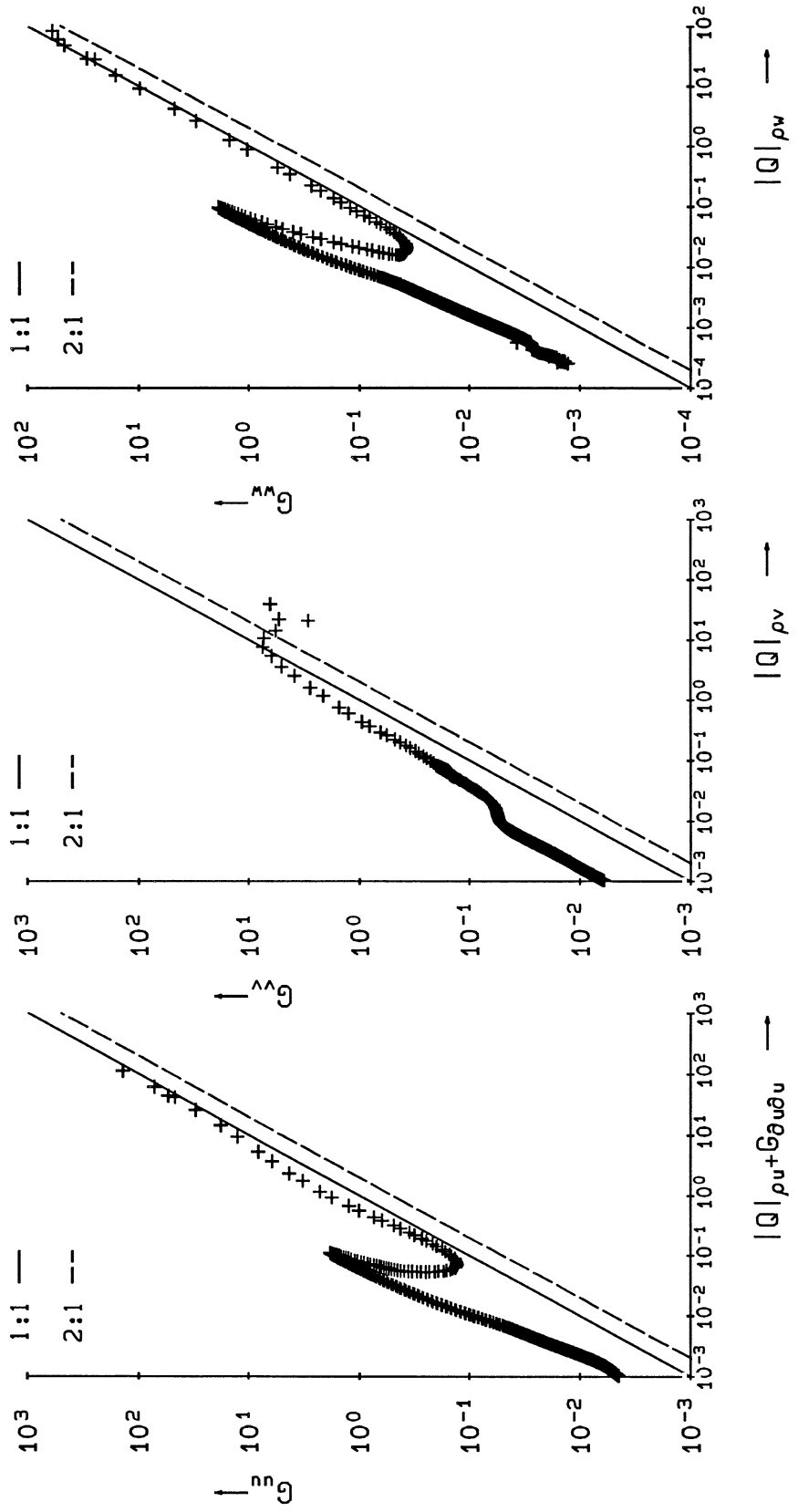

Absolute quad spectra compared with power spectra of velocity components u, v, and w.

06.05.09:13|19-49 min

tet913.inv

DELFT HYDRAULICS

Z 722

Fig.42[b]

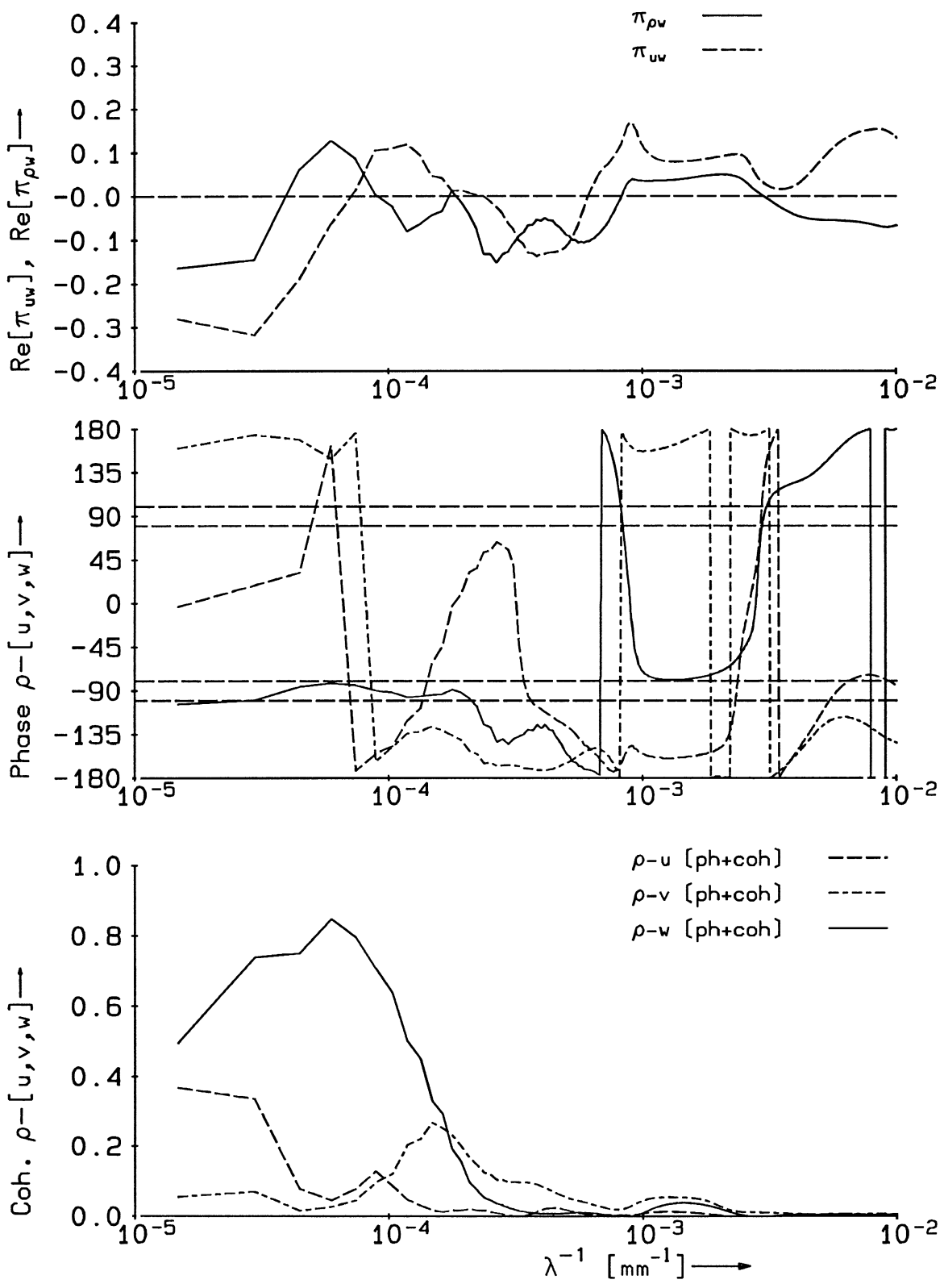

Phase, coherence, momentum and buoyancy fluxes.	06.05.09:13|19-49 min	
Caland channel (Ri=4.9;N=0.082 rad/s).	iwe913.inv	
DELFT HYDRAULICS	Z 722	Fig.42c

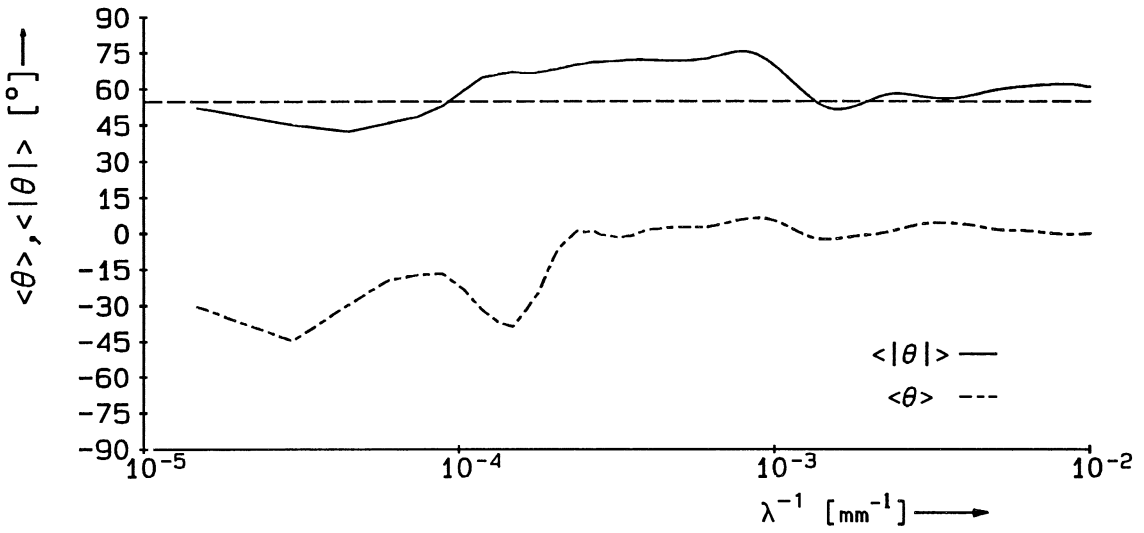

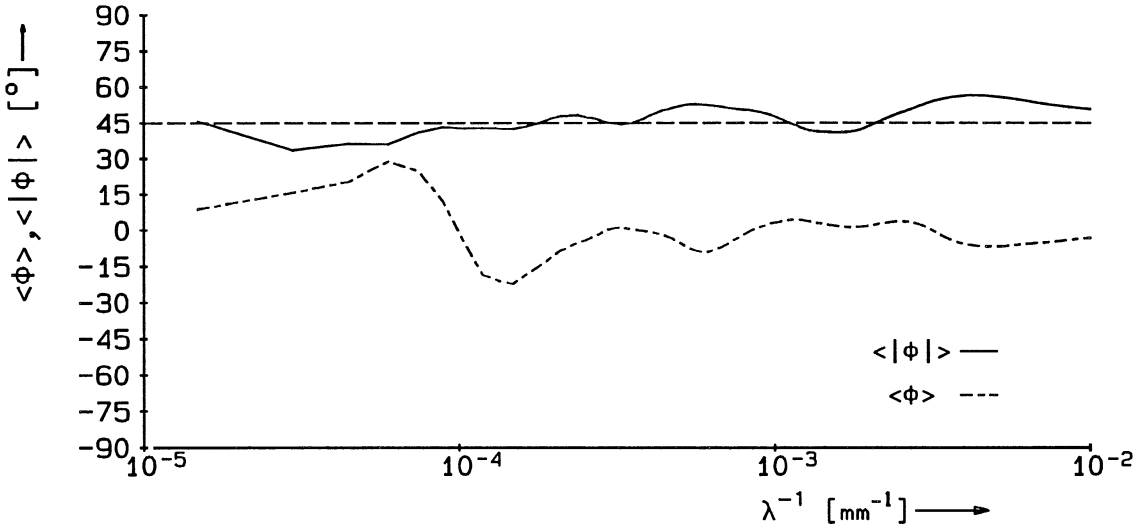

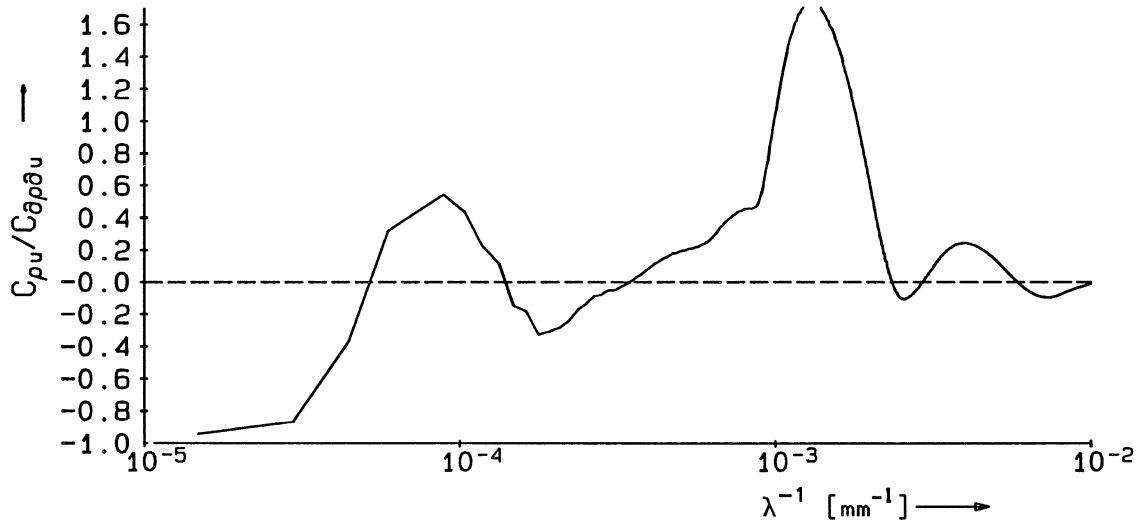

Normalized Stokes mass drift and IW angles. Rotterdam Waterway (Ri=4.9;N=0.082 rad/s).	06.05.09:13|19-49 min	
	stok913.inv	
DELFT HYDRAULICS	Z 722	Fig.42d

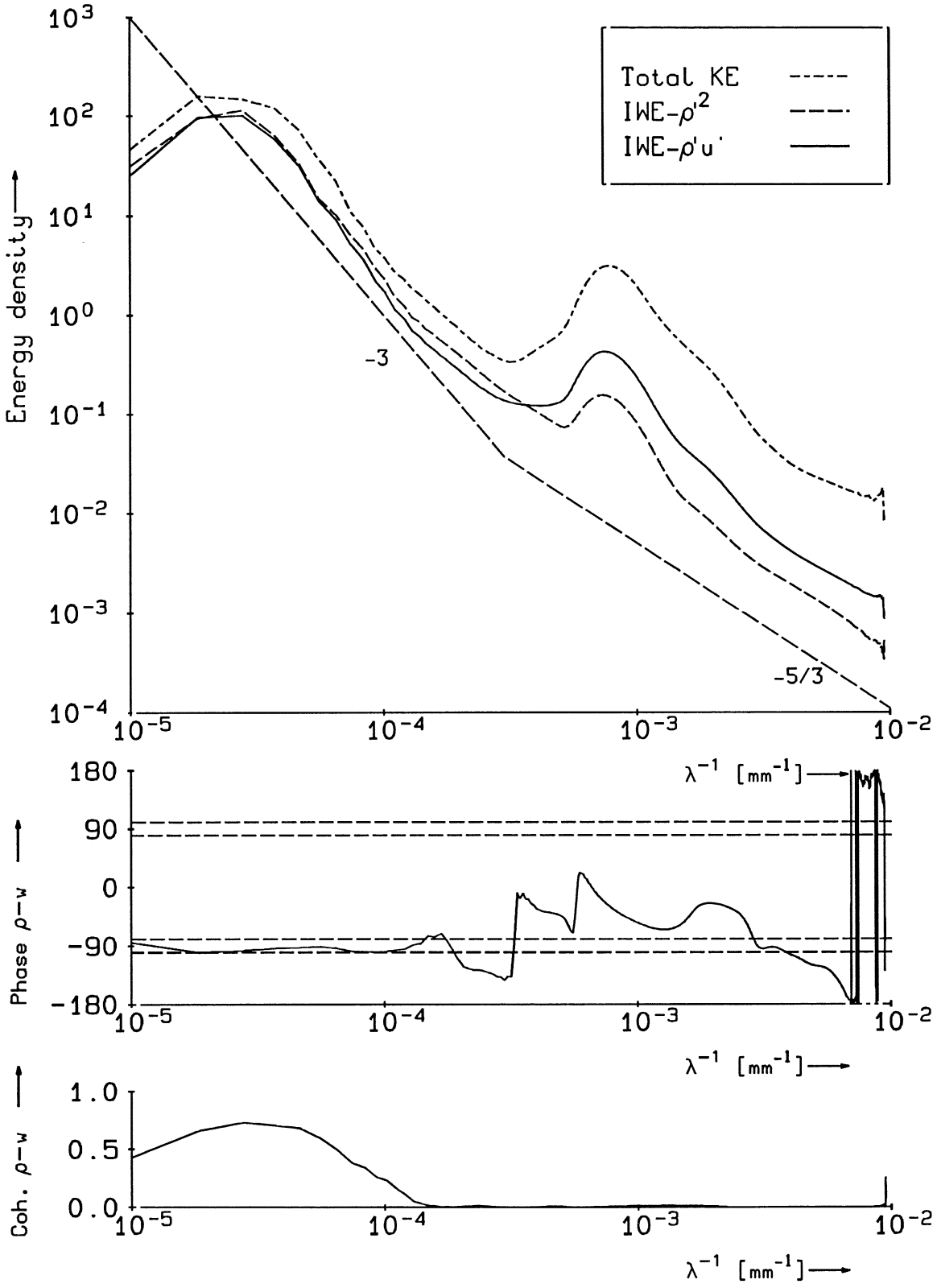

TKE-IWE decomposition. Field measurements in Caland channel (Ri=0.85;N=0.079 rad/s).

06.05.09:53|59-89 min

iwefield.953

DELFT HYDRAULICS

Z 722

Fig.43

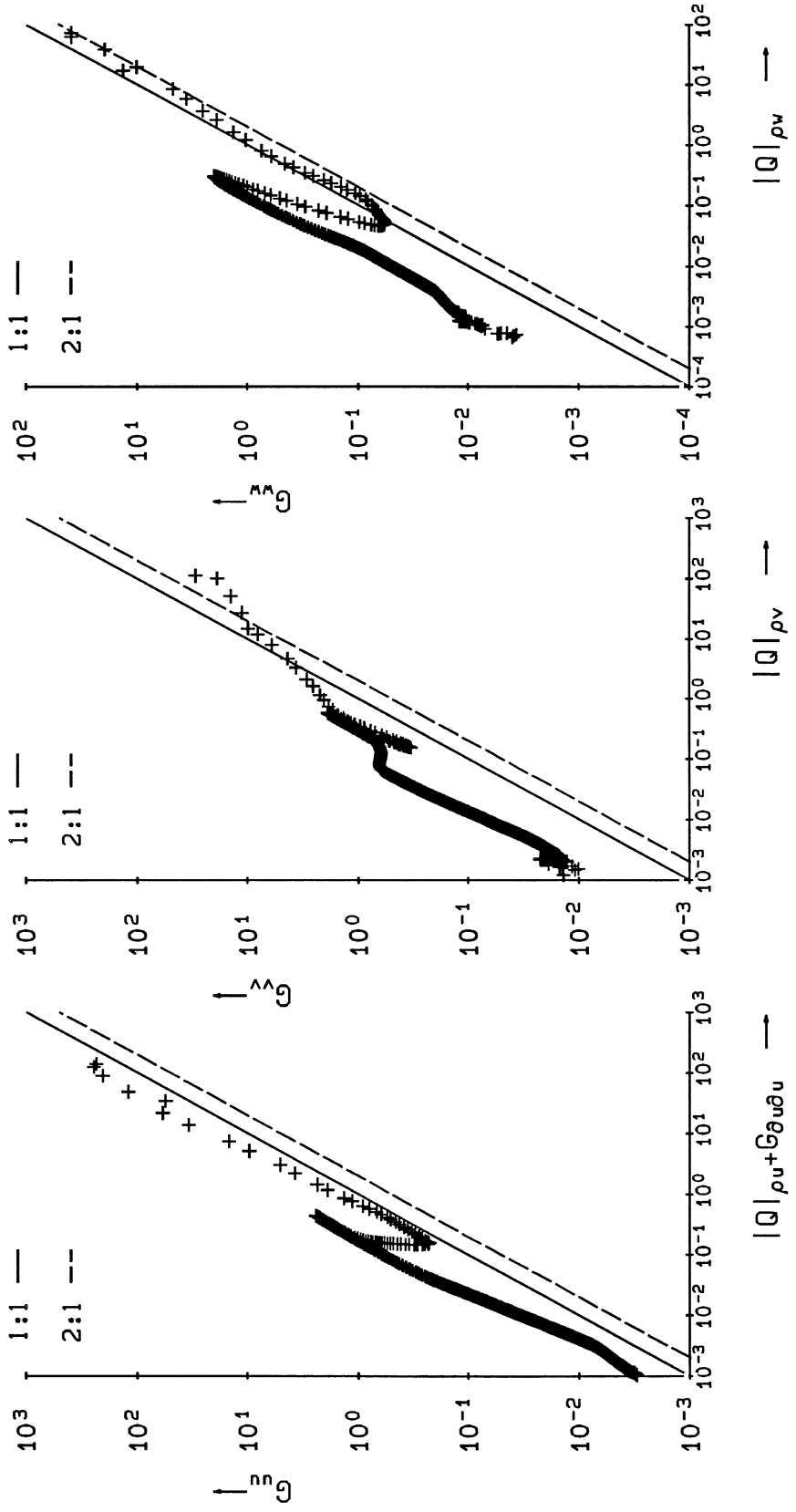

Absolute quad spectra compared with power spectra of velocity components u, v, and w.

06.05.09:53|59-89 min

tet953.inv

DELFT HYDRAULICS

Z 722

Fig.43[b]

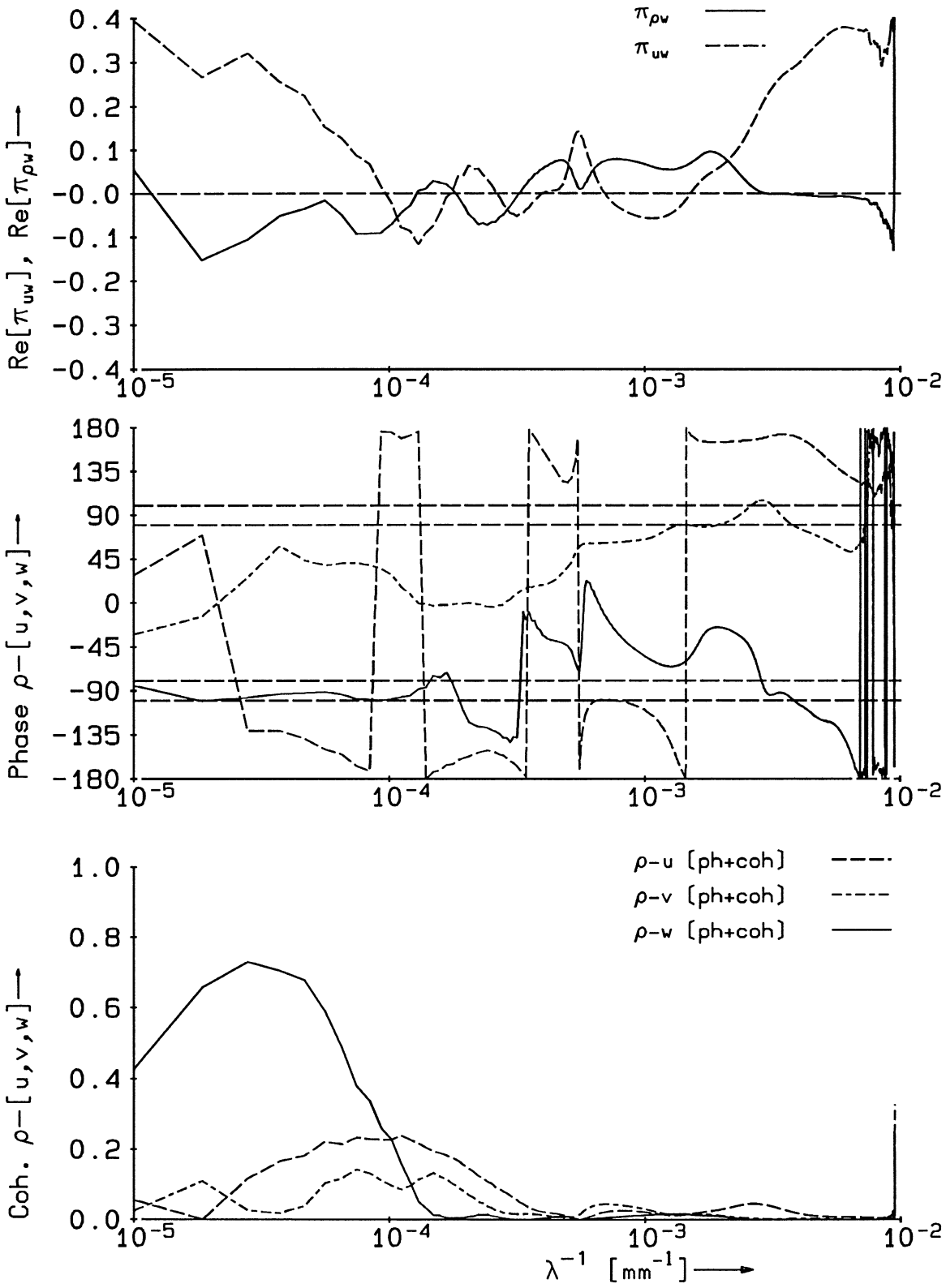

Phase, coherence, momentum and buoyancy fluxes.	06.05.09:53|59-89 min	
Caland channel [Ri=0.85;N=0.079 rad/s].	iwe953.inv	
DELFT HYDRAULICS	Z 722	Fig.43c

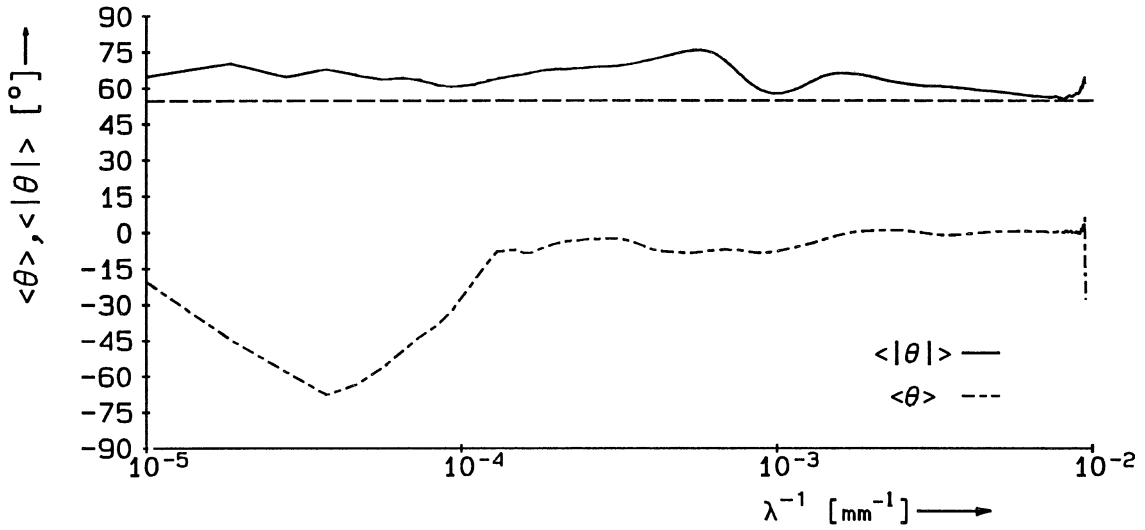

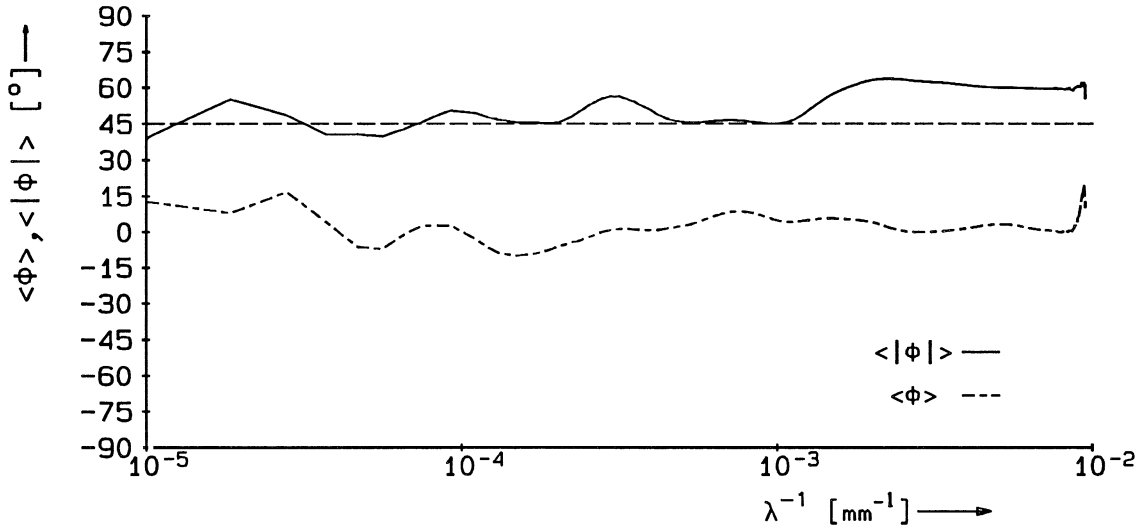

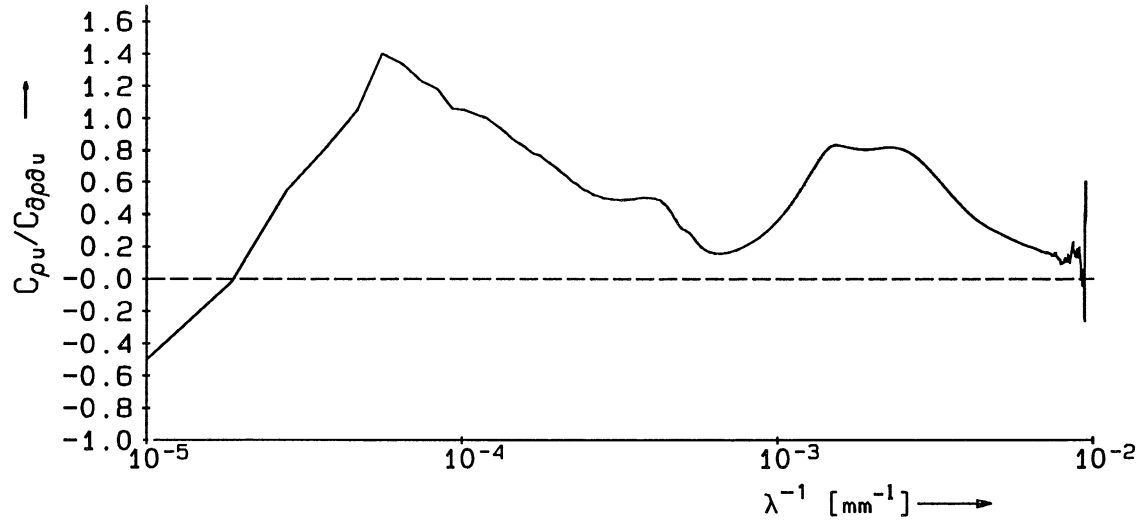

Normalized Stokes mass drift and IW angles.	06.05.09:53|59-89 min	
Rotterdam Waterway (Ri=0.85;N=0.079 rad/s).	stok953.inv	
DELFT HYDRAULICS	Z 722	Fig.43[d]

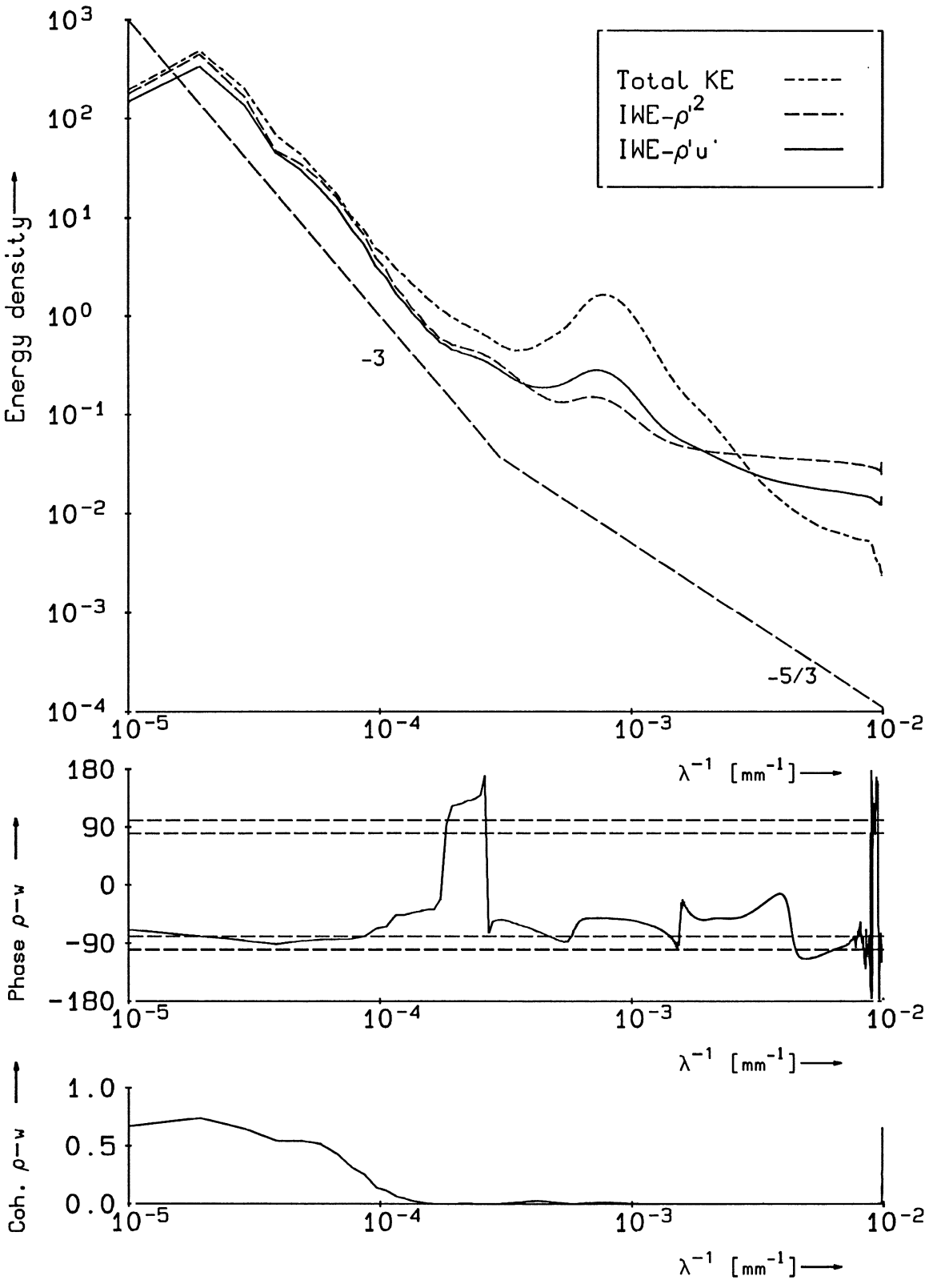

TKE-IWE decomposition. Field measurements in Caland channel (Ri=3.9;N=0.063 rad/s).	06.05.10:35\101-131 min iwefield.103	
DELFT HYDRAULICS	Z 722	Fig.44

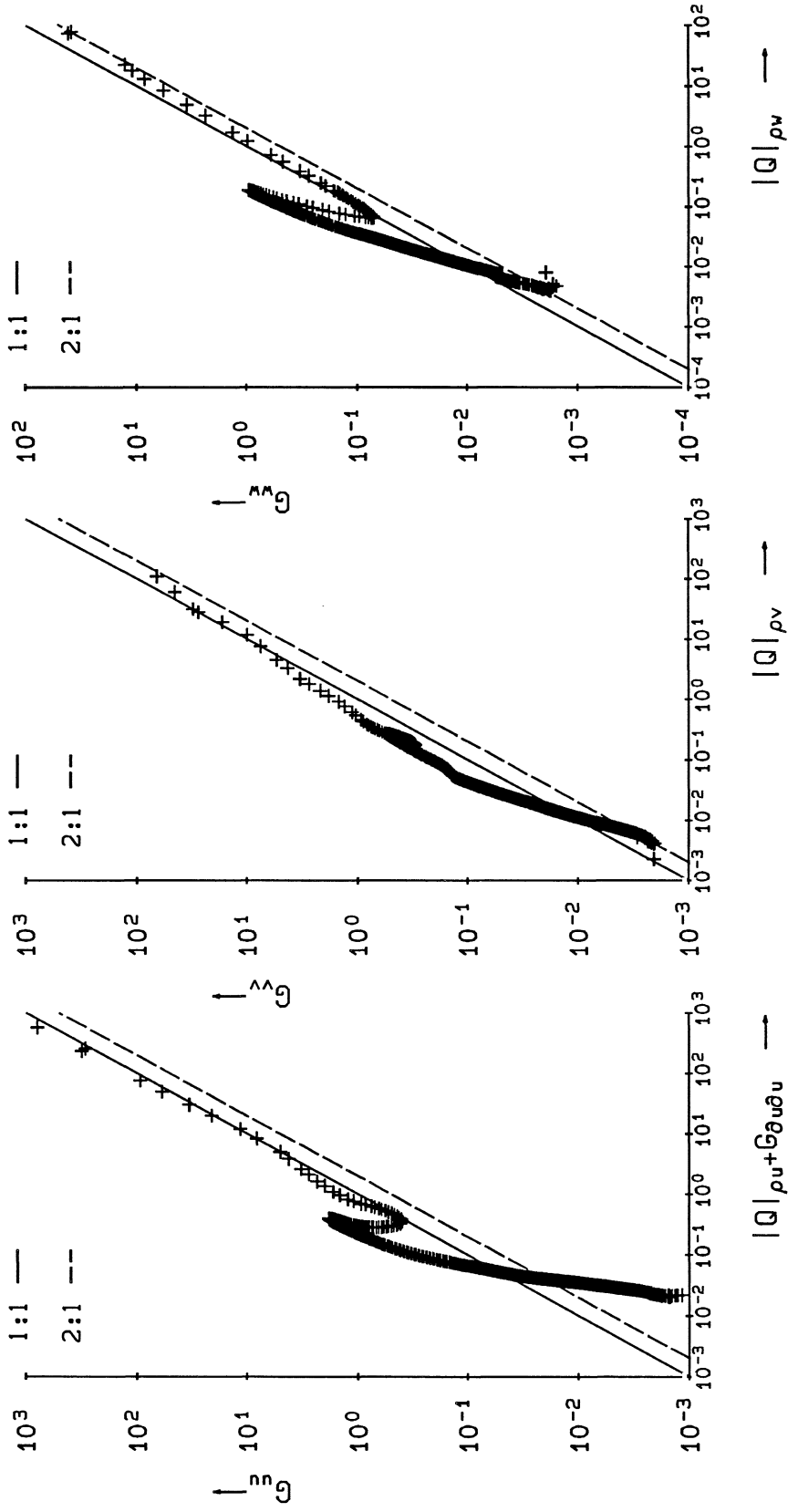

Absolute quad spectra compared with power spectra of velocity components u, v, and w.

06.05.10:35|101-131 min

tet103.inv

DELFT HYDRAULICS

Z 722

Fig.44b

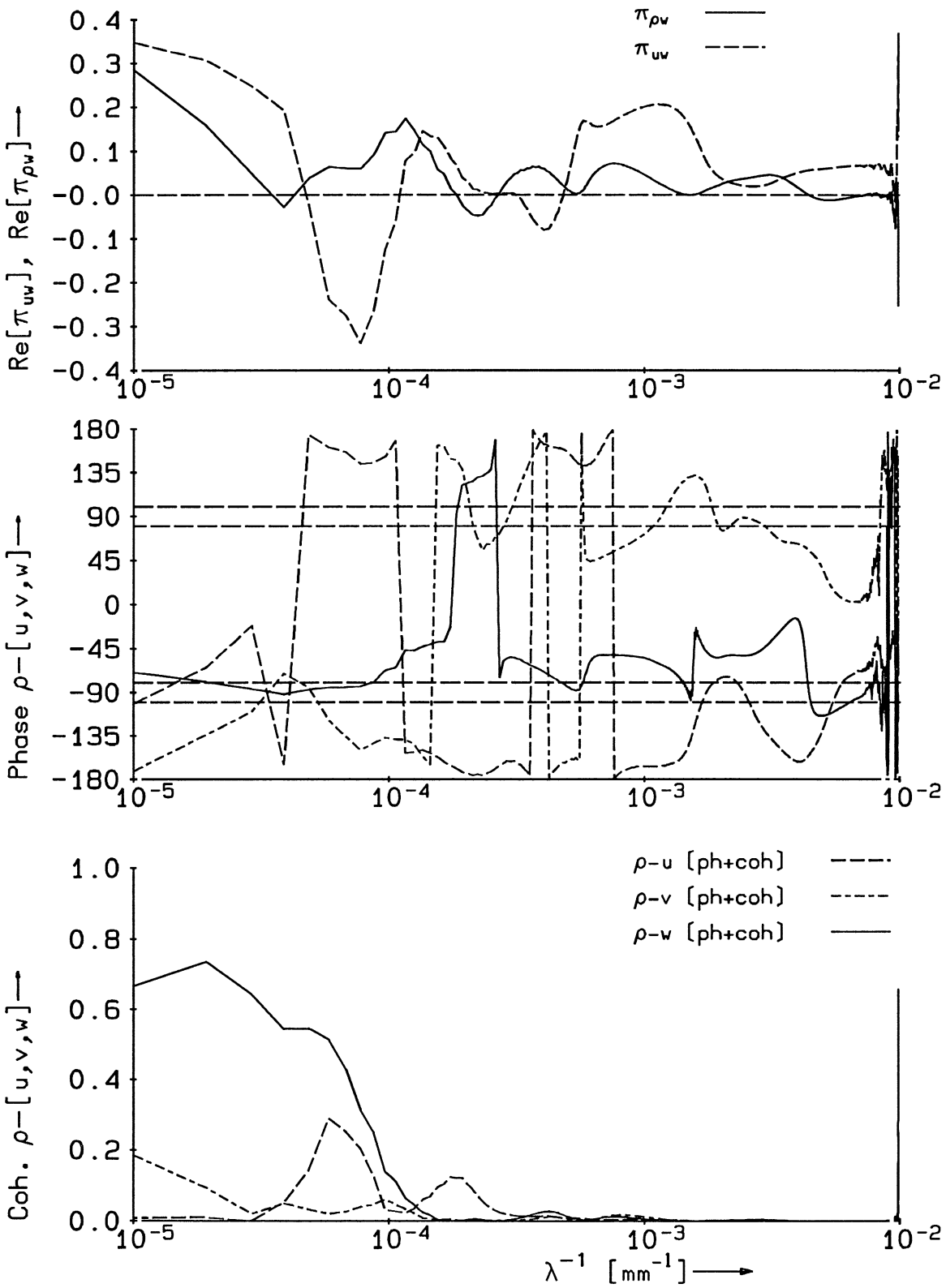

Phase, coherence, momentum and buoyancy fluxes.	06.05.10:35|101-131 mir	
Caland channel (Ri=3.9;N=0.063 rad/s).	iwe103.inv	
DELFT HYDRAULICS	Z 722	Fig.44c

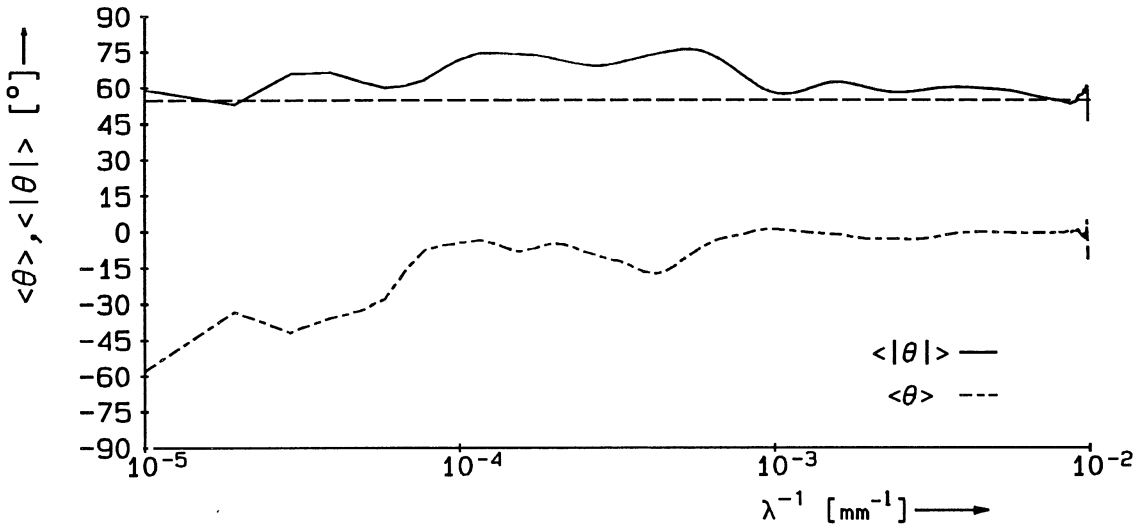

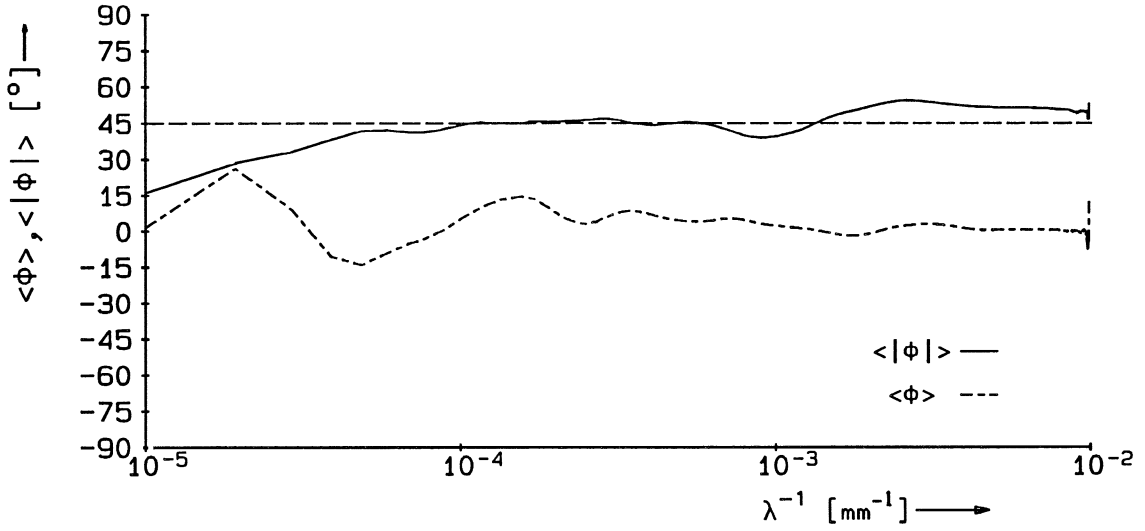

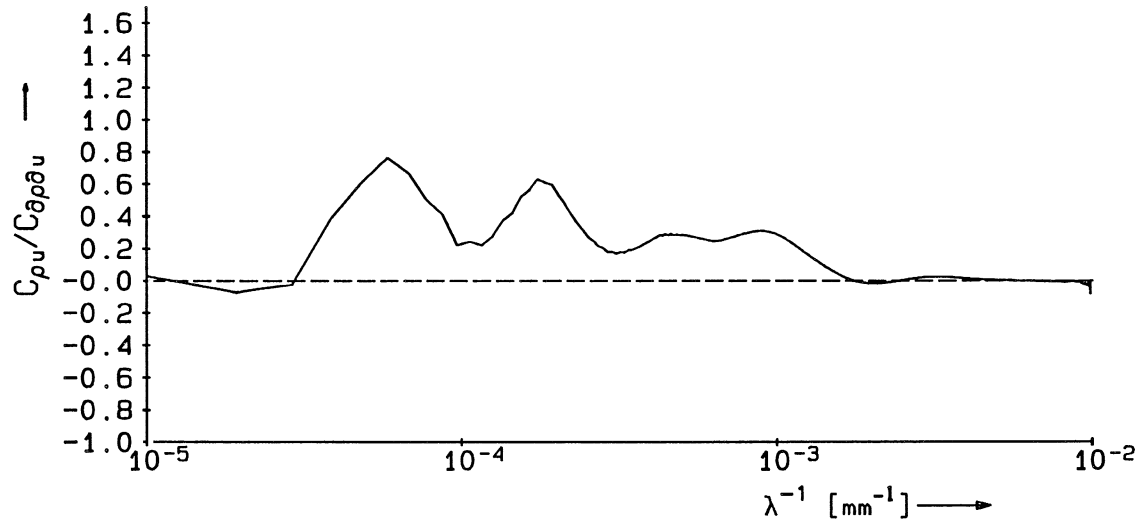

Normalized Stokes mass drift and IW angles. Rotterdam Waterway (Ri=3.9;N=0.063 rad/s).	06.05.10:35\101-131 mir	
	stok103.inv	
DELFT HYDRAULICS	Z 722	Fig.44d

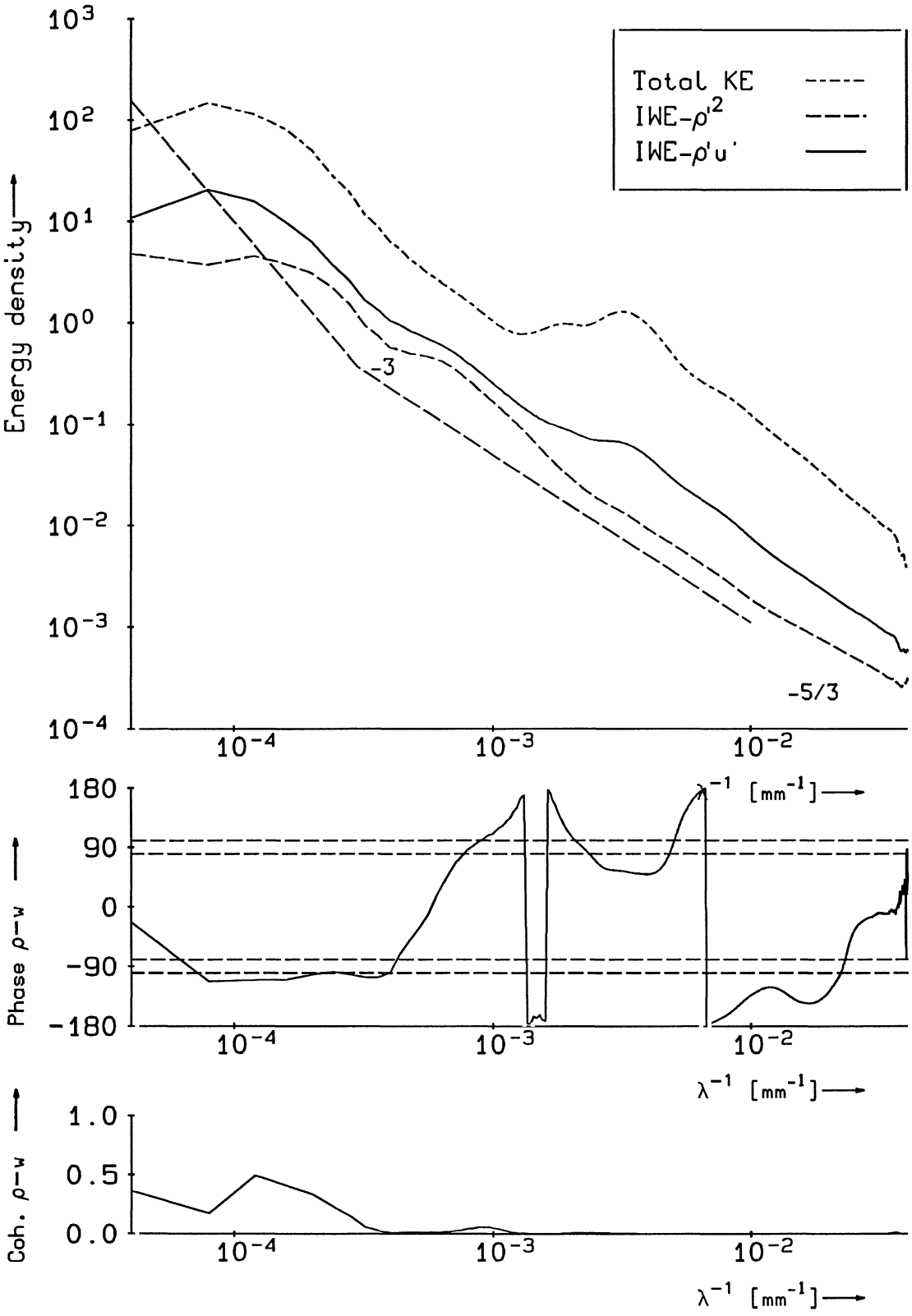

TKE-IWE decomposition. Field measurements in Caland channel (Ri=3.6;N=0.062 rad/s).

06.05.11:11|137-167 mir

iwefield.111

DELFT HYDRAULICS

Z 722

Fig.45

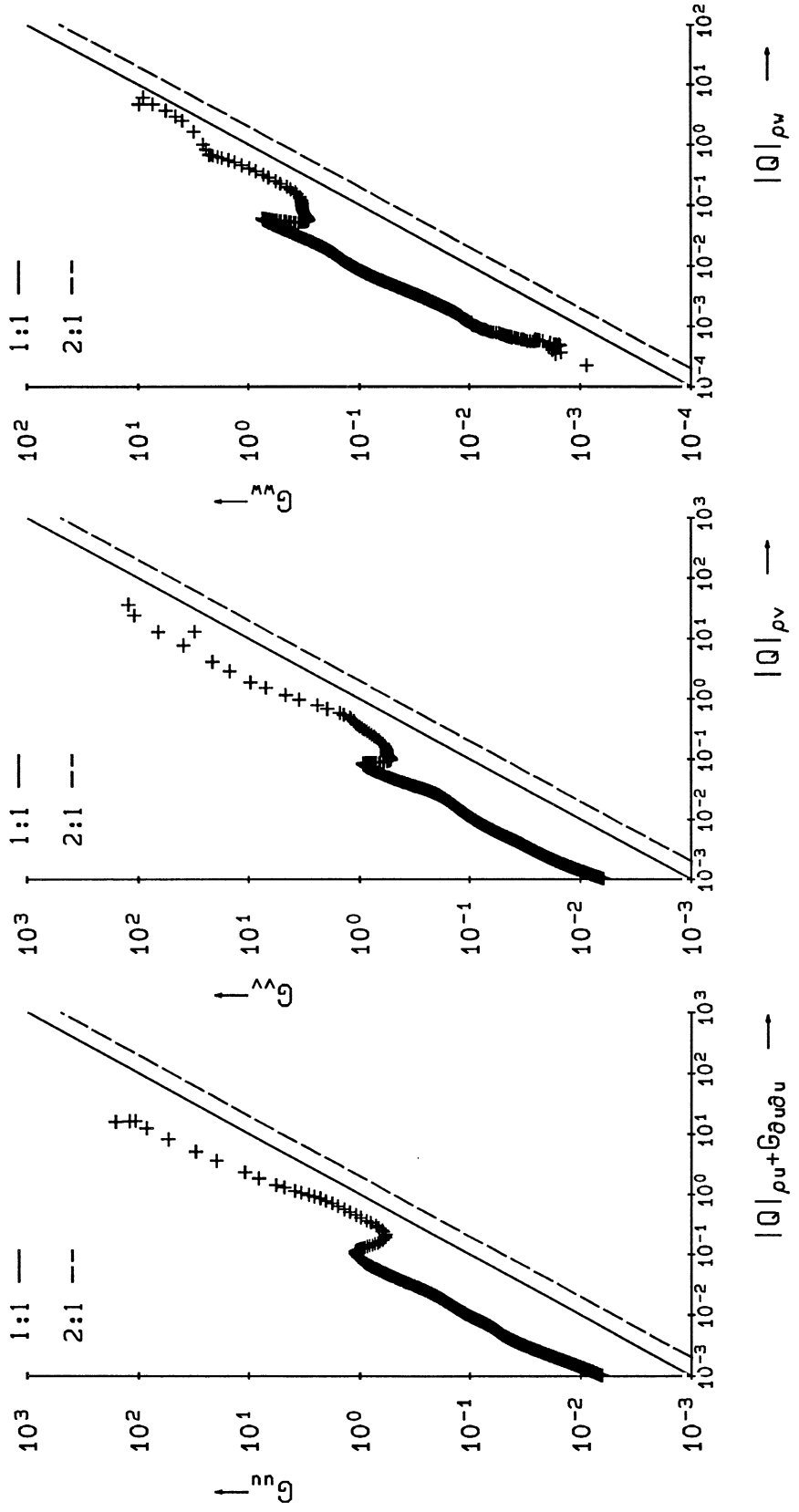

Absolute quad spectra compared with power spectra of velocity components u, v, and w.

06.05.11:11|137-167 mi

tet111.inv

DELFT HYDRAULICS

Z 722

Fig.45b

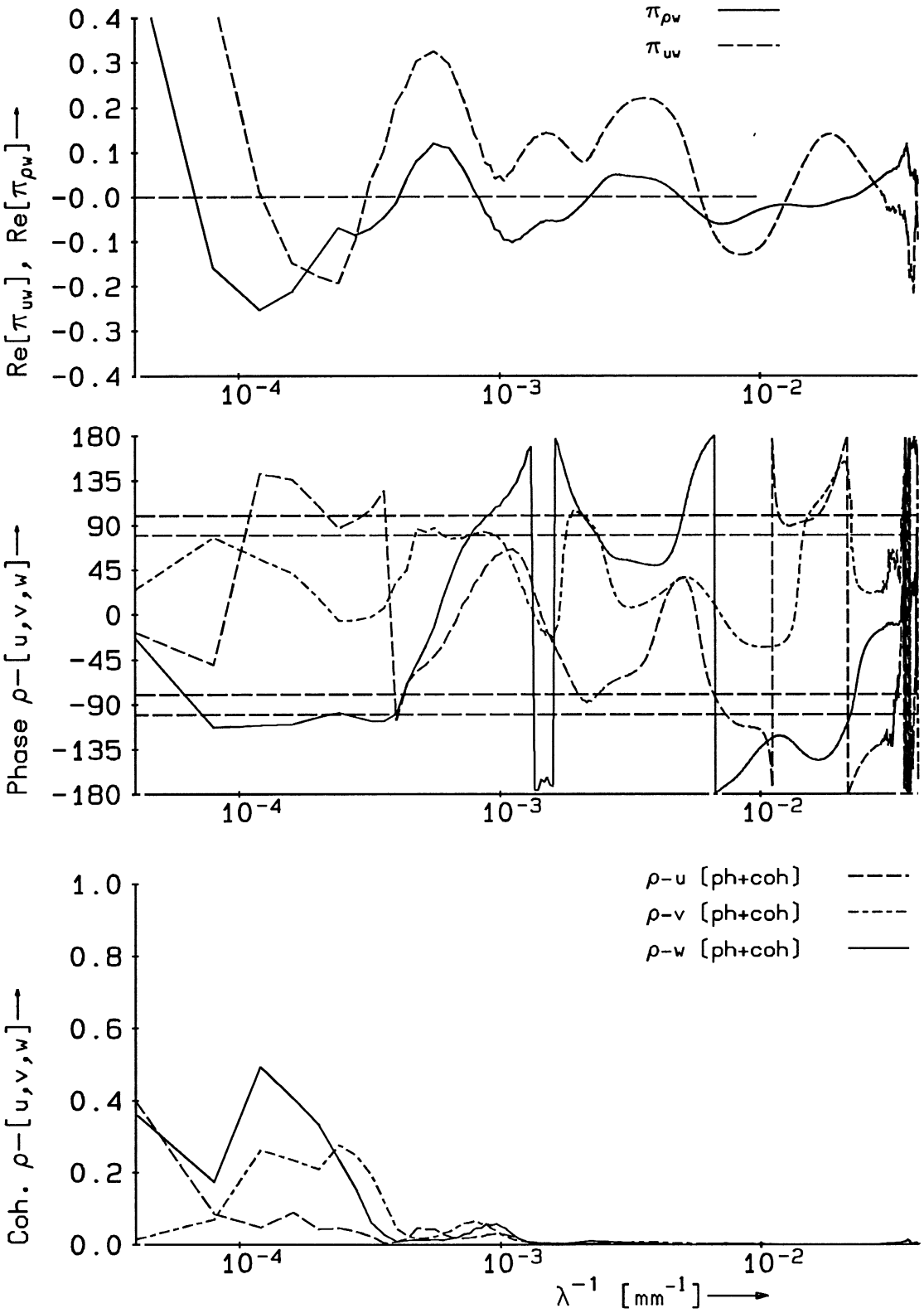

Phase, coherence, momentum and buoyancy fluxes. Caland channel (Ri=3.6;N=0.062 rad/s).	06.05.11:11|137-167 mir iwe111.inv	
DELFT HYDRAULICS	Z 722	Fig.45c

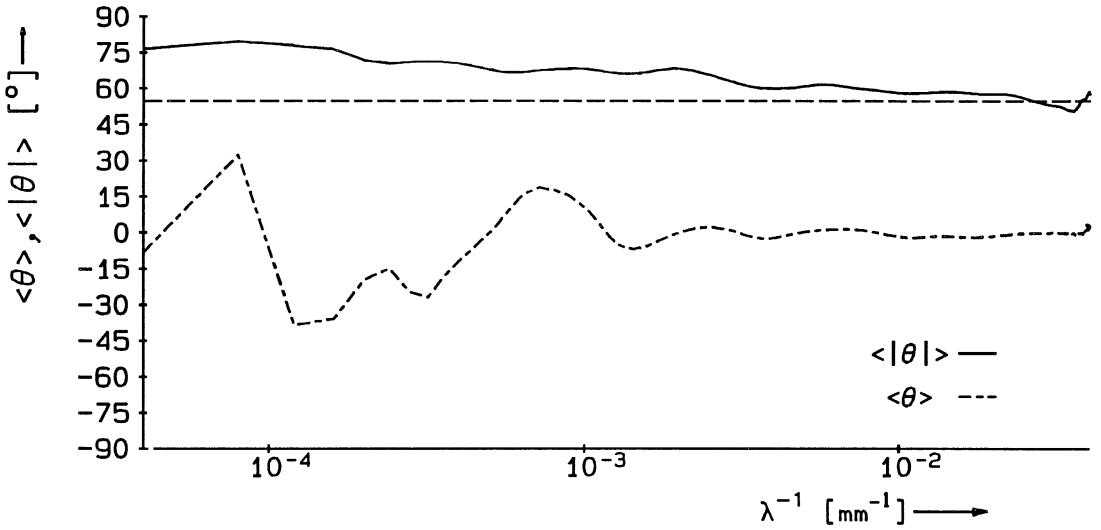

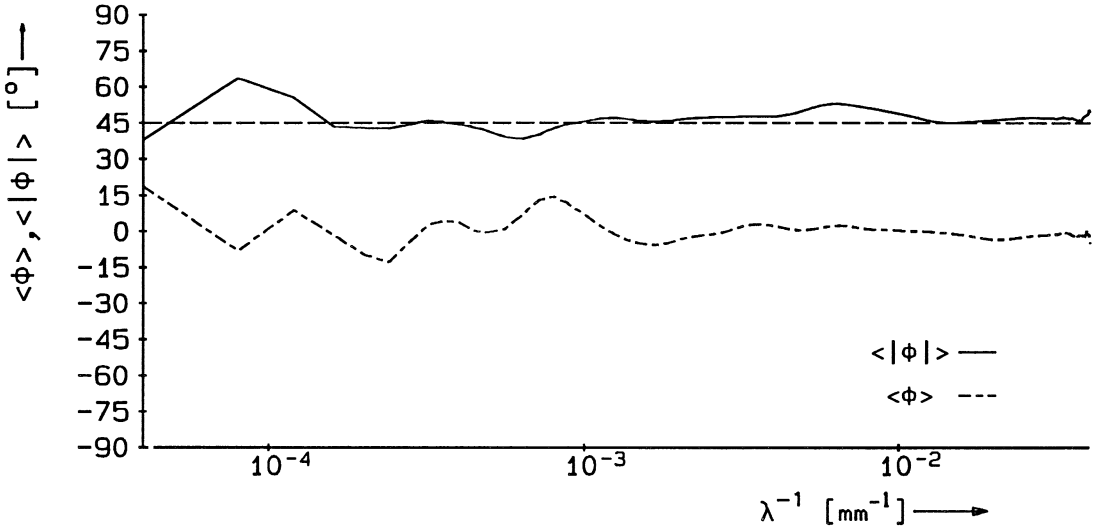

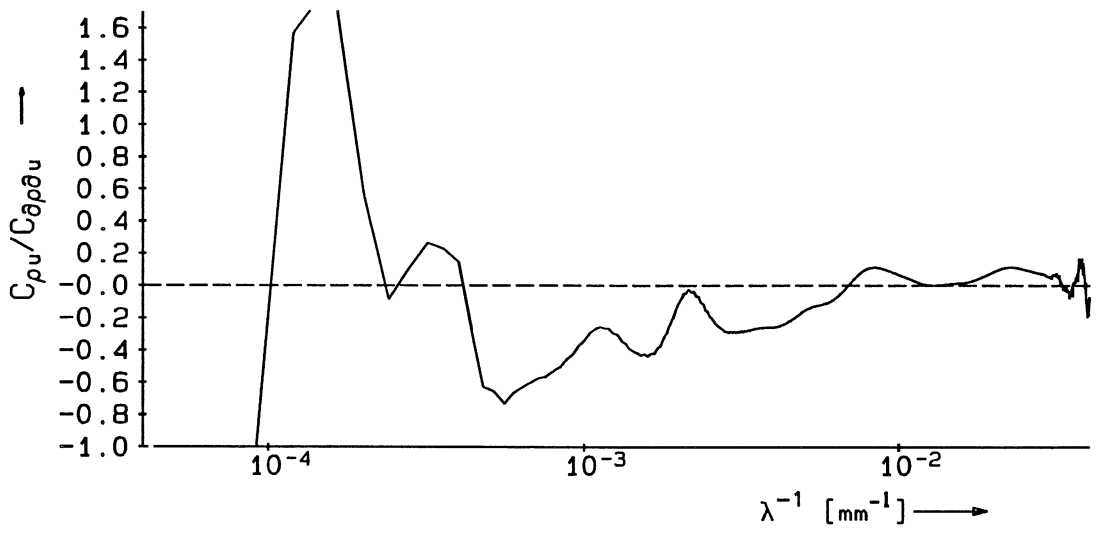

Normalized Stokes mass drift and IW angles. Rotterdam Waterway (Ri=3.6;N=0.062 rad/s).	06.05.11:11|137-167 mir	
	stok111.inv	
DELFT HYDRAULICS	Z 722	Fig.45[d]